Dual Endomembrane Recycling Pathways Function in Synapse Maintenance and Plasticity

by

Garrett Chavis

A dissertation submitted in partial fulfillment
of the requirements for the degree of
Doctor of Philosophy
(Molecular and Integrative Physiology)
at the University of Michigan
2026

Doctoral Committee:

Professor Michael Sutton, Chair
Professor Geoffrey Murphy
Professor Yatrik Shah
Professor Lois Weisman

Garrett Chavis

gchavis@umich.edu

ORCID iD: 0000-0001-5379-4180

© Garrett Chavis 2026

Dedication

This work is dedicated to the mentors who have guided me, challenged me, and believed in me even when I doubted myself. I am deeply grateful for the opportunities that have shaped my path and for the people who opened doors, sometimes when I didn't even know they were there. To those who offered wisdom, encouragement, and patience: your lessons go far beyond science.

There were moments when progress stalled, when experiments failed, or when the road ahead seemed unclear. Yet, in every setback, I found a way forward, through resilience, through support, or through sheer persistence. Each time I fell, I learned to stand again, and every time I stood, I grew. Looking back, I see not only the challenges but the strength, kindness, and community that lifted me here. For all of this—I am profoundly thankful.

Acknowledgements

First and foremost, I would like to thank all the remarkable people who have been part of my life, those who have challenged me, inspired me, and supported me both in science and far beyond. Each of you has shaped who I am today, not only as a scientist but as a person, and I am endlessly grateful for your presence and influence.

I owe special thanks to my mentors, who have guided my scientific journey, encouraged my professional growth, and helped me develop confidence in my own abilities. To Robert Poage (UNCP), thank you for introducing me to the wonders of neuroscience research and reminding me that where you come from does not define where you can go. Your belief in striving for excellence will always stay with me.

To Dan Michele, I will never forget the day you gave a talk at my small liberal arts college, a talk I almost missed but that changed my life forever. Your words and research inspired me to apply to one of the best research institutions in the world. Without you none of this would have been possible. Your leadership and passion for academia instilled in me the strength to apply to a place I never even dreamed of getting into to. Because of your encouragement, I found not only academic success but a community of dedicated and inspiring peers who became lifelong friends.

To Michael Sutton, my PI and mentor, thank you for taking a chance on a young scientist with limited lab experience and helping shape me into the researcher I am today. You pushed me when I wanted to quit, reminded me how far I had come, and continued to support me even when I doubted myself. Your guidance, patience, and encouragement have been instrumental in both my scientific and personal growth. I will always be grateful for your mentorship and belief in me. I am also deeply thankful to Christian Althaus and Cindy Carruthers, who reminded me of the importance of balance—of taking care of both my physical and mental health. Thank you for

always being there during long and difficult days in the lab, and for reminding me that perseverance does not mean neglecting oneself. To Takao Tsukahara, my day-to-day mentor in the beginning and friend, your support and insight have been invaluable. You taught me how to approach research thoughtfully and patiently, and your example has inspired me to be both a better scientist and a better colleague and mentor to others as well.

To my U-M friends and MIP cohort, thank you for being there for both the victories and the setbacks, the successful experiments and the failed ones. You were the ones to celebrate with, to vent and procrastinate with, and to lean on during the toughest stretches. Being surrounded by so many driven, passionate, and talented people kept me motivated to push through the challenges. We were in this together! To my friends from back home, thank you for your unwavering loyalty and laughter. You have known me the longest and seen me at my lowest. Even if you didn't always understand what I was doing, you were always there with an escape, a joke, or a reminder of where I came from. Watching us all grow and excel in our own paths has been one of the greatest rewards of this journey.

To my family, I owe everything. Mom, your resilience, kindness, and generosity continue to guide me every day. You taught me the power of compassion and respect and have always been my greatest supporter. Dad, you showed me what it takes to succeed—the value of hard work, discipline, and integrity. Because of your lessons, I learned early on that with determination, anything is possible. To my grandparents, even though you did not get to see the man I've become, your teachings and example shaped my foundation. I carry your lessons with me always, and I thank you for everything you did for me and for Mom.

Finally, to Steph and her dog Bodie who now has truly become this man's best friend, thank you for filling my life with love, joy, and balance. I never imagined finding such a profound connection during graduate school, but I thank God every day that I did. Your work ethic, and passion inspire me daily to be a better partner, scientist, and person. I am honored and proud to share life and this journey with you and I am beyond thrilled that we get to take our next steps together as we both complete our PhDs.

To everyone who has walked beside me, in science and in life, thank you. I am deeply grateful for every person and every moment that helped me reach this point.

Table of Contents

Dedication ii

Acknowledgements iii

List of Figures viii

Abstract x

Chapter 1 Introduction 1

1.1 Synaptic organization and plasticity 1

1.2 Structural plasticity of dendritic spines 2

1.3 The endomembrane system and endocytic recycling in eukaryotic cells 3

1.4 Retromer and the emergence of dedicated recycling machinery 4

1.5 The SNX27-Retromer pathway in non-neuronal cells 5

1.6 The SNX17-Retriever pathway in non-neuronal cells 6

1.7 Neurons as a specialized context for endosomal recycling 7

1.8 SNX27-Retromer function in neurons and synaptic plasticity 8

1.9 SNX17-Retriever in neurons: emerging evidence 9

1.10 Intersecting roles of SNX27-Retromer and SNX17-Retriever at excitatory synapses 10

1.11 References 12

Chapter 2 Dual Endomembrane Recycling Pathways Function in Parallel to Support Synapse Maintenance and Plasticity 19

2.1 Abstract 19

2.2 Introduction 19

2.3 Materials and methods 21

2.4 Results 29

2.4.1 Synapse loss after disruption of SNX17-Retriever/SNX27-Retromer pathways in vivo 29

2.4.2 SNX17-Retriever and SNX27-Retromer regulate dendritic spine density and morphology in vitro 32

2.4.3 SNX17 and SNX27 localize to the same cellular compartment in neurons 35

2.4.4 SNX17 and SNX27 regulate synapse integrity via parallel pathways 38

2.4.5 SNX17-Retriever and SNX27-Retromer are both required for cLTP and homeostatic upscaling 40

2.4.6 AMPAR recycling requires the SNX27-Retromer Pathway, but is independent of SNX17-Retriever 41

2.4.7 Long term synaptic depression is dependent on both SNX17-Retriever and SNX27-Retromer recycling pathways 44

2.5 Discussion 47

2.5.1 An emerging role for SNX17-Retriever in synapse regulation 47

2.5.2 SNX17-Retriever and SNX27-Retromer operate in the same cellular compartment but regulate synapse maintenance in parallel 49

2.5.3 Combinatorial roles of SNX17-Retriever and SNX27-Retromer in diverse forms of long-lasting synaptic plasticity 51

2.6 References 53

Chapter 3 Dual Recycling Pathways Function in Presynaptic Terminals 62

3.1 Abstract 62

3.2 Introduction 62

3.3 Materials and methods 65

3.4 Results 69

3.4.1 SNX17 and SNX27 are necessary to maintain presynaptic terminals in axons 71

3.4.2 SNX17-Retriever and SNX27-Retromer pathways are not required for spontaneous synaptic vesicle release 73

3.4.3 The SNX27-Retromer pathway, but not SNX17-Retriever, is required for normal evoked synaptic vesicle release 75

3.4.4 SNX27 regulates multiple vesicle pools that participate in AP-triggered neurotransmission 80

3.5 Discussion 82

3.5.1 The SNX27-Retromer and SNX17-Retriever pathways contribute to the maintenance of axonal boutons. 83

3.5.2 Unique roles for SNX17-Retriever and SNX27-Retromer pathways in supporting evoked neurotransmitter release 86

3.5.3 Mechanistic model and implications 86

3.6 References 87

Chapter 4 General Discussion 91

4.1.1 Dual recycling pathways as core regulators of excitatory synapse maintenance 91

4.1.2 Combinatorial control of long-lasting synaptic plasticity 93

4.1.3 Presynaptic specialization 94

4.1.4 Implications for neurological disease and synaptic vulnerability 95

4.1.5 New SNX17 cargoes and postsynaptic structure 97

4.1.6 New SNX17 cargoes with presynaptic influence 97

4.1.7 Expanded SNX27 cargo space and glutamatergic signaling 98

4.1.8 Dual-pathway control of synaptic vulnerability 99

4.1.9 Open questions and gaps in the field 100

4.1.10 Limitations and technical considerations 101

4.1.11 Future directions and concluding model 103

4.2 References 104

List of Figures

Figure 2.1 Synapse loss after disruption of SNX17-Retriever and SNX27-Retromer pathways *in vivo* 30

Figure 2.2 Validation of SNX17 and SNX27 shRNAs 31

Figure 2.3 SNX17-Retriever and SNX27-Retromer regulate synapse density and morphology *in vitro* 33

Figure 2.4 Synapse loss following depletion of the core Retriever subunit VPS26C and core Retromer subunit VPS26B 34

Figure 2.5 SNX17 and SNX27 localize to the same cellular compartment in neurons 36

Figure 2.6 Retriever and Retromer complexes colocalize in dendrites 37

Figure 2.7 SNX17 and SNX27 control synapse maintenance in parallel 39

Figure 2.8 Additive synapse loss following coincident depletion of SNX17 and the core Retromer subunit VPS26B, but not the core Retriever subunit VPS26C 40

Figure 2.9 SNX17-Retriever and SNX27-Retromer are both required for cLTP 42

Figure 2.10 Homeostatic upscaling requires both SNX17-Retriever and SNX27-Retromer pathways 43

Figure 2.11 AMPARs recycle selectively via the SNX27-Retromer pathway, not the SNX17-Retriever pathway 45

Figure 2.12 SNX17 and SNX27 are both required for long term synaptic depression 46

Figure 2.13 Model for functional organization of SNX27-Retromer and SNX17-Retriever pathways at excitatory synapses 48

Figure 3.1 SNX17 colocalizes with presynaptic terminals 71

Figure 3.2 SNX17 and SNX27 are necessary to maintain presynaptic terminals in axons 72

Figure 3.3 Depletion of SNX17 and SNX27 induces non-additive loss of presynaptic boutons . 74

Figure 3.4 Measuring basal AP-independent synaptic vesicle release via live labeling of synaptotagmin 1 in the vesicle lumen 76

Figure 3.5 SNX17-Retriever and SNX27-Retromer pathways are not required for spontaneous synaptic vesicle release 77

Figure 3.6 Using mCherry-vGlut1-pHluorin to measure evoked synaptic vesicle release from individual presynaptic boutons 80

Figure 3.7 The SNX27-Retromer pathway, but not SNX17-Retriever, is required for normal evoked synaptic vesicle release 81

Figure 3.8 Depletion of core Retromer and Retriever subunits reveals unique roles for the SNX27-Retromer and SNX17-Retriever pathways in regulating evoked vesicle release 83

Figure 3.9 The SNX27-Retromer pathway regulates multiple synaptic vesicle pools that participate in evoked neurotransmission 85

Abstract

The proper recycling of synaptic membrane proteins is a fundamental requirement for the stability and adaptability of neuronal connections, yet the molecular systems governing this process across pre- and postsynaptic compartments remain poorly understood. This research investigates how two evolutionarily conserved endosomal recycling pathways - the SNX27-Retromer and SNX17-Retriever complexes - coordinate to maintain synaptic structure, function, and plasticity in mammalian neurons. Using a combination of *in vivo* manipulations in developing rat hippocampus and quantitative imaging, electrophysiological, and optical assays in cultured neurons, I demonstrate that SNX27-Retromer and SNX17-Retriever operate in largely parallel yet distinct pathways essential for synaptic maintenance. Postsynaptically, disruption of either pathway causes progressive loss of excitatory synapses in CA1 pyramidal neurons and impairs multiple forms of activity-dependent plasticity, including long-term potentiation (LTP), long-term depression (LTD), and homeostatic scaling. Both SNX27 and SNX17 colocalize extensively within early endosomes, indicating shared subcellular localization, but the additive synapse loss following dual disruption reveals parallel, nonredundant functions. Cargo analyses further identify pathway-specific substrates, suggesting that SNX17-Retriever and SNX27-Retromer selectively govern the recycling of complementary sets of synaptic proteins required for long-lasting forms of synaptic plasticity. Presynaptically, both complexes localize within axonal endosomes and support the stability of presynaptic boutons. Knockdown of either SNX17 or SNX27 reduces bouton density, consistent with a shared requirement of endosomal recycling for terminal maintenance. However, combined depletion does not enhance this reduction, implying overlapping presynaptic cargos or sorting hubs. Functional imaging reveals that while spontaneous neurotransmitter release persists after loss of either pathway, depletion of SNX27 or the Retromer subunit VPS26B impairs action potential evoked release. Specifically, SNX27 loss reduces both the readily releasable and total recycling pools of synaptic vesicles, slowing evoked responses and diminishing active bouton density, whereas SNX17-Retriever disruption leaves evoked release largely intact. Together, these data establish the SNX27-Retromer and SNX17-

Retriever complexes as major regulators of neuronal endosomal trafficking. Their coordinated but distinct actions ensure the surface delivery and recycling of key pre- and postsynaptic proteins, enabling the structural integrity, functional precision, and adaptive responsiveness of excitatory synapses. This work highlights endosomal recycling as a central mechanism linking molecular trafficking to the maintenance and plasticity of neural circuits.

Chapter 1 Introduction

1.1 Synaptic organization and plasticity

Synapses are asymmetric intercellular junctions that enable neurons to communicate with one another and with their target cells, providing the fundamental basis for information transfer in neural circuits (Südhof, 2021; von Bohlen und Halbach, 2009). At most chemical synapses, an action potential coming through the presynaptic terminal triggers voltage-gated calcium channel opening, leading to synaptic vesicle fusion and quantal release of neurotransmitter into the synaptic cleft, where it binds postsynaptic receptors and alters the electrical and biochemical state of the postsynaptic neuron (Südhof, 2021; von Bohlen und Halbach, 2009). Through the integration of thousands of synaptic inputs distributed across dendritic areas, individual neurons transform incoming activity patterns, and the dynamic modulation of synaptic efficacy is widely viewed as a core mechanism by which neural circuits support learning, memory, and behavior (Rochefort and Konnerth, 2023; von Bohlen und Halbach, 2009).

Chemical synapses exhibit a highly organized architecture, comprising a presynaptic active zone enriched in synaptic vesicles and release machinery, a synaptic cleft, and a postsynaptic density (PSD) that contains neurotransmitter receptors, scaffolding proteins, and diverse signaling molecules (Südhof, 2021; Bourne and Harris, 2008). This molecular specialization ensures tight spatial coupling between sites of vesicle fusion and postsynaptic receptor clusters, supporting efficient neurotransmission and enabling synapses to alter their strength through activity-dependent changes in receptor content and PSD composition (Bourne and Harris, 2008; Bosch and Hayashi, 2012). Such changes often manifest as long-term potentiation (LTP) or long-term depression (LTD), which are considered principal cellular components of learning and memory across multiple brain regions (Rochefort and Konnerth, 2023; Bosch and Hayashi, 2012). In most excitatory neurons of mammals, the vast majority of glutamatergic synapses are formed on small actin-rich protrusions from dendrites known as dendritic spines (Bourne and Harris, 2008; Rochefort and Konnerth, 2023). Dendritic spines

typically consist of a rounded head connected to a thin neck, a geometry that creates a restricted biochemical and electrical compartment in which calcium dynamics and signaling pathways can be locally regulated during synaptic activity (Bourne and Harris, 2008; von Bohlen und Halbach, 2009). By acting as microdomains for excitatory input, spines help preserve input specificity and allow neighboring synapses on the same dendritic branch to undergo distinct patterns of plasticity in response to different activity (Segal and Korkotian, 2014; von Bohlen und Halbach, 2009).

1.2 Structural plasticity of dendritic spines

Dendritic spines are structurally highly dynamic, and their formation, elimination, and morphological remodeling occur over time scales ranging from minutes to days in response to synaptic activity, sensory experience, and learning paradigms (Bourne and Harris, 2008; Rochefort and Konnerth, 2023). Spine head enlargement, changes in neck geometry, and coordinated growth of the PSD correlate closely with enhanced synaptic efficacy, whereas spine shrinkage or loss is associated with synaptic weakening, indicating that structural features of spines encode aspects of synaptic strength (Arellano et al., 2019; von Bohlen und Halbach, 2009). Converging evidence from *in vivo* imaging and behavioral studies has shown that learning-related tasks induce clustered spine formation and stabilization, and that selective manipulation of spine dynamics can affect memory formation and persistence (Rochefort and Konnerth, 2023; Berry and Nedivi, 2017). Because dendritic spines host the majority of cortical and hippocampal excitatory synapses, their proper development, maintenance, and plasticity are essential for normal circuit function and cognitive performance (Bourne and Harris, 2008; Rochefort and Konnerth, 2023). Alterations in spine density, morphology, and stability have been consistently reported in a broad range of neurodevelopmental and neuropsychiatric disorders, including intellectual disability, autism spectrum disorders, schizophrenia, and some forms of epilepsy, suggesting that spine pathology represents a common cellular substrate for cognitive and behavioral dysfunction (von Bohlen und Halbach, 2009; Segal and Korkotian, 2014). Elucidating the mechanisms that govern synapse formation, spine structural plasticity, and the coupling between structural and functional changes at excitatory synapses is therefore crucial for understanding how neural circuits support behavior in health and how these processes are disrupted in disease (Bourne and Harris, 2008; Rochefort and Konnerth, 2023).

1.3 The endomembrane system and endocytic recycling in eukaryotic cells

Eukaryotic cells depend on an internal membrane system to keep compartments separate, control signaling, and regulate the composition of the plasma membrane (Maxfield and McGraw, 2004; Grant and Donaldson, 2009). This system includes the endoplasmic reticulum, Golgi apparatus, endosomes, lysosomes, and the plasma membrane, which are linked by vesicle transport pathways (Maxfield and McGraw, 2004). Constant two-way traffic between these organelles delivers newly synthesized proteins and lipids, retrieves missorted or damaged components, and adjusts surface receptor levels in response to external signals (Maxfield and McGraw, 2004; Grant and Donaldson, 2009). Endocytosis brings plasma membrane proteins, lipids, and extracellular ligands into early endosomes, which act as sorting stations (Maxfield and McGraw, 2004; Huotari and Helenius, 2011). From here, cargo can be recycled back to the plasma membrane, sent to the trans-Golgi network (TGN), or delivered to late endosomes and lysosomes for degradation (Maxfield and McGraw, 2004; Huotari and Helenius, 2011). The balance between recycling and degradation maintains receptor homeostasis and influences how cells respond to their environment (Sorkin and von Zastrow, 2009). If degradation is too strong or recycling is weak, nutrient transporters and growth factor receptors may fall to levels that impair metabolism and mitogenic signaling, whereas reduced downregulation can sustain or enhance signaling and contribute to disease, including cancer (Sorkin and von Zastrow, 2009). Endosome-to-plasma membrane recycling uses several routes. A fast route returns cargo directly from early endosomes to the surface, often within minutes, and depends on Rab4 (Grant and Donaldson, 2009). This route typically handles receptors that must return quickly, such as the transferrin receptor (TfnR) (Grant and Donaldson, 2009). A slower route delivers cargo from early endosomes to a perinuclear Rab11 recycling compartment before returning it to the plasma membrane (Green et al., 1997; Welz et al., 2014). This slower pathway is important for polarized trafficking and for recycling that is controlled by signals, including for adhesion molecules and receptors (Green et al., 1997; Welz et al., 2014). The identity of endosomal compartments is shaped by Rab GTPases, phosphoinositide lipids, coat proteins, motors, and scaffolding complexes (Cullen, 2008; Teasdale and Collins, 2012). Sorting nexins (SNXs) are key components that help define endosomal subdomains and select cargo for different routes (Cullen, 2008; Teasdale and Collins, 2012). All SNXs have a PI3P binding PX domain that targets them to PI3P rich early endosomes, and many also carry BAR or FERM domains that support

membrane curvature or protein–protein interactions (Cullen, 2008; Teasdale and Collins, 2012). By organizing discrete zones on endosomes and recruiting specific trafficking machinery, SNXs direct sets of transmembrane cargoes into either recycling or retrograde pathways (Cullen, 2008; Cullen and Steinberg, 2018).

1.4 Retromer and the emergence of dedicated recycling machinery

A major step in understanding endosomal sorting was the discovery of the Retromer complex. In yeast, Retromer was first identified as a factor that returns the vacuolar protein sorting receptor Vps10 from endosomes to the Golgi (Seaman et al., 1998; Seaman, 2004). Later work showed that Retromer is conserved in metazoans and acts in both retrograde and recycling routes (Seaman, 2004; Burd and Cullen, 2014). In mammals, the canonical cargo selective complex (CSC) contains VPS35, VPS26A/B, and VPS29 (Hierro et al., 2007). This trimer associates with SNX-BAR dimers, such as SNX1, SNX2 or SNX5, SNX6, which support formation of tubule vesicular carriers that bud from endosomes (Hierro et al., 2007; Cullen and Steinberg, 2018). Retromer was originally linked to endosome TGN transport, but it is now clear that it also mediates direct recycling to the plasma membrane, in part through specific SNX adaptors (Steinberg et al., 2013; Gallon and Cullen, 2015). This broader view led to the idea that there are distinct forms of Retromer dependent pathways, each defined by different adaptors and cargo specificity (Steinberg et al., 2013; Gallon and Cullen, 2015). Among these, SNX27 associated Retromer is a major regulator of endocytic recycling, especially in polarized and excitable cells, including neurons (Steinberg et al., 2013; McMillan et al., 2021).

An evolutionarily related complex, Retriever, was later identified in metazoans as a second major endosomal recycling system (McNally et al., 2017). Retriever shares VPS29 with Retromer but uses VPS35L and VPS26C in place of VPS35 and VPS26A/B (McNally et al., 2017). Unlike Retromer, Retriever does not bind SNX BAR proteins; instead, it associates with SNX17, a PX FERM domain sorting nexin that recognizes NPXY/NXXY motifs in cargo cytoplasmic tails (Böttcher et al., 2012; McNally et al., 2017). The SNX17-Retriever axis, together with the CCC (COMMD-CCDC22-CCDC93) complex and the WASH complex, defines a second major route for returning transmembrane proteins to the plasma membrane (Phillips-Krawczak et al., 2015; Simonetti and Cullen, 2019). These pathways control the surface

levels of many receptors, transporters, and adhesion molecules that are central to cell polarity, tissue organization, and cell migration (Simonetti and Cullen, 2019; Burd and Cullen, 2014).

1.5 The SNX27-Retromer pathway in non-neuronal cells

SNX27 is a multidomain sorting nexin that gives Retromer cargo specificity. It has an N-terminal PDZ domain, a central FERM-like domain, and a C-terminal PX domain (Gallon et al., 2014; Clairfeuille et al., 2016). The PX domain targets SNX27 to PI3P rich early endosomes, while the PDZ domain binds type I PDZ binding motifs (S/T-X-Φ) at the C-terminal of many transmembrane proteins (Gallon et al., 2014; Clairfeuille et al., 2016). The FERM like domain interacts with additional partners, including actin linked complexes, which helps couple cargo recognition to changes in membrane shape and downstream signaling (Clairfeuille et al., 2016; Steinberg et al., 2013). In non-neuronal cells, SNX27-Retromer controls recycling of a wide range of plasma membrane proteins. Proteomic studies and motif searches suggest that more than 400 proteins with PDZ motifs may depend on SNX27 for their retrieval from endosomes and return to the cell surface (Steinberg et al., 2013; Loo et al., 2014; McMillan et al., 2021). Confirmed SNX27 cargoes include nutrient transporters such as GLUT1 and GLUT4, ion channels and transporters, G protein coupled receptors (GPCRs), and signaling receptors such as the β_2-adrenergic receptor (Lauffer et al., 2010; Balana et al., 2011; Temkin et al., 2017). By binding these cargoes, SNX27 shields them from lysosomal degradation and promotes their return to the plasma membrane, thereby preserving their function and modulating signaling output (Lauffer et al., 2010; Gallon and Cullen, 2015).

SNX27-Retromer is closely linked to the WASH complex, which activates Arp2/3-dependent actin polymerization on endosomes (Gomez and Billadeau, 2009; Harbour et al., 2012). Actin networks driven by WASH help separate recycling cargoes from those set for degradation and support the formation of tubules that bud from endosomes (Gomez and Billadeau, 2009; Harbour et al., 2012). VPS35 binds FAM21, a WASH subunit, linking Retromer to WASH, and SNX27 strengthens this connection through its interactions with VPS26 and other subunits (Harbour et al., 2012; Jia et al., 2012). This arrangement coordinates cargo recognition with carrier formation and export from endosomes (Harbour et al., 2012; Jia et al., 2012). Through these roles, SNX27-Retromer supports processes that rely on repeated cycles of

receptor internalization and return to the surface. In epithelial cells, for example, SNX27-dependent recycling of nutrient transporters supports high metabolic demand and polarized trafficking to apical or basolateral membranes (Lauffer et al., 2010). In immune cells, SNX27 helps recycle receptors for antigen recognition and cytokine signaling, shaping immune responses (Gallon and Cullen, 2015; McMillan et al., 2021). In fibroblasts and endothelial cells, SNX27 regulates adhesion receptors and GPCRs that guide cell migration, angiogenesis, and tissue repair (McMillan et al., 2021). Given its broad impact on the surface proteome, defects in SNX27-Retromer function have been linked to cancer, metabolic disease, and neurodegeneration (Burd and Cullen, 2014; Wang et al., 2013; McMillan et al., 2021).

1.6 The SNX17-Retriever pathway in non-neuronal cells

The SNX17-Retriever axis defines a second conserved recycling pathway in metazoan cells. SNX17 contains a PX domain that targets it to PI3P positive endosomes and a C-terminal FERM domain that recognizes NPXY/NXXY motifs in cytoplasmic tails of transmembrane proteins (Böttcher et al., 2012). These motifs are common in LDL receptor family members, integrins, and several other adhesion and signaling receptors (Stockinger et al., 2002; Böttcher et al., 2012). Retriever is a heterotrimer composed of VPS35L, VPS26C, and VPS29 (McNally et al., 2017). VPS29 is shared with Retromer, but VPS35L and VPS26C are distinct paralogs of VPS35 and VPS26A/B (McNally et al., 2017). Retriever does not bind SNX-BAR proteins; instead, SNX17 recruits Retriever to endosomal membranes, bringing it near NPXY-containing cargoes (McNally et al., 2017). The CCC complex, which includes COMMD proteins and CCDC22/CCDC93, further supports this axis by scaffolding Retriever and WASH on endosomes and by regulating ion transport and copper homeostasis (Phillips-Krawczak et al., 2015; Chen et al., 2019; Simonetti and Cullen, 2019). A key function of SNX17-Retriever-CCC-WASH in non-neuronal cells is recycling integrins and other adhesion molecules. SNX17 binds β-integrin tails through NPXY motifs and prevents their lysosomal degradation, favoring their return to the cell surface (Böttcher et al., 2012). This recycling is needed to maintain cell matrix adhesion, support focal adhesion turnover, and allow directed migration (Zech et al., 2011; Böttcher et al., 2012). Loss of SNX17 or Retriever reduces β_1-integrin and other receptors at the surface, impairs motility, alters cell shape, and disrupts tissue morphogenesis (McNally et al., 2017; Chen et al., 2019).

SNX17-Retriever also controls LDL receptor related proteins (LRPs) and other receptors involved in endocytosis, nutrient uptake, and signaling. For example, SNX17 regulates recycling and signaling of LRP1, which affects lipoprotein metabolism and TGF-β signaling (Stockinger et al., 2002; van Kerkhof et al., 2005). Through these cargoes, SNX17-Retriever influences adhesion, migration, and signal integration in epithelial, endothelial, and immune cells (McNally et al., 2017; Simonetti and Cullen, 2019). Genetic disruption of Retriever or CCC components in animal models causes embryonic lethality or severe developmental defects, showing that this pathway is essential (Starokadomskyy et al., 2013; McNally et al., 2017). Mutations in CCDC22 and CCDC93 are linked to X-linked intellectual disability and Ritscher-Schinzel syndrome, indicating that this pathway is also important in the nervous system (Starokadomskyy et al., 2013; Rehmann et al., 2013).

1.7 Neurons as a specialized context for endosomal recycling

The core machinery of endosomal trafficking is conserved across eukaryotic cells, but neurons place special demands on these pathways. Neurons are highly polarized cells with long axons and complex dendritic trees, and synapses especially excitatory glutamatergic synapses on dendritic spines must adjust their molecular composition locally in response to activity and neuromodulators (Kennedy and Ehlers, 2006; Haucke et al., 2011). This requires tight spatial and temporal control of endocytic recycling at synaptic and perisynaptic sites that are often far from the soma (Kennedy and Ehlers, 2006; Haucke et al., 2011). At excitatory hippocampal synapses, synaptic strength and stability depend on the abundance and subunit composition of AMPA-type and NMDA-type glutamate receptors at the postsynaptic density, along with adhesion molecules and scaffold proteins that maintain synapse structure (Huganir and Nicoll, 2013; Diering and Huganir, 2018). These surface proteins undergo continual endocytosis and recycling through dendritic endosomes located in spines or adjacent shafts (Ehlers, 2000; Park et al., 2004). Activity dependent synaptic plasticity, including LTP and LTD, relies on changes in receptor trafficking that are mediated by these local endosomal systems (Ehlers, 2000; Park et al., 2004; Park et al., 2006).

Dendritic and spine endosomes show features of early and recycling endosomes, including Rab5, Rab4, and Rab11 markers, and they are linked to actin and microtubule tracks that support vesicle transport (Park et al., 2006; Kennedy and Ehlers, 2006). Small GTPases, kinases, and phosphatases activated by synaptic signaling converge on trafficking adaptors to control sorting, recycling, and degradation of postsynaptic receptors and adhesion molecules (Kennedy and Ehlers, 2006; Diering and Huganir, 2018). This regulation allows synapses to respond to patterns of activity and to encode information as lasting structural and functional changes. Disrupted endosomal trafficking is implicated in many neurological and psychiatric disorders. Changes in receptor recycling and degradative sorting can alter synaptic strength, spine morphology, and circuit connectivity, contributing to intellectual disability, autism spectrum disorders, Alzheimer's disease, and Parkinson's disease (Li et al., 2016; Small and Petsko, 2015; McDonald, 2020; Saitoh, 2022). Understanding endosomal recycling in neurons is therefore important both for explaining the cellular basis of learning and memory and for identifying mechanisms and targets in disease (Li et al., 2016; Small and Petsko, 2015).

1.8 SNX27-Retromer function in neurons and synaptic plasticity

Among endosomal pathways, SNX27-Retromer is a key regulator of postsynaptic receptor recycling in excitatory neurons. SNX27 is highly expressed in the brain and enriched in hippocampal neurons, where it localizes to endosomes within dendrites and near excitatory synapses (Wang et al., 2013; Loo et al., 2014; McMillan et al., 2021). Proteomic and biochemical studies have identified more than 200 neuronal transmembrane proteins as SNX27-Retromer cargoes, including neurotransmitter receptors, ion channels, transporters, and various signaling receptors (Steinberg et al., 2013; McMillan et al., 2021). A well-studied neuronal cargo of SNX27-Retromer is the AMPA-type glutamate receptor (AMPAR), which mediates most fast excitatory transmission in the hippocampus. The GluA1 subunit contains a C-terminal PDZ-binding motif recognized by the SNX27 PDZ domain, which allows internalized AMPARs to enter SNX27-Retromer positive endosomes (Loo et al., 2014; Hussain et al., 2014). Through its association with the Retromer CSC (VPS35, VPS26A/B, VPS29) and the WASH complex, SNX27 promotes AMPAR recycling to the postsynaptic membrane rather than delivery to lysosomes (Harbour et al., 2012; Mao et al., 2021; McMillan et al., 2021). SNX27-Retromer dependent AMPAR recycling is critical for LTP. During LTP induction, synaptic activity drives

insertion of additional AMPARs into the postsynaptic membrane, which strengthens transmission (Huganir and Nicoll, 2013; Diering and Huganir, 2018). Loss of SNX27 or interference with its interaction with Retromer lowers surface AMPAR levels, impairs activity dependent AMPAR insertion, and disrupts LTP (Loo et al., 2014; Temkin et al., 2017; McMillan et al., 2021). Conversely, enhancing SNX27-Retromer function stabilizes synaptic AMPARs and supports synaptic potentiation (Wang et al., 2013; McMillan et al., 2021).

Beyond AMPARs, SNX27-Retromer regulates other synaptic proteins, including NMDA receptors, GABA/B receptors, GPCRs, and transporters and channels involved in ion homeostasis and neuromodulation (Temkin et al., 2017; McMillan et al., 2021). By coordinating recycling of multiple receptor classes, SNX27-Retromer tunes synaptic responsiveness and excitability in response to neuronal activity (McMillan et al., 2021). SNX27-Retromer dysfunction has been linked to neurodevelopmental and neurodegenerative disease. Lower levels of SNX27 have been reported to be observed in postmortem tissue of the cortex recovered from individuals diagnosed with Down syndrome as well as in the hippocampus of Ts65Dn mice. (Wang et al., 2013; Wang et al., 2014; McGough et al., 2014). Retromer dysfunction due to VPS35 mutations or reduced VPS35 expression is associated with Parkinson's disease and late-onset alzheimer's disease, which feature synaptic loss and protein homeostasis defects (Small and Petsko, 2015; McGough et al., 2014; Asadzadeh et al., 2022). These findings highlight SNX27-Retromer as a pathway important for both physiological plasticity and long-term synapse integrity (Small and Petsko, 2015; McMillan et al., 2021).

1.9 SNX17-Retriever in neurons: emerging evidence

Compared with SNX27-Retromer, the neuronal roles of SNX17 and Retriever have only recently been explored. Given the importance of SNX17-Retriever in recycling integrins and other adhesion receptors in non-neuronal cells, it has been proposed that this pathway could also regulate neuronal adhesion molecules and influence synapse formation, stability, and plasticity (Böttcher et al., 2012; Simonetti and Cullen, 2019). Initial work showed that SNX17 is expressed in the brain and localizes to endosomal structures in dendrites, suggesting a role in postsynaptic trafficking (McNally et al., 2017; Chen et al., 2019). Emerging data suggest that SNX17-Retriever regulates additional neuronal cargoes. Proteomic and interactome analyses implicate

SNX17 in recycling other adhesion receptors, including certain protocadherins and LRP family members, as well as signaling receptors that affect synaptic development and plasticity (McNally et al., 2017; Phadke et al., 2025). In cortical neurons, disruption of Retriever or CCC components alters postsynaptic membrane composition and dendritic spine morphology, indicating a broader role in synapse maintenance (McDonald, 2020; Simonetti and Cullen, 2019).

Together, these findings support a potential model in which SNX17-Retriever operates in neurons as an adhesion and signaling focused recycling pathway that complements the receptor and transporter rich cargo spectrum of SNX27-Retromer (Simonetti and Cullen, 2019). SNX27-Retromer primarily ensures recycling of neurotransmitter receptors and transporters, whereas SNX17-Retriever may maintain adhesion receptors and co-receptors that provide structural and signaling support at synapses (McMillan et al., 2021).

1.10 Intersecting roles of SNX27-Retromer and SNX17-Retriever at excitatory synapses

Excitatory hippocampal synapses rely on tightly regulated trafficking of surface proteins, and endocytic recycling is a key way neurons adjust the composition of receptors, adhesion molecules, and transporters in response to activity (Diering and Huganir, 2018; van Oostrum et al., 2020). Disturbances in these recycling routes impair synaptic plasticity and are associated with neurodevelopmental and neurodegenerative conditions (Li et al., 2016; McDonald, 2020; Saitoh, 2022). SNX27-Retromer and SNX17-Retriever define two major endosome-to-plasma membrane recycling pathways that are both relevant to excitatory synapses. SNX27-Retromer is comparatively well characterized and mediates recycling of a large set of neuronal transmembrane proteins, including neurotransmitter receptors, ion channels, and signaling receptors (Steinberg et al., 2013; McMillan et al., 2021). SNX27 uses its PDZ domain to recognize specific cargoes and cooperates with the core Retromer complex (VPS35, VPS26A/B, VPS29) and the WASH complex to promote cargo exit from endosomes (Harbour et al., 2012; Steinberg et al., 2013; Mao et al., 2021). AMPA-type glutamate receptors are a central SNX27 cargo in hippocampal neurons, and SNX27-Retromer dependent AMPAR recycling is critical for synaptic potentiation and other forms of plasticity (Loo et al., 2014; Hussain et al., 2014; Temkin et al., 2017; McMillan et al., 2021).

In parallel, SNX17 and Retriever form a recycling system that operates independently of SNX27 and canonical Retromer (McNally et al., 2017). SNX17 is a PX-FERM protein that recognizes NPXY/NXXY motifs in cargo cytoplasmic tails and requires Retriever (VPS35L, VPS26C, VPS29), the CCC complex, and WASH for efficient cargo retrieval from endosomes (McNally et al., 2017; Simonetti and Cullen, 2019). In non-neuronal cells, SNX17-Retriever regulates surface levels of many adhesion molecules and transporters, including β-integrins and LDL receptor related proteins, thereby shaping cell matrix adhesion, migration, and signaling (Böttcher et al., 2012; van Kerkhof et al., 2005; Chen et al., 2019; McNally et al., 2017). These cargo profiles suggest that, in neurons, SNX17-Retriever is well placed to control adhesion receptors and co-receptors that support synapse structure and signal integration (Simonetti and Cullen, 2019). Although their cargoes and core architectures differ, both SNX27-Retromer and SNX17-Retriever are implicated in processes that are essential for excitatory synapse function (Asadzadeh et al., 2022; McMillan et al., 2021; Phadke et al., 2025). The two complexes share cofactors such as VPS29 and engage the WASH complex, raising the possibility that they may be coordinated or compete within specialized endosomal subdomains (McNally et al., 2017; Mao et al., 2021). Their inferred cargo specializations are complementary: SNX27-Retromer focuses on neurotransmitter receptors and transporters, whereas SNX17-Retriever likely emphasizes adhesion receptors and co-receptors, together providing the signaling and structural components needed for stable and plastic synapses (Simonetti and Cullen, 2019; McMillan et al., 2021). However, how these pathways operate at excitatory synapses in intact circuits, which cargoes are handled by each route in neurons, and whether they act redundantly or in parallel for synapse maintenance and plasticity remain open questions. The work in this thesis is designed to address these gaps by defining the roles of SNX27-Retromer and SNX17-Retriever in supporting excitatory synapse integrity and activity dependent plasticity in hippocampal neurons.

What is presented later in this thesis is designed to address a subset of these questions by (1) defining how SNX27-Retromer and SNX17-Retriever are organized on neuronal endosomes at excitatory synapses, (2) identifying synaptic cargoes that depend selectively on each pathway, and (3) determining how disruption of each pathway, alone and in combination, affects synapse maintenance and multiple forms of plasticity in hippocampal circuits. Together with ongoing and

future studies, these experiments aim to establish a framework for how recycling pathways cooperate to maintain synaptic connectivity and how their failure contributes to brain disease.

1.11 References

Arellano, J.I., et al. (2019). Neuronal plasticity affects correlation between the size of dendritic spine and postsynaptic density. *Scientific Reports*, 9, 16936.

Asadzadeh, J., Ruchti, E., Jiao, W., Limoni, G., MacLachlan, C., Small, S.A., Knott, G., Santa-Maria, I., McCabe, B.D. (2022). Retromer deficiency in Tauopathy models enhances the truncation and toxicity of Tau. *Nature Communications*, 13(1), 5049.

Balana, B., Maslennikov, I., Kwon, Y., et al. (2011). Mechanism underlying selective regulation of G protein–gated inwardly rectifying potassium channels by sorting nexin 27. *Proceedings of the National Academy of Sciences USA*, 108(49), 20172–20177.

Böttcher, R.T., Stremmel, C., Meves, A., et al. (2012). Sorting nexin 17 prevents lysosomal degradation of β1-integrins by binding to the β1-integrin tail. *Nature Cell Biology*, 14(6), 584–592.

Bosch, M., & Hayashi, Y. (2012). Structural plasticity of dendritic spines. *Current Opinion in Neurobiology*, 22(3), 383–388.

Bourne, J.N., & Harris, K.M. (2008). Balancing structure and function at hippocampal dendritic spines. *Annual Review of Neuroscience*, 31, 47–67.

Burd, C., & Cullen, P.J. (2014). Retromer: A master conductor of endosome sorting. *Cold Spring Harbor Perspectives in Biology*, 6(2), a016774.

Chan, C.S., Weeber, E.J., Zong, L., et al. (2006). Beta1-integrins are required for hippocampal AMPA receptor-dependent synaptic transmission, synaptic plasticity, and working memory. *Journal of Neuroscience*, 26(1), 223–232.

Chen, Y., Schindler, C., Limonciel, A., et al. (2019). The CCC complex cooperates with the WASH complex to regulate endosomal trafficking of the LDL receptor and transferrin receptor. *Journal of Cell Science*, 132(3), jcs217141.

Clairfeuille, T., Mas, C., Chan, A.S.M., et al. (2016). A molecular code for endosomal recycling of phosphorylated cargos by the SNX27–Retromer complex. *Nature Structural & Molecular Biology*, 23(10), 921–932.

Cullen, P.J. (2008). Endosomal sorting and signaling: An emerging role for sorting nexins. *Nature Reviews Molecular Cell Biology*, 9, 574–582.

Cullen, P.J., & Steinberg, F. (2018). To degrade or not to degrade: Mechanisms and significance of endocytic recycling. *Trends in Cell Biology*, 28(12), 879–894.

Diering, G.H., & Huganir, R.L. (2018). The AMPA receptor code of synaptic plasticity. *Neuron*, 100(2), 314–329.

Ehlers, M.D. (2000). Reinsertion or degradation of AMPA receptors determined by activity-dependent endocytic sorting. *Neuron*, 28(2), 511–525.

Gallon, M., & Cullen, P.J. (2015). Retromer and sorting nexins in endosomal sorting. *Biochemical Society Transactions*, 43(1), 33–47.

Gallon, M., Clairfeuille, T., Steinberg, F., et al. (2014). A unique PDZ domain and arrestin-like fold interaction reveals mechanistic details of endosomal cargo recognition by SNX27–Retromer. *Proceedings of the National Academy of Sciences USA*, 111(1), E12–E21.

Gomez, T.S., & Billadeau, D.D. (2009). A FAM21-containing WASH complex regulates retromer-dependent sorting. *Nature Cell Biology*, 11(2), 122–131.

Grant, B.D., & Donaldson, J.G. (2009). Pathways and mechanisms of endocytic recycling. *Nature Reviews Molecular Cell Biology*, 10(9), 597–608.

Green, S.A., Setiadi, H., McEver, R.P., & Kelly, R.B. (1997). The cytoplasmic domain of P-selectin contains a sorting determinant that mediates rapid degradation in lysosomes. *Journal of Cell Biology*, 139(2), 417–428.

Harbour, M.E., Breusegem, S.Y., Antrobus, R., et al. (2012). The cargo-selective Retromer complex is a recruiting hub for protein complexes that regulate endosomal tubule dynamics. *Nature Cell Biology*, 14, 24–35.

Haucke, V., Neher, E., & Sigrist, S.J. (2011). Protein scaffolds in the coupling of synaptic exocytosis and endocytosis. *Nature Reviews Neuroscience*, 12(3), 127–138.

Hierro, A., Rojas, A.L., Rojas, R., et al. (2007). Functional architecture of the Retromer cargo-recognition complex. *Nature*, 449, 1063–1067.

Huganir, R.L., & Nicoll, R.A. (2013). AMPARs and synaptic plasticity: The last 25 years. *Neuron*, 80(3), 704–717.

Huotari, J., & Helenius, A. (2011). Endosome maturation. *EMBO Journal*, 30(17), 3481–3500.

Hussain, N.K., Diering, G.H., Sole, J., et al. (2014). Sorting Nexin 27 regulates basal and activity-dependent trafficking of AMPA receptors by binding to the GluA1 subunit. *Neuron*, 82(2), 441–454.

Jia, D., Gomez, T.S., Metlagel, Z., et al. (2012). WASH and WAVE actin regulators of the Arp2/3 complex in endosomal trafficking. *Small GTPases*, 3(4), 226–230.

Kennedy, M.J., & Ehlers, M.D. (2006). Organelles and trafficking machinery for postsynaptic plasticity. *Annual Review of Neuroscience*, 29, 325–362.

Lauffer, B.E.L., Melero, C., Temkin, P., et al. (2010). SNX27 mediates PDZ-directed sorting from endosomes to the plasma membrane. *Journal of Cell Biology*, 190(4), 565–574.

Li, J., et al. (2016). Endocytic recycling and neurodevelopmental disorders. *Neuron*, 91(4), 857–872.

Loo, L.S., Tang, N., Al-Haddawi, M., et al. (2014). A role for sorting nexin 27 in AMPA receptor trafficking. *Nature Communications*, 5, 3176.

Mao, L., Nie, H., Cai, Q., et al. (2021). Structural insights into SNX27–Retromer assembly and endosomal cargo recycling. *Cell Reports*, 34(13), 108880.

Maxfield, F.R., & McGraw, T.E. (2004). Endocytic recycling. *Nature Reviews Molecular Cell Biology*, 5(2), 121–132.

McDonald, F.J. (2020). Explosion in the complexity of membrane protein recycling. *American Journal of Physiology – Cell Physiology*, 320, C483–C495.

McGough, I.J., Steinberg, F., Jia, D., et al. (2014). Retromer binding to FAM21 and the WASH complex are perturbed by the Parkinson disease-linked VPS35(D620N) mutation. *Journal of Neuroscience*, 34(26), 8538–8547.

McMillan, K.J., Korswagen, H.C., & Cullen, P.J. (2021). The emerging role of Retromer in neuroprotection. *Nature Reviews Neuroscience*, 22, 289–304.

McNally, K.E., Faulkner, R., Steinberg, F., et al. (2017). Retriever is a multiprotein complex for retromer-independent endosomal cargo recycling. *Nature Cell Biology*, 19, 1214–1225.

Park, M., & Goda, Y. (2016). Integrins in synapse regulation. *Nature Reviews Neuroscience*, 17(11), 745–756.

Park, M., Salgado, J.M., Ostroff, L., et al. (2006). Plasticity-induced growth of dendritic spines by exocytic trafficking from recycling endosomes. *Neuron*, 52(5), 817–830.

Park, M., Penick, E.C., Edwards, J.G., et al. (2004). Recycling endosomes supply AMPA receptors for LTP. *Science*, 305(5692), 1972–1975.

Phadke, R.A., Brack, A., Fournier, L.A., et al. (2025). The schizophrenia risk gene C4 induces pathological synaptic loss by impairing AMPAR trafficking. *Molecular Psychiatry*, 30(2), 796–809.

Phillips-Krawczak, C.A., Singla, A., Starokadomskyy, P., et al. (2015). COMMD1 is linked to the WASH complex and regulates endosomal trafficking of the copper transporter ATP7A. *Molecular Biology of the Cell*, 26(1), 91–103.

Rehmann, H., Wittinghofer, A., & Bos, J.L. (2013). A role of CCDC22 in Ritscher-Schinzel syndrome. *Human Molecular Genetics*, 22(6), 1249–1257.

Rivero-Ríos, P., et al. (2023). Recruitment of the SNX17-Retriever recycling pathway regulates synaptic function and plasticity. *J Cell Biol*. doi: 10.1083/jcb.202207025.

Rochefort, N.L., & Konnerth, A. (2023). Dendritic spines in learning and memory: From first discoveries to insights. *Progress in Neurobiology*, 219, 102388.

Saitoh, F. (2022). Endosomal trafficking defects in neurodegeneration. *Neuron*, 110(14), 2283–2300.

Seaman, M.N. (2004). Cargo-selective endosomal sorting for retrieval to the Golgi requires Retromer. *Journal of Cell Biology*, 165(1), 111–122.

Seaman, M.N., Marcusson, E.G., Cereghino, J.L., & Emr, S.D. (1998). Endosome to Golgi retrieval of the vacuolar protein sorting receptor requires the VPS29, VPS30, and VPS35 gene products. *Journal of Cell Biology*, 142(3), 665–681.

Segal, M., & Korkotian, E. (2014). Dendritic spines: The locus of structural and functional plasticity. *Physiological Reviews*, 94(1), 141–188.

Simonetti, B., & Cullen, P.J. (2019). Actin-dependent endosomal receptor recycling. *Nature Reviews Molecular Cell Biology*, 20(9), 517–532.

Small, S.A., & Petsko, G.A. (2015). Retromer in Alzheimer disease, Parkinson disease and other neurological disorders. *Nature Reviews Neuroscience*, 16(3), 126–136.

Sorkin, A., & von Zastrow, M. (2009). Endocytosis and signalling: Intertwining molecular networks. *Nature Reviews Molecular Cell Biology*, 10(9), 609–622.

Starokadomskyy, P., et al. (2013). CCDC22 deficiency in humans leads to impaired WASH complex function and developmental defects. *Nature Immunology*, 14(8), 735–743.

Steinberg, F., Gallon, M., Winfield, M., et al. (2013). A global analysis of SNX27–Retromer cargo reveals a function in glucose and metal ion transport. *Nature Cell Biology*, 15(5), 461–471.

Stockinger, W., et al. (2002). The PX-domain protein SNX17 interacts with members of the LDL receptor family and modulates endocytosis of the LDL receptor. *EMBO Journal*, 21(15), 4259–4267.

Südhof, T.C. (2021). The cell biology of synapse formation. *Journal of Cell Biology*, 220(7), e202103052.

Teasdale, R.D., & Collins, B.M. (2012). Insights into the PX (phox-homology) domain and SNX (sorting nexin) family. *Biochemical Journal*, 441(1), 39–59.

Temkin, P., Lauffer, B., Jäger, S., et al. (2017). SNX27 mediates PDZ-directed sorting from endosomes to the plasma membrane. *Neuron*, 96(4), 873–887.

van Kerkhof, P., et al. (2005). Sorting nexin 17 facilitates LRP recycling in the early endosome. *EMBO Journal*, 24(16), 2851–2861.

van Oostrum, M., Gschewtsch, A., et al. (2020). Proteomics of endocytic recycling at synapses. *Cell Reports*, 30(4), 1178–1191.

Vilariño-Güell, C., Wider, C., Ross, O.A., et al. (2011). VPS35 mutations in Parkinson disease. *American Journal of Human Genetics*, 89(1), 162–167.

von Bohlen und Halbach, O. (2009). Dendritic spine: A crucial structure for learning and memory. *Progress in Brain Research*, 175, 161–182.

Wang X, Zhao Y, Zhang X., et al. (2013). Loss of sorting nexin 27 contributes to excitatory synaptic dysfunction by modulating glutamate receptor recycling in Down's syndrome. *Nature medicine*. 19:473–480. doi: 10.1038/nm.3117.

Wang X, Huang T, Zhao Y., et al. (2014). Sorting nexin 27 regulates Aβ production through modulating γ-secretase activity. *Cell Rep*. 2014 Nov 6;9(3):1023-33. doi: 10.1016/j.celrep.2014.09.037.

Welz, T., Wellbourne-Wood, J., & Kerkhoff, E. (2014). Orchestration of cell surface proteins by Rab11. *Trends in Cell Biology*, 24(7), 407–415.

Zech, T., et al. (2011). The WAVE2 complex is required for lamellipodia formation and motility in migrating cells. *Journal of Cell Science*, 124(19), 3433–3442.

Chapter 2 Dual Endomembrane Recycling Pathways Function in Parallel to Support Synapse Maintenance and Plasticity

2.1 Abstract

The SNX27-Retromer and more recently discovered SNX17-Retriever complexes are key drivers in recycling internalized cargoes back to the cell surface in eukaryotic cells, but the extent to which these pathways have unique or redundant roles in neurons is not known. Here, we show similar, but non-overlapping, roles of the SNX17-Retriever and SNX27-Retromer pathways in the maintenance and plasticity of excitatory synapses. We find that *in vivo* disruption of either pathway in developing rats leads to a marked loss of excitatory synapses in CA1 pyramidal neurons, a phenotype that is recapitulated in cultured hippocampal neurons. Further analysis in cultured neurons confirms that SNX17 and SNX27 colocalize prominently with each other and Retriever/Retromer in early endosomes, indicating a largely shared cellular localization of the two pathways. Interestingly, coordinate disruption of both pathways produced an additive loss of excitatory synapses, suggesting parallel roles in synapse maintenance. We further show that certain cargoes are specific for each pathway and that both recycling pathways are essential for numerous forms of synaptic plasticity, including long-term potentiation (LTP), long-term depression (LTD), and homeostatic synaptic scaling. Together, our results support a model where the SNX17-Retriever and SNX27-Retromer pathways function largely in parallel at synapses, with their combinatorial action a key requirement for long-lasting forms of synaptic plasticity.

2.2 Introduction

Excitatory synapses in the hippocampus are highly dynamic structures that depend on the regulated trafficking of cell-surface proteins to support synaptic signaling, structural plasticity,

Chavis GD, Rivero-Ríos P, Uygun T, Tsukahara T, Hayami T, Lee GY, Lee M, Pace C, Czesak FN, Hilde KL, Li F, Iwase S, Murphy GG, Morrow JD, Akil H, Weisman LS, Sutton MA. (2025). Dual endomembrane recycling pathways function in parallel to support synapse maintenance and plasticity. *Neuroscience*. 15;591:205-221. doi: 10.1016/j.neuroscience.

and memory formation. Endocytic recycling, in which internalized surface proteins are routed back to the plasma membrane, is a key mechanism by which neurons control the composition of surface receptors, adhesion molecules, and transporters in response to synaptic activity (Diering and Huganir, 2018; van Oostrum et al., 2020). Disruptions in protein recycling impair synaptic plasticity and have been linked to neurodevelopmental and neurodegenerative disorders (Li et al., 2016; McDonald, 2020; Saitoh, 2022; Li et al., 2016; Collins and Cullen, 2025).

The SNX27-Retromer and SNX17-Retriever pathways have been described in eukaryotic cells and mediate routes of cargo retrieval from endosomes to the plasma membrane. The better characterized SNX27- Retromer pathway mediates the retrieval of over 200 transmembrane proteins in neurons, including neurotransmitter receptors, ion channels, and signaling receptors (McMillan et al., 2021). SNX27 (Sorting Nexin 27) contains a PDZ domain that enables selective cargo recognition and facilitates recycling by interacting with the trimeric core Retromer complex (VPS35, VPS26A/B, VPS29), and the actin remodeling WASH complex (Steinberg et al., 2013; Harbour et al., 2012; Mao et al., 2021). A key SNX27 cargo in hippocampal neurons is the AMPA-type glutamate receptor (AMPAR), and SNX27 Retromer-dependent AMPAR recycling is essential for synaptic potentiation and plasticity (Loo et al., 2014; Hussain et al., 2014; McMillan et al., 2021; Temkin et al., 2017). In contrast, SNX17 (Sorting Nexin 17) and the Retriever complex has been shown to define a distinct recycling pathway that is independent of SNX27 and Retromer (McNally et al., 2017); however, there are only a handful of studies that have assessed this separate recycling pathway in neurons. SNX17 is a PX-FERM domain containing protein that recognizes NPXY/NXXY motifs in the cytoplasmic tails of its cargoes and requires the Retriever complex (VPS35L, VPS26C, VPS29), the CCC complex, and the WASH complex for cargo retrieval (McNally et al., 2017; Simonetti and Cullen, 2019). In non-neuronal cells, SNX17 regulates the surface levels of numerous adhesion molecules and transporters (McNally et al., 2017; Chen et al., 2019), but its neuronal cargoes are less well defined. Recent work has identified β1-integrin as a key SNX17 cargo in hippocampal neurons, where its recycling is required for long-term potentiation of synapse strength (Rivero-Ríos et al., 2023).

Despite their independent cargo profiles and molecular machinery, both SNX17-Retriever and SNX27-Retromer pathways are crucial for maintaining excitatory synapse function (Rivero Rios et al., 2023; Asadzadeh et al., 2022; Phadke et al., 2025). However, the differential contributions of the two pathways to hippocampal synaptic plasticity, as well as the potential for convergence or coordination in response to neuronal activity, remain largely unexplored. Here, we investigate the roles of each pathway in supporting excitatory synapse integrity and plasticity in hippocampal neurons. We show that both the SNX17- Retriever and SNX27-Retromer pathway are essential for maintaining excitatory synapses in CA1 pyramidal neurons and in cultured hippocampal neurons. Importantly, disrupting both pathways produces additive effects on synapse loss, demonstrating that each act in parallel for synapse maintenance. In addition, we demonstrate that certain cargoes are specific for each pathway and that both recycling pathways are essential for numerous forms of synaptic plasticity, including long-term potentiation (LTP), long-term depression (LTD), and homeostatic synaptic scaling. Together, our results support a model where the SNX17- Retriever and SNX27-Retromer pathways function largely in parallel at synapses, with their combinatorial action a key requirement for long-lasting forms of synaptic plasticity.

2.3 Materials and methods

Subjects

Pregnant Female Sprague Dawley rats, purchased from Charles River Laboratories, were housed on a 12hr light–dark cycle and had food and water available ad libitum. Neonatal rat pups (P0-1) of either sex were used to generate primary hippocampal neuron cultures, while P8-10 pups of both sexes were used for stereotaxic delivery of AAV vectors into hippocampus. All procedures were in accordance with the Guide for the Care and Use of Laboratory Animals from the National Institutes of Health and were approved by the University Committee on the Use and Care of Animals (PRO00012210; University of Michigan; Ann Arbor, MI).

Stereotaxic surgery

Surgeries were performed under aseptic conditions. Anesthesia was induced with 5% isoflurane (Fluriso VetOne) in an induction chamber, then maintained with 1–2.5% isoflurane during surgery. Rats received carprofen (5 mg/kg, s.c.) for analgesia and were mounted in a

KOPF model 942 stereotaxic frame with a heating pad. The surgical area was prepared with betadine followed by 70% alcohol as an antiseptic. The skull was leveled and small holes were drilled at the following coordinates (relative to Bregma) to target the CA1 region for infusion: AP -3.0; LH ±2.2. 5 µl Hamilton syringes were lowered to DV -2.3 and 0.4 µl of virus was infused at 100 nl/min with a UMP3T microinjection syringe pump (World Precision Instruments). Each animal received unilateral infusions of control AAV9 SCR shRNA along with AAV9 SNX17 or SNX27 shRNA on the contralateral side. After completion of the surgery, the incision was closed with surgical glue and rats monitored for 30 min in a recovery chamber with a heating pad and bedding from the home cage. Rat pups were returned to the home cage once fully aware and ambulatory. During the 14-day recovery period, animals were monitored daily to ensure proper healing of surgical wounds and for any sign of distress.

Perfusions and cryosectioning

14 days post-surgery, rats were deeply anesthetized with an intraperitoneal injection of 100 mg/kg pentobarbital and transcardially perfused through left ventricle with ~200 mL of ice-cold saline solution, followed by ~200 mL of ice cold 4% paraformaldehyde (diluted in 1XPBS). Brains were then extracted and post-fixed overnight in 4% formaldehyde at 4˚C. Brains were cryoprotected over three nights in sucrose solution (30%, dissolved 1XPBS) at 4˚C. Following cryo-protection, brains were encased in Tissue-Plus O.C.T. (Fisher Healthcare), frozen using dry ice in methanol butanol and subsequently sectioned in the coronal plane (50 µm) using a cryostat (Leica CM 1860). Brain slices containing the hippocampus were collected and mounted onto SuperFrost Plus microscope slides (Fisher Scientific, #1255015) with antifade mounting medium (VectarShield, #H-1200), cover slipped (Fisher Scientific, #12541042) and stored at -20˚C until imaging

DNA constructs and site-directed mutagenesis

For knockdown experiments, we used the following shRNA lentiviral plasmids: SNX17 (pLKO.1-puro with shRNA target sequence 5′-CCAGATGACTTGATCGGATAT-3′, TRCN0000190340, Millipore Sigma); SNX27 (pLKO.005-puro with shRNA target sequence 5′-GAACCAGGTAATAG-3′, TRCN0000253473, Millipore Sigma); VPS26C (pGIPZ vector with shRNA target sequence 5′-GAGT-3′, V3LMM_455807, Horizon Discovery), VPS26B

(pLKO.005- puro with shRNA target sequence 5′-TGCAGCCTAGGTAGGGATAAG-3′, TRCN0000306336, Millipore Sigma); and scrambled control (MISSION pLKO.1 scrambled non-target shRNA SHC002, Millipore Sigma). The constructs mNeonGreen-SNX17 and the shRNA-resistant variant of SNX17 were previously described (Rivero-Ríos et al., 2023). For GFP- SNX27, the SNX27 coding sequence was amplified from rat whole brain cDNA using primers 5′-CGCTCGCTTACTCGCAAGA-3′ and 5′-GCTAAGAGGCTGAGGGCAAA-3′. A synthetic GFP fragment with an 18 bp GS linker and a 5′ KpnI site was obtained from Twist Bioscience. To produce overlapping sequences for assembly, SNX27 was re-amplified using primers 5′-CAGGGGGTGGAAGCGGTGGTGCGGACGAGGACGGGGAA GGG-3′ and 5′-CAC-3′. The expression vector pCDNA4:TO (Rivero-Ríos et al., 2023) was digested with ApaI and KpnI and assembled with the SNX27 and GFP fragments using NEBuilder HiFi DNA Assembly (New England Biolabs), yielding pTO-GFP-SNX27. To make this construct resistant to SNX27 shRNA, six silent mutations were introduced into the target site (5′-AGCTGGAGAACCAGGTAATAG-3′) using two rounds of Q5 Site- Directed Mutagenesis (New England Biolabs). The first round (primers: 5′-CAGGTAATAGCGTTTGAATGGGATGAGATGC-3′ and 5′-GTTTTCAAGTTGCCCTTCTTCAGTGCAGG-3′) yielded an intermediate sequence (5′-AACTTGAAAACCAGGTAATAG-3′), and the second round (primers: 5′-CAAGTGATAGCGTTTGAATGGGATGAGATGC-3′ and 5′-ATTTTCAAGTTGCCCTTCTTCAGTGCAGG-3′) completed the mutation to 5′-AACTTGAAAATCAAGTGATAG-3′, resulting in pCDNA4:TO-GFP- SNX27-R. To generate mNeonGreen-SNX17, the region containing the GS linker and SNX27 was PCR-amplified from pTO-GFP-SNX17 using primers 5′-CAAGGAATTCGGGGGCGGTTCAGGGGGT-3′ and 5′-TATCGATAAGCTTGATATCGACCGGTTTACAGATCCTCATCTCCAATGCC-3′, which add restriction sites for EcoRI an AgeI at 5′ and 3′, respectively. mNeonGreen was PCR-amplified from a modified pAAV vector, pAAV- eno-mNeonGreen (Rivero-Ríos et al., 2023), using the oligos 5′- CCGCCACTACCACCGGGTACGGTACCGCCACCATGGTG-3′ and 5′-AACC GCCCCCGAATTCCTTGTACAGCTCGTCC-3′ to delete the stop codon and add an EcoRI site at the 3′ end. Note that the mNeonGreen fragment contains a KpnI site at 5′. Both PCR products were digested with the corresponding restriction enzymes and purified. pAAV-eno- mNeonGreen was digested with KpnI and EcoRI to release the mNeonGreen fragment, and

the purified vector was used for the ligation reaction. This generated the pAAV-eno-mNeonGreen-SNX17.

To generate mScarlet-tagged SNX27, the SNX27 fragment with the GS linker was PCR-amplified from pTO-GFP-SNX27 using primers incorporating EcoRI and AgeI restriction sites (5′-CAAGGAATTCGGGGGCGGTTCAGGGGGT-3′ and 5′-TATCGACCGGTCTAGGTGGCCACATCC-3′). The mScarlet2 coding region was synthesized by Twist Bioscience and amplified with primers introducing NheI and EcoRI sites (5′-CACCGGGTACCGCTAGCGCCACCATGGTG-3′ and 5′-GAATTCCTTGTACAGCTCGTCC-3′). After digestion and purification, the mNeonGreen insert was excised from pAAV-eno-mNeonGreen using KpnI and EcoRI, and the vector backbone was ligated with the mScarlet and SNX27 fragments to generate pAAV-eno-mScarlet- SNX27.

To produce mNeonGreen-VPS35, the VPS35 coding sequence was amplified from rat brain cDNA with oligos 5′-GAGTAGGCGCTGCTGCTTG-3′ and 5′-TGTCTGGAGGTGCTGGGTAA-3′, and cloned into a GFP-tagged pTO backbone using primers 5′-taagcttggtaccATGCCTACAACACAGCAATC-3′ and 5′-ccacccccctgaaccgc ccccAAGGATGAGACCTTCATAGATTG-3′. The construct was then subcloned into a pAAV vector under the neuron-specific enolase (NSE) promoter by amplifying VPS35 with primers 5′-tacGCCACCATGCCTACAACACAGC-3′ and 5′-ACCATGGTGGCGGTACCC GTACCACCGCTTCCACCCCC-3′. The recipient vector was linearized with KpnI and assembled with the insert using NEBuilder HiFi DNA Assembly.

To generate mScarlet-VPS35L, VPS35L was PCR-amplified from rat cDNA with primers 5′-GATCATGTGACTGGGAAGATGG-3′ and 5′- TGTCAATTCCCCTTCCGTCAG-3′, followed by amplification with primers 5′-tttaaacttaagcttggtaccATGGCTGTCTTTCCCTGG-3′ and 5′- CCACCCCCTGAACCGCCCCCAGTCCTGGTTTGCAGAGG-3′ for NEBu ilder HiFi DNA assembly into a linearized pTO vector. VPS35L was then subcloned into a modified pAAV vector by PCR (primers: 5′-taccaccgggtaccGCCACCATGGCTGTCTTTCC-3′ and 5′-CTGCCTCGCCC TTGCTCACGCTAGCACCACCGCTTCCACCCCC-3′). The

mScarlet fragment (Twist Bioscience) and the vector backbone (from pAAV-eno- mNeonGreen, digested with KpnI and EcoRI) were assembled using NEBuilder.

DNA was prepared from bacterial cultures grown at 37˚C using a Maxiprep kit (Endofree Plasmid Maxiprep System, QIAGEN) according to the manufacturer's instructions. In all cases, the identity of the constructs was verified by sequencing the entire coding region.

AAV9 and lentiviral vectors

AAV9 and Lentiviral transduction-ready viral particles were produced for SNX17, SNX27 and scramble shRNAs by the University of Michigan Vector Core with a concentration of 10^7 transduction units per ml. For lentivirus infection, neurons were infected on DIV7 at an MOI of 2, without polybrene. After overnight incubation, the virus-containing medium was replaced with conditioned medium. Experiments were performed 7 days after lentivirus transduction.

Cell culture and transfection

Dissociated hippocampal or cortical neuron cultures from P0–2 rat pups of either sex were prepared as previously described (Henry et al., 2018). Hippocampal neurons were plated at a density of 230–460 mm^2 in poly-D-lysine-coated 35-mm glass-bottom Petri dishes (Mattek), while cortical neurons were seeded at 3–4 x10^6 cells/well on 6-well plates (Costar). Neurons were maintained at 37◦C and 5% CO^2 in growth medium (Neurobasal A [Invitrogen] containing 2% B27 [Invitrogen] and 1% Glutamax [Invitrogen]) supplemented with 15% glial conditioned media and 10% cortical conditioned media until DIV14; after DIV14, neurons were maintained in growth medium alone until experiments.

For plasmid transfection, neurons were transfected at DIV12-14 using Lipofectamine 2000 (Invitrogen) according to the manufacturer's recommendations and used 4–5 d after shRNA transfection. For lentiviral delivery of shRNAs, neurons were infected on DIV7 and used for experiments on DIV14.

CRISPR/Cas9 ORANGE

ORANGE was performed as previously described (Willems et al., 2020). The target sequence CTCGCTTACTCGCAAGATGGCGG was chosen based on the MIT guide specificity score and the absence of premature stop codons between the insert and the endogenous SNX27 gene. To generate a knock-in construct, the pORANGE cloning template vector was purchased from Addgene (plasmid 131471). Oligos containing the target sequences (caccgCTCGCTTACTCGCAAGATGG and cGAGCGAATGAGCGTTCTACCcaaa) were annealed and ligated into the BbsI sites of pORANGE. A synthetic gene containing the mScarlet insert flanked by two Cas9 target sites identical to the genomic target site was purchased from Twist Bioscience and inserted into the pOrange restriction sites HindIII and XhoI. Hippocampal neurons were transfected at DIV3 with 1ug of the template vector using Lipofectamine 2000 and maintained at 37°C and 5% CO^2 for 2 weeks before fixation and imaging.

Electrophysiology

Whole-cell patch-clamp recordings of mEPSCs were made with a MultiClamp 700B amplifier from hippocampal neurons bathed in HEPES-buffered saline (HBS; 119 mM NaCl, 5 mM KCl, 2 mM $CaCl_2$, 2 mM $MgCl_2$, 30 mM glucose, 10 mM HEPES [pH 7.4]) plus 1 µM TTX and 10 µM bicuculline. The pipette internal solution contained 100 mM cesium gluconate, 0.2 mM EGTA, 5 mM $MgCl_2$, 40 mM HEPES, 2 mM Mg-ATP, 0.3 mM Li-GTP, and 1 mM QX314 (pH 7.2) and had a resistance of 4–6 MΩ. mEPSCs were recorded from a holding potential of –70 mV and analyzed offline using MiniAnalysis (Synaptosoft) and Clampfit (Molecular Devices). For induction of chemical LTP (cLTP), growth media was removed, and neurons were subjected to a brief 5-min exposure to a Mg^{2+}free HBS solution supplemented with 0.4 mM Glycine (Thermo Fisher Scientific), 0.02 mM Bicuculline (Abcam), and 0.003 mM Strychnine (Tocris). Neurons were then washed and maintained in HBS for 20–60 min prior to recordings. To induce synaptic scaling, neurons were treated with either 1 µM TTX or vehicle (0.1% v/v distilled H_20) in growth media for 24 hr prior to recording. For chemical induction of LTD (cLTD), neurons were exposed to a brief 5-min exposure to 20 µM NMDA (Sigma-Aldrich) in HBS, washed, then returned to regular HBS for 20–60 min prior to recordings. To determine the effect of ß1-integrin on LTP and LTD, cells were treated with function-blocking anti-ß1-integrin monoclonal antibodies (MAB1987Z; Millipore Sigma) or IgG2a isotype control antibodies (MABC004; Millipore Sigma) at a concentration of 10 µg/ml 30 min prior to LTP/LTD

stimulation; antibodies were also present throughout the post- stimulation interval until recording 20–60 min post-LTP/LTD.

Immunocytochemistry

Neurons were fixed with 4% paraformaldehyde/4% sucrose in phosphate-buffered saline (PBS) with 1 mM $MgCl_2$ and 0.1 mM $CaCl_2$ (PBS-MC) for 15 min, permeabilized with 0.1% Triton X-100 for 10 min and blocked with 2% BSA for 1 hr. Neurons were then incubated with primary antibody in blocking buffer overnight followed by 3X 5 min washes in PBS-MC and incubation with secondary antibodies for 1 hr. The primary antibodies used were: goat anti-VPS35 (1:200; Abcam, ab10099), mouse anti-EEA1 (1:200; Cell Signaling, 48453), and rabbit anti-VPS35L (1:200; kindly provided by Dr. Daniel D. Billadeau, previously described in Phillips-Krawczak et al., 2015). To label surface GluA1 in the recycling assays, neurons were incubated live with 30 µg/ ml dilution of GluA1 primary antibody (#ABN241, Millipore) for 15 min at 37˚C, washed 2X with warm PBS-MC, and returned to conditioned media for 60 min to allow labeled GluA1 internalization to occur. Neurons were then live labeled with Goat Anti-Rabbit Alexa Fluor 555 (#A21429, Invitrogen, 1:250) secondary antibody for 10 min, washed 2X with warm PBS-MC, followed by saturating labeling with unconjugated Goat Anti-Rabbit IgG (#31210, Invitrogen, 1:50) for 5 min. Neurons were then washed 2X with warm PBS-MC, returned to mentioned media for 0, 30, or 60 min at 37˚C prior to fixation. Neurons were fixed with 4% paraformaldehyde/4% sucrose in PBS-MC for 15 min, washed, then blocked with 2% BSA in PBS-MC solution for 60 min. After blocking, Goat Anti-Rabbit Alexa Fluor 488 (#A11034, Invitrogen, 1:250) was applied in 2% BSA for 1 hr to label recycled GluA1. Cells were washed 3X for 5 min with PBS-MC, then maintained in PBS-MC until imaging (within a week).

Image acquisition and analysis

Images were acquired with either an Olympus FV1000 or Leica Stellaris 5 laser-scanning confocal microscope systems with a Plan- Apochromat 63 ×/1.4 oil objective. Z-stacks were captured at 0.4 µm intervals with sequential single-wavelength excitation. The same laser settings and acquisition parameters were used for all treatment conditions in individual experiments. Images were analyzed and processed using Image J.

Dendritic spine numbers were quantified manually by an observer blind to the experimental conditions in 30 μm segments of dendrites after the first dendritic branchpoint. Spine morphology classification followed the criteria described by Henry et al. (2017). The Image J line tool was used to measure head diameter, spine length, and neck width. Filopodia are defined as protrusions with a length of at least 5 μm. Mushroom spines are defined as a head-to-neck ratio equal to or greater than 2.5. Flat spines are defined as a head width to length ratio of at least 1. Thin spines are defined as a length-to-neck width ratio greater than or equal to 3. A spine that does not satisfy any of the previous conditions is considered a stubby spine. The class of each spine is determined by checking against these conditions sequentially. The JACoP plugin of ImageJ was used to quantify the colocalization between components of the SNX17-Retriever and SNX27-Retromer pathways or with the endolysosomal markers EEA1 and LAMP1. Manders' overlap coefficient was obtained after thresholding the images, and the percentage of colocalization was obtained by multiplying the coefficient by 100. The dendritic shaft and spines were manually segmented in ImageJ to determine the colocalization between mNeonGreen-SNX17 and mScarlet-SNX27 in these regions. To prepare representative images, the brightness and contrast were adjusted uniformly over all images of the respective assays using Image J.

Western Blot

Neurons were collected in lysis buffer containing 100 mM NaCl, 10 mM $NaPO_4$, 10 mM $Na_4P_2O_7$, 10 mM lysine, 5 mM EDTA, 5 mM EGTA, 50 mM NaF, 1 mM $NaVO_3$, 1% Triton-X, 0.1% SDS, and 1 tablet Complete Mini protease inhibitor mixture (Sigma, #118361153001), pH 7.4. Protein concentrations in each sample were determined with a modified Lowry assay (DC Protein Assay kit, BioRAD). Equal amounts of protein for each sample were loaded and separated on 4–20% gradient gels (mini-Protean TGX gels, #4561094), then transferred to PVDF membranes. Blots were blocked with Tris-buffered saline containing 0.1% Triton-X (TBST) and 5% nonfat milk for 120 min at room temperature, and incubated with rabbit or mouse polyclonal primary antibodies overnight at 4°C (Rabbit Anti-SNX27, 1:1000, Abcam #ab241128, Rabbit Anti-SNX17, 1:1000, Atlas HPA043867, Mouse Anit-β-Tubulin, Sigma, 1:2000, T6074). After washing with TBST, blots were incubated with HRP-conjugated Goat anti-rabbit or Goat anti-mouse secondary antibody (1:2000; Invitrogen), followed by enhanced chemiluminescent

detection (BioRAD). After probing for SNX17 or SNX27, blots were stripped and re-probed with a mouse monoclonal antibody against β-tubulin to confirm equal loading. Band intensity was quantified with ImageJ Fiji and normalized to β-tubulin protein levels relative to SCR.

Statistical analysis

All experiments were repeated at least three times. Statistical tests and the size of the samples are described in the respective figure legends. Data distribution was assumed to be normal, but this was not formally tested. Unless stated otherwise, statistical differences between groups were made using unpaired Student's t-test (2 groups) or one-way Analysis of Variance (ANOVA) with Fisher's LSD posthoc tests (>2 groups). All comparisons were 2-tailed. Data were plotted and analyzed using Microsoft Excel and GraphPad Prism 10.

2.4 Results

2.4.1 Synapse loss after disruption of SNX17-Retriever/SNX27-Retromer pathways in vivo

Endomembrane recycling of surface proteins in neurons has been studied primarily in the context of the SNX27-Retromer pathway, with only a handful of studies examining the more recently identified SNX17- Retriever pathway. Rivero-Rios et al. (2023) reported that acute knockdown of SNX17 or Retriever subunits in cultured hippocampal neurons led to a ~40% loss of dendritic spines and functional excitatory synapses in cultured hippocampal neurons. Likewise, Cui et al. (2024) found impaired excitatory synaptic function in CA1 pyramidal neurons of 60-day old SNX17 heterozygous knockout mice (homozygous SNX17 mice are early embryonic lethal), though the deficit in this case was due to impaired spine maturation, without a change in synapse density. The unique nature of the synaptic changes observed in the two studies could be due to differences in the manner of SNX17 depletion (acute vs constitutive), species (rats vs mice), developmental state, or *in vitro* vs *in vivo* context. To distinguish between these possibilities, we performed stereotaxic microinfusion of AAV9 vectors expressing shRNA against SNX17 into the CA1 area of P8-10 rats to examine the impact of acute SNX17 depletion *in vivo*. These infusions were unilateral, with the contralateral side receiving AAV9 expressing scrambled (scr) shRNA as a control. To compare effects with disruption of the SNX27-Retromer

pathway, we employed a similar strategy in parallel with AAV9 vectors expressing SNX27 shRNA (Fig. 1); all vectors expressed mNeonGreen to label infected cells. Dendritic spine

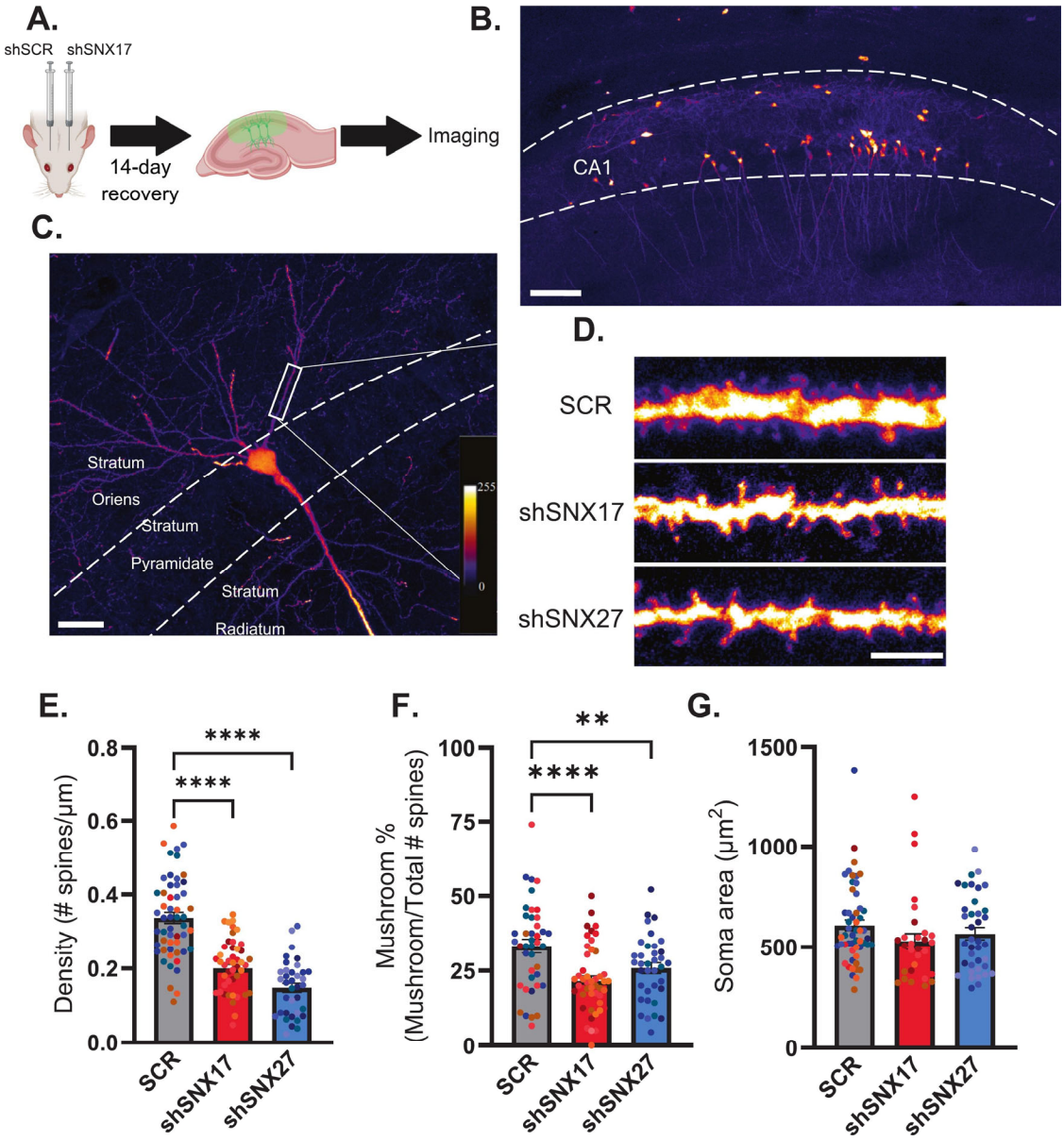


Figure 2.1 Synapse loss after disruption of SNX17-Retriever and SNX27-Retromer pathways *in vivo*

(A). Procedural schematic: Unilateral stereotaxic injections of AAV9 vectors expressing shRNA against SNX17 or SNX27 in hippocampal area CA1 coupled with contralateral infusion of AAV9 vectors expressing scrambled shRNA were made at P8-10, followed by perfusion/fixation 14 days later. mNeonGreen (expressed by all vectors) was imaged by confocal microscopy **(B)**. Representative low power mNeonGreen image of CA1 hippocampal region with injection site at P22. Scale bar =50 µm. **(C)**. Representative high-power image of CA1 pyramidal neuron expressing AAV9-mNeonGreen fluorescent reporter. Scale bar =20 µm. **(D)**. Representative images of dendritic spines in CA1 basal dendrites in each of the indicated treatment conditions. Scale bar =5 µm. **(E–G)**. Mean ±SEM spine density in basal dendrites ($F_{2,136}$ =56.16, p <0.0001) **(E)**, percent spines with mature mushroom morphology ($F_{2,124}$ =10.36, p <0.0001) **(F)**, and soma area ($F_{2,120}$ =0.20, NS) **(G)** in CA1 pyramidal neurons for the indicated conditions. SCR, N =53 neurons; shSNX17, N =50 neurons; shSNX27, N =36 neurons from 7 animals (5 male, 2 female) receiving shSNX17/SCR and 5 animals (3 male, 2 female) receiving shSNX27/SCR. ** P <0.01, ****P

<0.0001 by Fisher's LSD. Data in **(E–G)** from the same animal is reflected with a common shade of red (SNX17 shRNA) or blue (SNX27 shRNA). When neurons from the same condition are averaged into a single value per animal: Mean ±SEM Spines per µm =0.32 ±0.04 (Scr), 0.26 ±0.03 (shSNX17), 0.20 ±0.03 (shSNX27); ($F_{2,18}$ =2.47, p <0.11); Mean ±SEM % Mushroom Spines =32.2 ±2.0 (Scr), 21.2 ±1.2 (shSNX17), 29.1 ±3.1 (shSNX27); $F_{2,18}$ =8.04, p <0.01; Mean ±SEM Soma area (µm^2) =605.1 ±44.7 (Scr), 523.5 ±86.4 (shSNX17), 576.2 ±66.4 (shSNX27); $F_{2,18}$ =0.45, p =0.65. Fig. 1A was created in BioRender. Chavis, G. (2025) https://BioRender.com/izig63v.

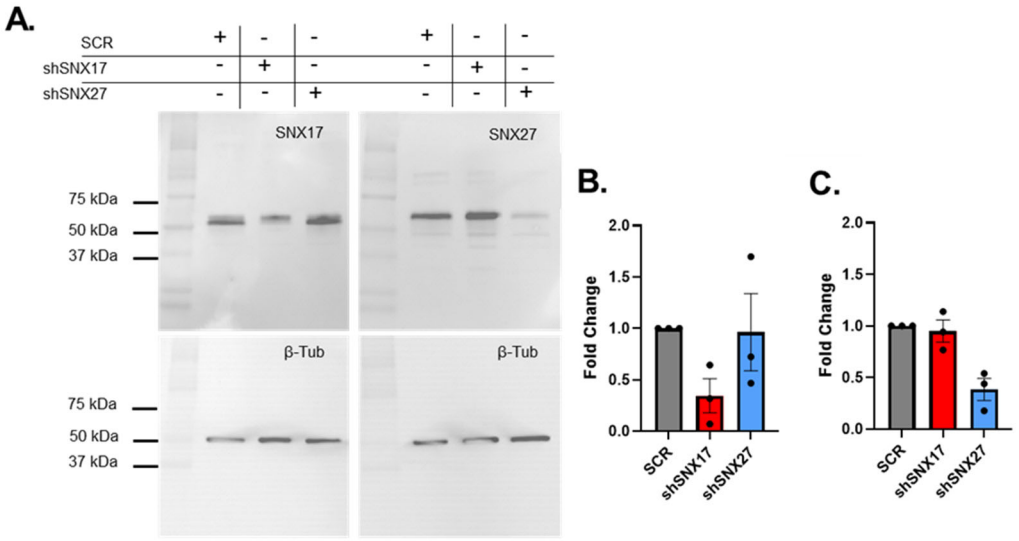


Figure 2.2 Validation of SNX17 and SNX27 shRNAs

(A). Representative Western blots probed for SNX17 (top, left) or SNX27 (top, right) following lentiviral expression of shRNAs against SNX17 or SNX27, or SCR shRNA as a control, as indicated above the blots. Bottom panels show the same blots above that have been stripped and re-probed for β-Tubulin as a loading control. Molecular weight markers are depicted to the left of the blots. **(B).** Mean ± SEM normalized expression of SNX17 (relative to SCR control) for each indicated treatment condition, as measured by densitometry (N = 3 experiments). **(C).** Mean ± SEM normalized expression of SNX27 (relative to SCR control) for each indicated treatment condition, as measured by densitometry (N = 3 experiments).

density in the basal dendrites of CA1 pyramidal neurons was assessed two weeks post- injection using confocal microscopy (Fig. 1A-D). Similar to cultured neurons (Rivero-Rios et al., 2023), our analysis revealed a pronounced reduction in dendritic spine density in SNX17-depleted CA1 pyramidal neurons, which showed a 40% decrease in spine density compared to control neurons expressing SCR shRNA (Fig. 1E). Similarly, AAV9- mediated knockdown of SNX27 expression reduced spine density by 58% in comparison to control neurons (Fig. 1E).

Interestingly, like the SNX17 heterozygous knockout mice (Cui et al., 2024), we found that SNX17 knockdown impaired the maturation of dendritic spines, as these cells exhibited a significantly reduced proportion of dendritic spines that were mature mushroom-like relative to SCR shRNA-expressing neurons; a similar spine maturation deficit was observed with SNX27

knockdown assessed in parallel (Fig. 1F). By contrast, soma areas were indistinguishable across experimental conditions, suggesting no overt changes in neuronal health associated with acute SNX17/27 knockdown (Fig. 1G). These findings highlight the critical role of the SNX17-Retriever and SNX27-Retromer complexes in the maintenance of dendritic spines, suggesting that deficits in the recycling of membrane proteins due to SNX17 or SNX27 disruption have a detrimental effect on spine stability and composition.

2.4.2 SNX17-Retriever and SNX27-Retromer regulate dendritic spine density and morphology in vitro

As both the SNX17-Retriever and SNX27-Retromer pathways appear to be crucial for maintaining excitatory synaptic contacts, we next turned to cultured hippocampal neurons as a more tractable system to explore their localization in neurons and respective roles in controlling other aspects of synaptic function. We first asked whether the spine density and morphology changes we observed *in vivo* would be similarly recapitulated *in vitro*. To also examine the potential cell autonomous nature of these effects, we used a sparse co-transfection strategy (<1% efficiency) with plasmids expressing shRNAs against SNX17 or SNX27 (or SCR control) and those expressing GFP for visualization. As we observed with *in vivo* depletion, SNX17 and SNX27 knockdown each elicited a significant reduction in overall dendritic spine density when compared to control conditions expressing SCR shRNA (Fig. 3A-B). Moreover, the extent of synapse loss was also comparable between in vivo (~40–60%) and in vitro (~50%) experiments, and between SNX17 and SNX27 knockdown conditions in both experiments. We also targeted VPS26C and VPS26B, core subunits of Retriever and Retromer respectively, for knock down with shRNA and saw a comparable loss of dendritic spines (~50–60%, Fig. 4). Also, similar to

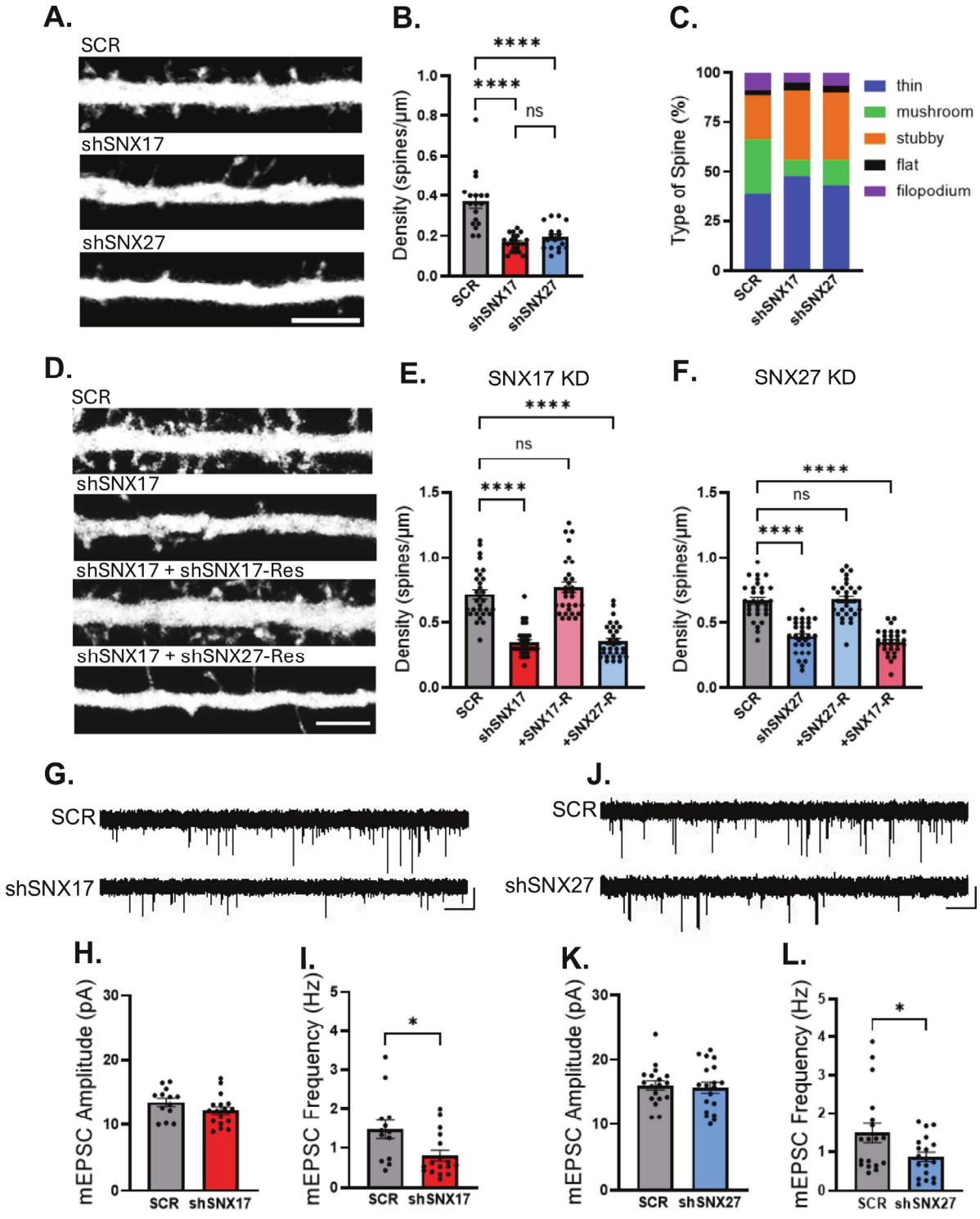


Figure 2.3 SNX17-Retriever and SNX27-Retromer regulate synapse density and morphology *in vitro*

(A). Representative dendritic images of DIV 18–20 primary hippocampal neurons for the indicated conditions. Scale bar = 5 µm. **(B).** Mean ± SEM spine density in neurons expressing the indicated constructs ($F_{2,52} = 27.41$, $p < 0.0001$). SCR, N = 18 neurons, shSNX17, N = 20 neurons, shSNX27, N = 17 neurons. **(C).** Distribution of spine morphology by spine type from the indicated conditions. SCR: Thin = 38.5%, Stubby = 22.7%, **Mushroom = 27.6%**, Filopodium = 8.6%, Flat = 2.6%. shSNX17: Thin = 47.8%, Stubby 35.3%, **Mushroom = 8%**,

Filopodium = 5%, Flat = 4%. shSNX27: Thin = 43.2%, Stubby = 34.4%, **Mushroom = 12.6%**, Filopodium = 6.6%, Flat = 3.3%. The proportion of Mushroom spines was significantly reduced in shSNX17 and shSNX27 conditions relative to SCR control, $F_{2,52} = 10.70$, $p < 0.0001$, Fisher's LSD $p < 0.05$. **(D).** Representative dendrite images of DIV 18–20 primary hippocampal neurons expressing the indicated constructs with SNX17 or SNX27 knockdown (KD) or SCR control. Scale bar = 5 µm. **(E).** Quantification of spine density rescue with indicated constructs following SNX17 KD; "-R" = co-expression of RNAi-resistant SNX17 or SNX27; $F_{3,116} = 54.46$, $p < 0.0001$; N = 30 neurons/group. **(F).** Quantification of spine density rescue with indicated constructs following SNX27 KD; "-R" = co-expression of RNAi-resistant SNX17 or SNX27; $F_{3,116} = 55.85$, $p < 0.0001$; N = 30 neurons/group. **(G, J).** Representative mEPSC recordings in DIV 18–20 hippocampal neurons expressing the indicated constructs. Scale bar = 20 pA, 2s. (**H-I**). Mean ± SEM mEPSC amplitude ($t_{28} = 1.46$, $p = 0.16$) **(H)** and frequency ($t_{28} = 2.59$, $p = 0.02$) **(I)** following SNX17 KD or SCR control; SCR, N = 13 neurons, shSNX17, N = 17 neurons. **(K-L).** Mean ± SEM mEPSC amplitude ($t_{35} = 0.30$, $p = 0.76$) **(K)** and frequency ($t_{35} = 2.26$, $p = 0.03$) **(L)** following SNX27 KD or SCR control; SCR, N = 18 neurons, shSNX27, N = 19 neurons. *P < 0.05, ****P < 0.0001, ns = not significant by Fisher's LSD or unpaired t-test.

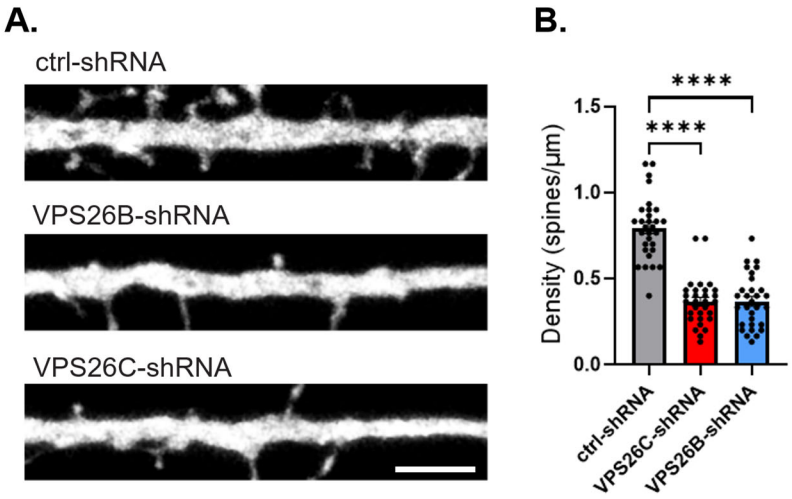


Figure 2.4 Synapse loss following depletion of the core Retriever subunit VPS26C and core Retromer subunit VPS26B

(A). Representative images of DIV 14 hippocampal neurons expressing the indicated constructs along with soluble GFP as a filler. Scale bar = 5 µm. **(B).** Mean ± SEM spine density from the indicated KD conditions. Ctrl-shRNA, N = 30 neurons; VPS26C-shRNA, N = 30 neurons; VPS26B-shRNA, N = 30 neurons ($F_{2,87} = 73.48$, $p < 0.0001$). *P<0.05, ****P<0.0001 by Fisher's LSD.

previous observations (Cui et al., 2024; see also Fig. 1), detailed morphological assessment showed that the percentage of mushroom spines, typically associated with mature synaptic connections, was significantly diminished following SNX17 knockdown, with a corresponding increase in immature morphologies such as stubby and thin spines (Fig. 3C). Again, SNX27 knockdown produced very similar results in spine morphology (Fig. 3C).

To ensure that the shRNA-mediated effects were specific, we also examined whether expression of RNAi-resistant versions of SNX17 and SNX27 could rescue the effects on spine density. We found that reintroducing RNAi-resistant SNX17, but not SNX27, indeed rescued

spine density back to control levels after SNX17 knockdown (Fig. 3D and E), while expression of RNAi-resistant SNX27, but not SNX17, rescued spine density after SNX27 knockdown (Fig. 3F). We also measured functional properties of excitatory synapses, focusing on whole-cell voltage clamp recordings of miniature excitatory postsynaptic currents (mEPSCs). Consistent with loss of functional synapses, we found that both SNX17 (Fig. 3G–I) and SNX27 (Fig. 3J–L) knockdown induced a significant ~50% reduction in mEPSC frequency. mEPSC amplitude, on the other hand, was not significantly altered by either knockdown condition, which is somewhat surprising given the spine maturation phenotype observed in these conditions.

2.4.3 SNX17 and SNX27 localize to the same cellular compartment in neurons

We next examined the relative localization of SNX17 and SNX27 in neurons. We first approached this question by expressing fluorescently tagged recombinant proteins – mNeonGreen-SNX17 and mScarlett- SNX27. Both SNX17 and SNX27 exhibited a punctate pattern of distribution (Fig. 5A) and displayed robust colocalization, with ~70–80% of SNX17 puncta colocalizing with SNX27 puncta, and vice versa (Fig. 5B and C). This close spatial relationship between these two sorting nexins was evident in both dendritic shafts and dendritic spines (~80%, Fig. 5D and E). To ensure that this strong colocalization was not an artifact of overexpression, we measured colocalization between endogenous SNX17 and SNX27. There is a well-validated antibody (Rivero Rios et al., 2023; Osborne et al., 2015) that recognizes endogenous SNX17, but not one suitable for immunocytochemical localization of rodent SNX27. Thus, we used CRISPR/Cas9 based ORANGE (Willems et al., 2020) to tag endogenous SNX27 with mScarlet. Using this approach, we again observed strong co-localization of SNX17 and SNX27 puncta in hippocampal neurons (~80%, Fig. 5F–H). We next examined the subcellular compartment where SNX17 and SNX27 reside. We found that mNeonGreen-SNX17 exhibited prominent colocalization with the early endosomal marker EEA1, and weaker colocalization with the lysosomal marker LAMP1(Fig. 5I and J). A highly similar distribution pattern was observed with mScarlett-SNX27, EEA1, and LAMP1, with SNX27 exhibiting strong colocalization with early endosomes and weaker association with lysosomes (Fig. 5K and L).

Finally, we also found that both recombinant and endogenous VPS35 and VPS35L, core subunits of the Retromer and Retriever complex, exhibited strong colocalization in neuronal

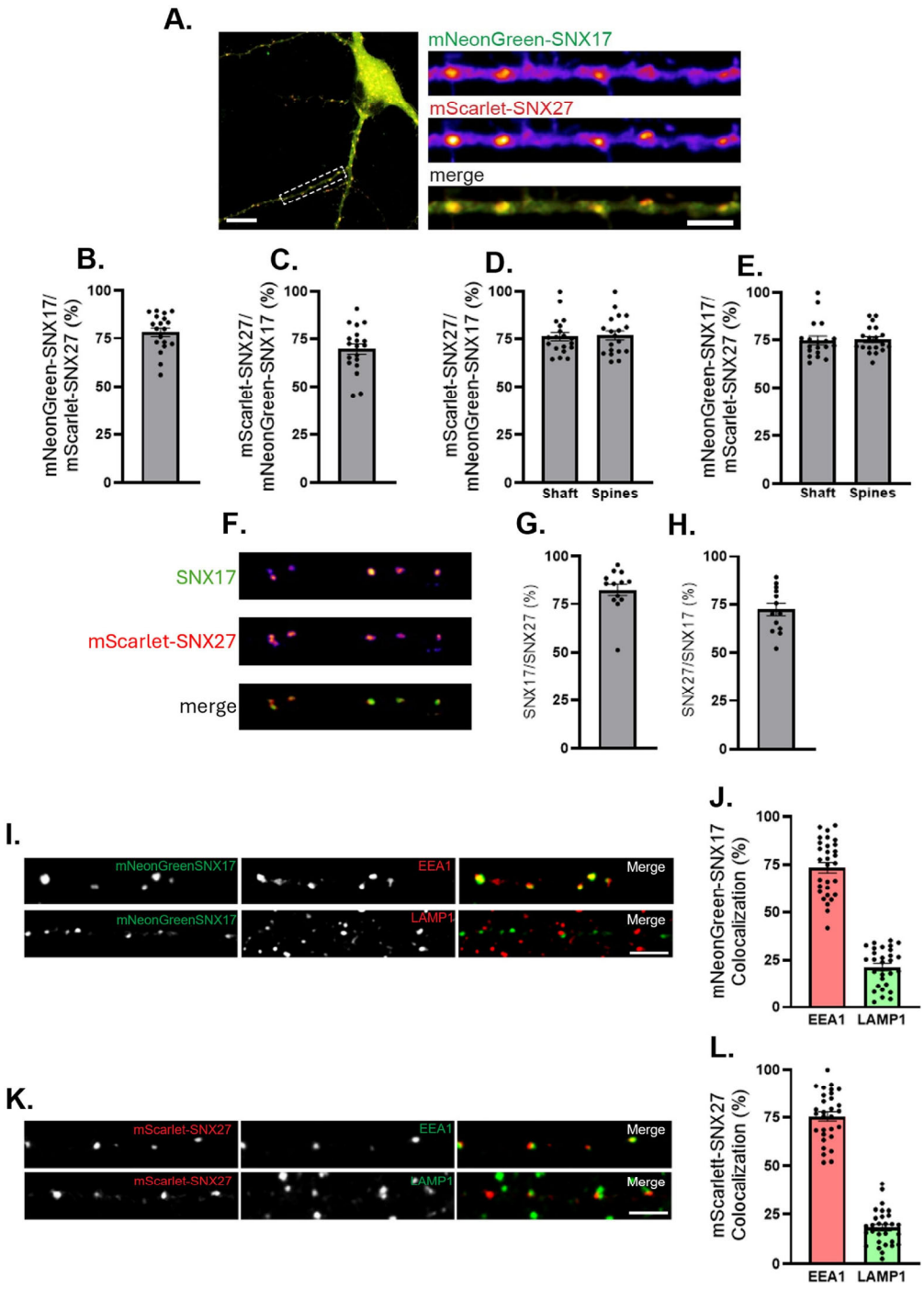


Figure 2.5 SNX17 and SNX27 localize to the same cellular compartment in neurons

(A). Representative images of DIV 18–20 primary hippocampal neurons expressing recombinant mNeonGreen-tagged SNX17 and mScarlet-tagged SNX27. Scale bars = 20 µm (left) and 5 µm (right). **(B-C).** Mean ± SEM percent of (**B**) mNeonGreen-SNX17 colocalized with mScarlet-SNX27, and (**C**) and mScarlet-SNX27 puncta colocalized with mNeonGreen-SNX17; (N = 19). Colocalization = 78.16%, N = 19. **(D-E).** Comparison of colocalization of (**D**) mScarlet-SNX27 with mNeonGreen-SNX17 and, (**E**) mNeonGreen-SNX17 with mScarlet-SNX27 in dendritic shafts vs. spines; N = 19. **(F).** Representative images of DIV 18–20 hippocampal neuron dendrites expressing endogenous SNX27 tagged with mScarlet and immunostained with an antibody against SNX17. Scale bar = 5 µm. (**G-H**) Mean ± SEM percent of (**G**) SNX17 colocalized with mScarlet-SNX27, and (**H**)

and mScarlet-SNX27 puncta colocalized with SNX17; N = 19. **(I).** Representative images of DIV 18–20 hippocampal neuron dendrites expressing mNeonGreen-SNX17 with the early endosome marker EEA1 and the lysosome marker LAMP1. Scale bar = 5 µm. **(J).** Mean ± SEM percent mNeonGreen-SNX17 colocalizing with EEA1 and LAMP1; N = 30/group. **(K).** Representative images of DIV 18–20 hippocampal neuron dendrites expressing mScarlet-SNX27 with the early endosome marker EEA1 and the lysosome marker LAMP1. Scale bar = 5 µm. **(L).** Mean ± SEM percent mScarlet-SNX27 colocalizing with EEA1 and LAMP1; N = 30/group.

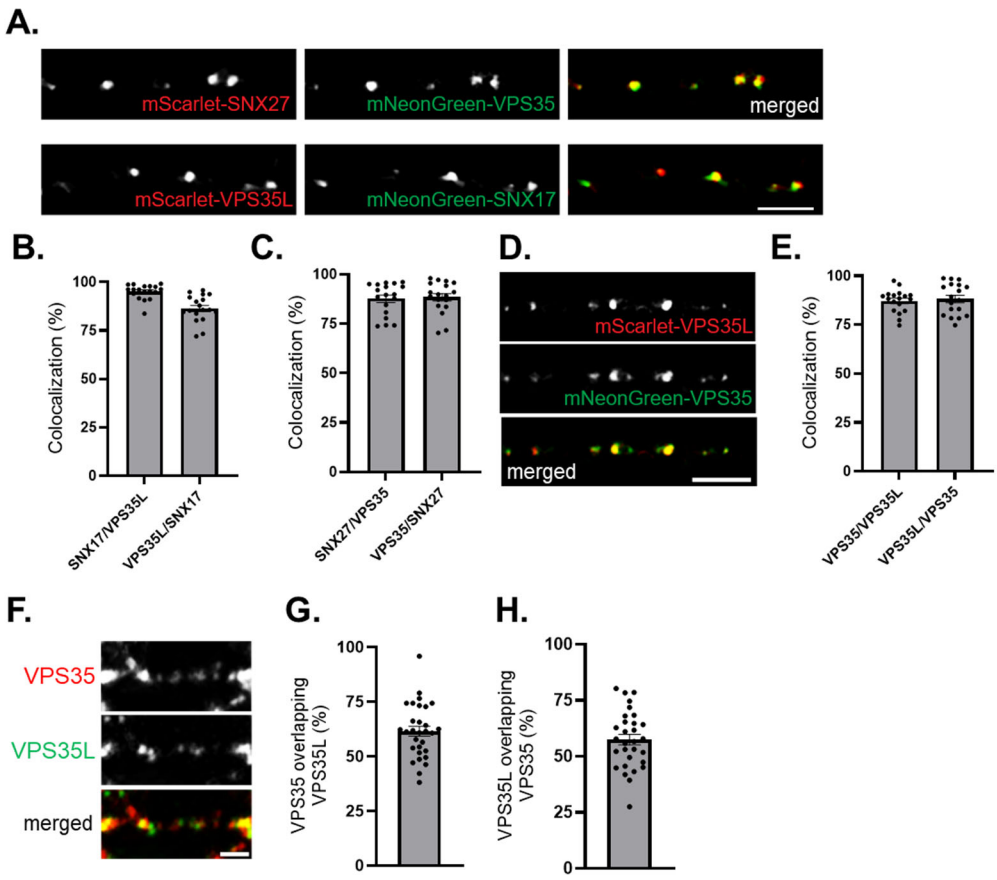


Figure 2.6 Retriever and Retromer complexes colocalize in dendrites

(A). Representative dendrite images from DIV18-20 hippocampal neurons co-expressing mScarlet-SNX27 and mNeonGreen-VPS35 and those co-expressing mScarlet-VPS35L and mNeonGreen-SNX17. Scale bar = 5 µm. **(B).** Mean ± SEM percent colocalization between SNX17:VPS35L and VPS35L:SNX17 from experiments in (A); N = 18 neurons. **(C).** Mean ± SEM percent colocalization between SNX27:VPS35 and VPS35:SNX27 from experiments in (A); N = 18 neurons. **(D).** Representative dendrite images from DIV18-20 hippocampal neurons co-expressing mScarlet-VPS35L and mNeonGreen-VPS35. Scale bar = 5 µm. **(E).** Mean ± SEM percent colocalization of VPS35:VPS35L and VPS35L:VPS35 from the experiment shown in (D); N = 18 neurons. **(F).** Representative dendrite images from DIV18-20 hippocampal neurons depicting endogenous VPS35 and VPS35L detected by immunocytochemistry. Scale bar = 5 µm. **(G-H).** Mean ± SEM percent colocalization of (**G**) VPS35 puncta with VPS35L and (**H**) VPS35L puncta with VPS35; N = 30 neurons.

dendrites (Fig. 6). Collectively, these results demonstrate that SNX17 and SNX27 colocalize in the same subcellular compartment within neurons, predominantly within EEA1-positive early

endosomes. This colocalization recapitulates what is observed in non-neuronal cells and is consistent with the known role of these proteins in regulating endosomal trafficking processes (Gallon and Cullen, 2015; Li et al., 2016; McNally et al., 2017; Chandra, et al., 2020, 2001).

2.4.4 SNX17 and SNX27 regulate synapse integrity via parallel pathways

The data presented thus far illustrate that SNX17 and SNX27 localize to the same cellular compartment, each is required to maintain excitatory synapses, and loss of either leads to a defect in spine maturation. These similarities raise the question of whether SNX17 and SNX27 participate in a common pathway needed to maintain synapses or whether each subserves a parallel recycling pathway, each of which is needed for synaptic integrity. To distinguish between these possibilities, we examined the effects of combinatorial SNX17/SNX27 knockdown on synapse density. If SNX17 and SNX27 comprise a common pathway, knocking down one of these effectors should occlude the effects of depleting the other. If they comprise parallel pathways, then the effects of knocking down both should be additive. We transfected hippocampal neurons with shSNX17, shSNX27, or both (shSNX17 +shSNX27). Spine density and miniature excitatory postsynaptic currents (mEPSCs) were measured to assess the impact on synaptic structure and function. Consistent with our earlier observations, we found that individual knockdown of SNX17 and SNX27 each led to a significant reduction in spine density compared to control neurons transfected with a non- targeting shRNA (Fig. 7A and B). Notably, the combined knockdown of both SNX17 and SNX27 led to a significantly larger loss of dendritic spines than either SNX17 or SNX27 knockdown on their own. Similarly, we found a decrease in mEPSC frequency in neurons expressing shSNX17 or shSNX27 alone (relative to SCR control), but a significant additive reduction of mEPSC frequency with combined SNX17 and SNX27 knockdown (Fig. 7C and E). By contrast, mEPSC amplitude was not significantly altered by any treatment conditions (Fig. 7D). In a separate series of experiments, we addressed the same question by combining SNX17 knockdown with coincident knockdown of either the core Retriever subunit VPS26C (same pathway) or the core Retromer subunit VPS26B (different pathway). We found that coincident knockdown of VPS26B, but not VPS26C, induced an additive loss of dendritic spines (Fig. 8). Taken together, these findings support the idea that

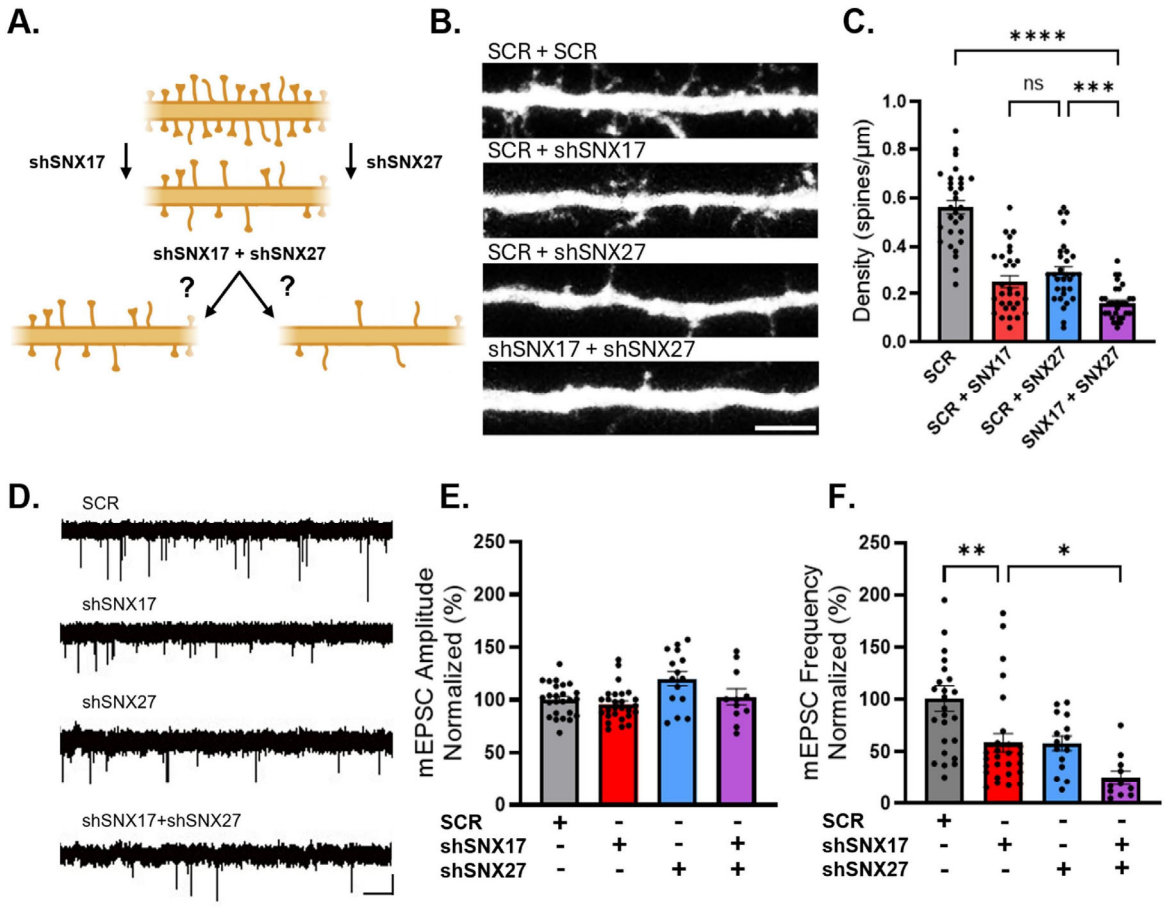


Figure 2.7 SNX17 and SNX27 control synapse maintenance in parallel

(A). Experimental schematic and potential outcomes. Disruption of SNX17 or SNX27 each results in synapse loss, and disruption of both could have the same effect as disrupting each individually (left) or an additive effect (right). **(B).** Representative images of DIV 18–20 primary hippocampal neurons expressing indicated constructs. Scale bar = 5 µm. **(C).** Mean ± SEM spine density from the indicated KD conditions ($F_{3,116} = 57.31$, $p < 0.0001$). SCR, N = 30 neurons; SCR + shSNX17; N = 30 neurons, SCR + shSNX27; N = 30 neurons; shSNX17 + shSNX27, N = 30 neurons. **(D).** Representative mEPSC traces from DIV 18–20 primary hippocampal neurons expressing indicated constructs. Scale bar = 20 pA, 2.5 s. **(E-F).** Mean ± SEM mEPSC amplitude ($F_{3,74} = 5.15$, $p = 0.02$) **(E)** and frequency ($F_{3,74} = 7.89$, $p < 0.0001$) **(F)** normalized to SCR control within each experimental run for each of the indicated experimental conditions (SCR, N = 25 neurons, shSNX17, N = 27 neurons, shSNX27, N = 15 neurons, shSNX17 + shSNX27, N = 11 neurons). *P < 0.05, ** P < 0.01, ***P < 0.001, ****P < 0.0001, ns = not significant by Fisher's LSD. Data are shown normalized to more effectively combine data from multiple experimental runs. Raw data, Mean ± SEM mEPSC amplitude (pA) = 13.4 ± 0.4 (SCR), 12.36 ± 0.4 (shSNX17), 16.8 ± 1.0 (shSNX27), 15.0 ± 1.1 (shSNX17 + shSNX27); Mean ± SEM mEPSC frequency (Hz) = 1.33 ± 0.17 (SCR), 0.69 ± 0.09 (shSNX17), 0.80 ± 0.10 (shSNX27), 0.43 ± 0.10 (shSNX17 + shSNX27). Fig. 7A was created in BioRender. Chavis, G. (2025) https://BioRender.com/20kqe3g.

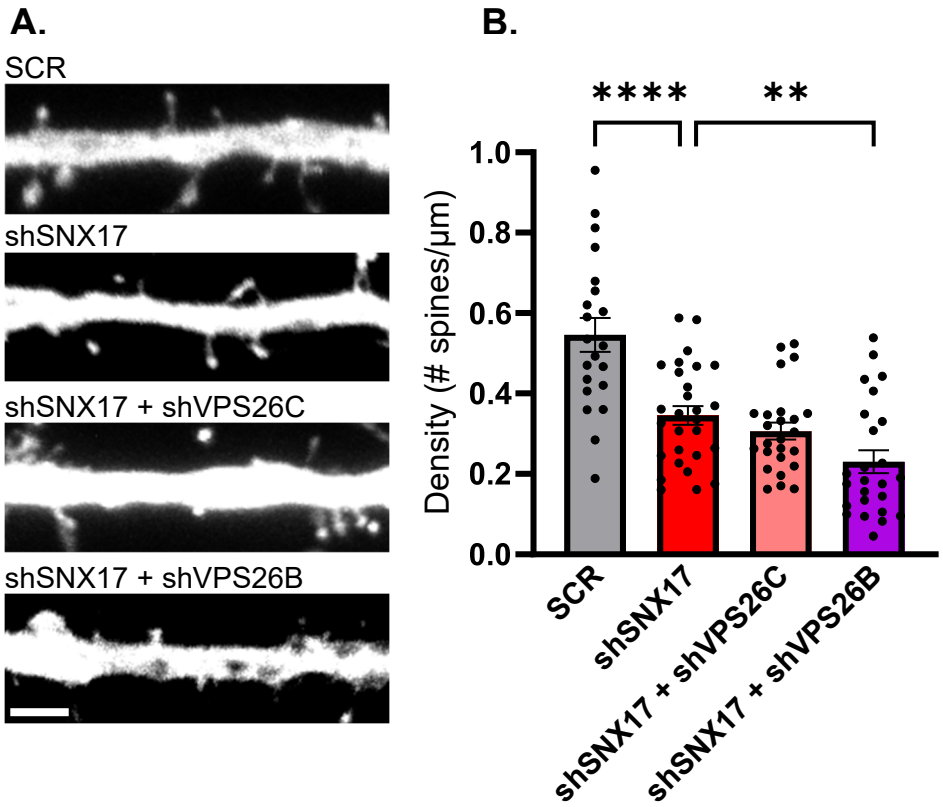


Figure 2.8 Additive synapse loss following coincident depletion of SNX17 and the core Retromer subunit VPS26B, but not the core Retriever subunit VPS26C

(A). Representative images of DIV 14 hippocampal neurons expressing the indicated constructs along with soluble GFP as a filler. Scale bar = 5 µm. **(B).** Mean ± SEM spines/µm from the indicated KD conditions. SCR = 0.55 ± 0.04, N = 21 neurons; shSNX17 = 0.35 ± 0.02, N = 28 neurons; shSNX17 + shVPS26C = 0.31 ± 0.02, N = 25 neurons; shSNX17 + shVPS26B = 0.23 ± 0.03, N = 25 neurons; ($F_{3,95}$ = 20.07, p <0.0001), **P<0.01, ****P<0.0001 by Fisher's LSD.

SNX17-Retriever and SNX17-Retromer constitute parallel endomembrane recycling pathways that independently control maintenance of excitatory synapses.

2.4.5 SNX17-Retriever and SNX27-Retromer are both required for cLTP and homeostatic upscaling

We next assessed the role of SNX17-Retriever and SNX27-Retromer pathways in synaptic plasticity. Following knockdown of SNX17 and SNX27 in cultured rat hippocampal neurons using shRNA, we assessed changes in synaptic function following chemically induced long-term potentiation (cLTP) using a well-established protocol (Lu et al., 2001; Park et al.,

2004; Henry et al., 2018; Fig. 9A). cLTP was induced via brief (5 min) exposure to Mg2+-free ringer supplemented with 0.4 mM glycine, 20 μM bicuculine, and 3 μM strychnine followed by return to regular ringer solution prior to recordings. Under control conditions (SCR shRNA), we observed robust increases in mEPSC amplitude 20–60 min post-cLTP induction relative to mock-treated sister cultures (Fig. 9B and C). Consistent with a previous study (Rivero-Rios et al., 2023), we found that knockdown of SNX17 blocked this cLTP induction (Fig. 9B and D). Similarly, knockdown of SNX27 also blocked cLTP (Fig. 9E–G), again similar to earlier reports (Loo et al., 2014; Hussain et al., 2014; see also, Temkin et al., 2017).

We next examined roles for these recycling pathways in a different form of synaptic enhancement, homeostatic upscaling driven by chronic silencing of network activity. This form of plasticity is thought to play a key role in stabilizing neuronal activity through compensatory synaptic adaptations to offset chronic changes in neuronal firing rate (Wen and Turrigiano, 2024). The role of either the SNX17-Retriever or SNX27- Retromer pathway in this form of plasticity is currently unknown. To induce homeostatic upscaling, we treated neurons with 1 μM tetrodotoxin (TTX) for 24 hrs prior to mEPSC recordings. In neurons expressing SCR shRNA, we found a significant increase in mEPSC amplitude (Fig. 10A–C), as well as a clear rightward shift of the cumulative mEPSC amplitude distribution (Fig. 10D), a signature of homeostatic scaling. By contrast, SNX17 knockdown prevented both the TTX-induced increase in mEPSC amplitude and the shift in the cumulative distribution. In a second set of experiments, we observed a similar pattern of results following SNX27 knockdown – loss of SNX27 prevented homeostatic upscaling of synaptic strength induced by activity silencing (Fig. 10E–G). Together, these results demonstrate a role for both recycling pathways in multiple forms of synaptic plasticity characterized by synaptic enhancement.

2.4.6 AMPAR recycling requires the SNX27-Retromer Pathway, but is independent of SNX17-Retriever

Given that both recycling pathways are required for distinct forms of synaptic potentiation, we considered the possibility that a recycled cargo key for these forms of plasticity might be jointly regulated by the 2 pathways. One cargo whose dynamic surface expression is

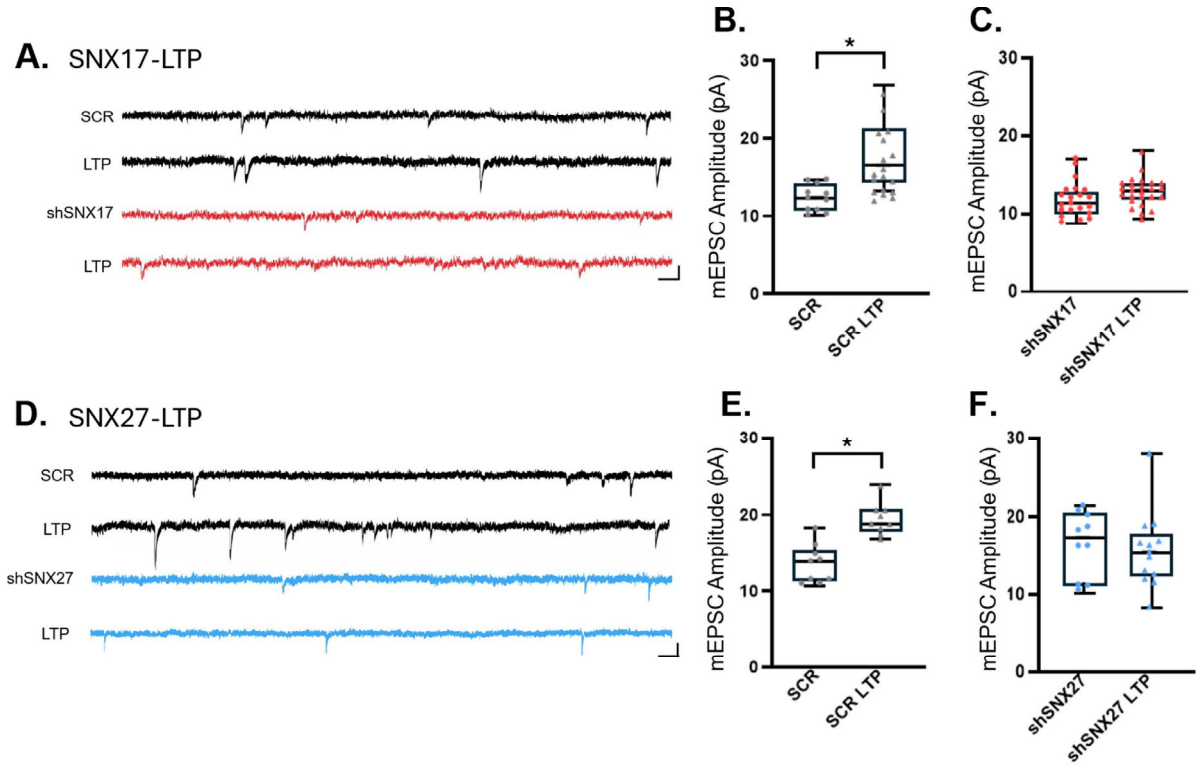


Figure 2.9 SNX17-Retriever and SNX27-Retromer are both required for cLTP

(A,D). Representative mEPSC traces of DIV 17–20 primary hippocampal neurons 20–60 min following cLTP or mock stimulation. Scale bars = 10 pA, 50 ms. **(B-C).** Box plots of mEPSC amplitude in neurons expressing SCR shRNA **(B)** or SNX17 shRNA **(C)** 20–60 min following cLTP or mock stimulation. SCR, N = 11 neurons; SCR + LTP, N = 18 neurons ($t_{27} = 3.16$, $p = 0.004$); shSNX17, N = 21 neurons; shSNX17 + LTP, N = 25 neurons ($t_{44} = 1.60$, $p = 0.12$). **(E-F).** Box plots of mEPSC amplitude in neurons expressing SCR shRNA **(E)** or SNX27 shRNA **(F)** 20–60 min following cLTP or mock stimulation. SCR, N = 9 neurons; SCR + LTP, N = 9 neurons ($t_{16} = 5.29$, $p < 0.0001$); shSNX27, N = 10 neurons; shSNX27 + LTP, N = 13 neurons ($t_{21} = 0.46$, $p = 0.65$). *P < 0.05 by unpaired *t*-test. For box and whisker plots, the box depicts the interquartile range, and the whiskers depict the min and max values.

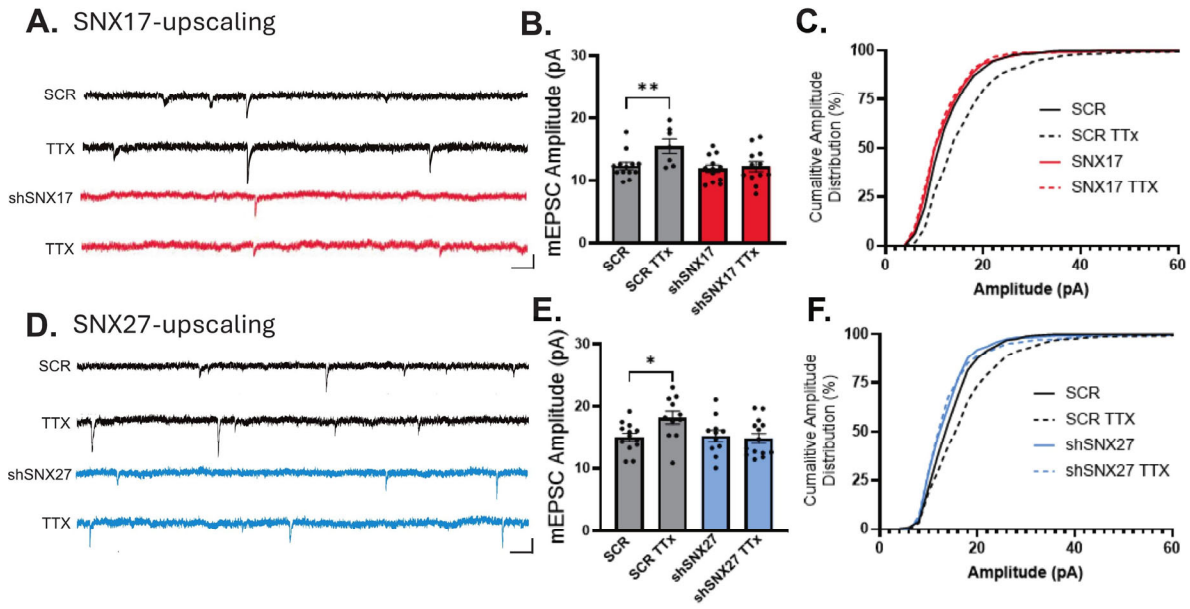


Figure 2.10 Homeostatic upscaling requires both SNX17-Retriever and SNX27-Retromer pathways

(A,D). Representative mEPSC traces of DIV 18–21 primary hippocampal neurons expressing the indicated constructs and treated for 24 hrs with 1 µM TTX or Vehicle. Scale bars = 10 pA, 50 ms. **(B).** Mean ± SEM mEPSC amplitude in neurons expressing shRNA against SNX17 or SCR control shRNA ± TTX treatment. SCR, N = 13 neurons, SCR + TTX, N = 7 neurons, shSNX17, N = 12 neurons, shSNX17 + TTX, N = 12 neurons; $F_{3,40} = 3.63$, p = 0.03. **(C).** Cumulative mEPSC amplitude distribution for the 4 experiments conditions in (B) − a rightward shift in the distribution is induced by TTX in SCR-expressing, but not shSNX17-expressing neurons. **(E).** Mean ± SEM mEPSC amplitude in neurons expressing shRNA against SNX27 or SCR control shRNA ± TTX treatment. SCR, N = 13 neurons; SCR + TTX, N = 11 neurons; shSNX27, N = 11 neurons; shSNX27 + TTX, N = 14 neurons; $F_{3,45} = 3.22$, p = 0.03. **(F).** Cumulative mEPSC amplitude distribution for the 4 experiments conditions in (E) − a rightward shift in the distribution is induced by TTX in SCR-expressing, but not shSNX27-expressing neurons.. *P < 0.05, **P < 0.01 by Fisher's LSD.

known to play a key role in many forms of long-lasting synaptic plasticity is the AMPAR (Chen et al., 2009). In particular, AMPAR recycling is known to be a key source of additional receptors for LTP (Park et al., 2004; Diering and Huganir, 2018), and the SNX27-Retromer pathway is known to be required for proper AMPAR recycling (Choy et al., 2014; Hussain et al., 2014; Temkin et al., 2017). If AMPARs are a cargo of both pathways, it could explain why both pathways are needed for long-lasting forms of synaptic enhancement.

To examine this question, we adapted an imaging protocol used previously to monitor recycling of endogenous AMPARs in hippocampal neurons (Kim et al., 2005; see methods). In brief, surface AMPARs were live-labeled with a well-validated antibody against a surface epitope of the AMPAR subunit GluA1 and allowed to internalize these labeled receptors for 60

min. The remaining surface receptors were labeled with an Alexa 555-conjugated secondary antibody followed by saturating labeling with an unlabeled secondary antibody. Internalized and newly inserted surface AMPARs were then labeled with an Alexa 488-gated secondary antibody after recycling times of 0 – 60 min (Fig. 11A).

To investigate the roles of each recycling pathway, we used lentivirus to express a scrambled shRNA (control) or shRNAs against SNX17 or SNX27. Neurons were infected on DIV7 and used for recycling assays on DIV14. Under control conditions (SCR), we observed a time-dependent increase in the surface expression of previously internalized GluA1 (Fig. 11B–E). Loss of SNX17 had no effect on the rate of this GluA1 recycling, but SNX27 knockdown virtually abolished GluA1 recycling over the 60 min period. Together, these results show that AMPAR recycling is mediated exclusively by the SNX27-Retromer pathway and is independent of the SNX17-Retriever pathway.

2.4.7 Long term synaptic depression is dependent on both SNX17-Retriever and SNX27-Retromer recycling pathways

We next examined the relative roles of each recycling pathway in long-term synaptic depression. We induced chemical LTD (cLTD) using a well-established protocol (Lee et al., 1998; Fern´andez-Monreal et al., 2012), exposing neurons to 20 μM NMDA for 5 min, followed by return to normal ringer solution and recording mEPSCs 20–60 min later. In control neurons (SCR shRNA), this protocol led to a significant and sustained decrease in mEPSC amplitude (Fig. 12A–C), consistent with other studies (McCartney et al., 2014). This cLTD was markedly disrupted following knockdown of SNX17 (Fig. 12D) or SNX27 (Fig. 12E). These results demonstrate that, as was the case with enduring forms of synaptic enhancement, long-lasting synaptic depression is also dependent on both endocytic recycling pathways.

Since the results above establish a role for the SNX17-Retriever pathway in LTD for the first time, we sought to examine the role of an established SNX17 neuronal cargo, β1 integrin, in this effect. Rivero Rios et al. (2023) previously demonstrated a key role for the SNX17-dependent recycling of β1 integrin in maintaining synaptic enhancement following LTP induction, raising the question of whether β1 integrin function also contributes to activity-

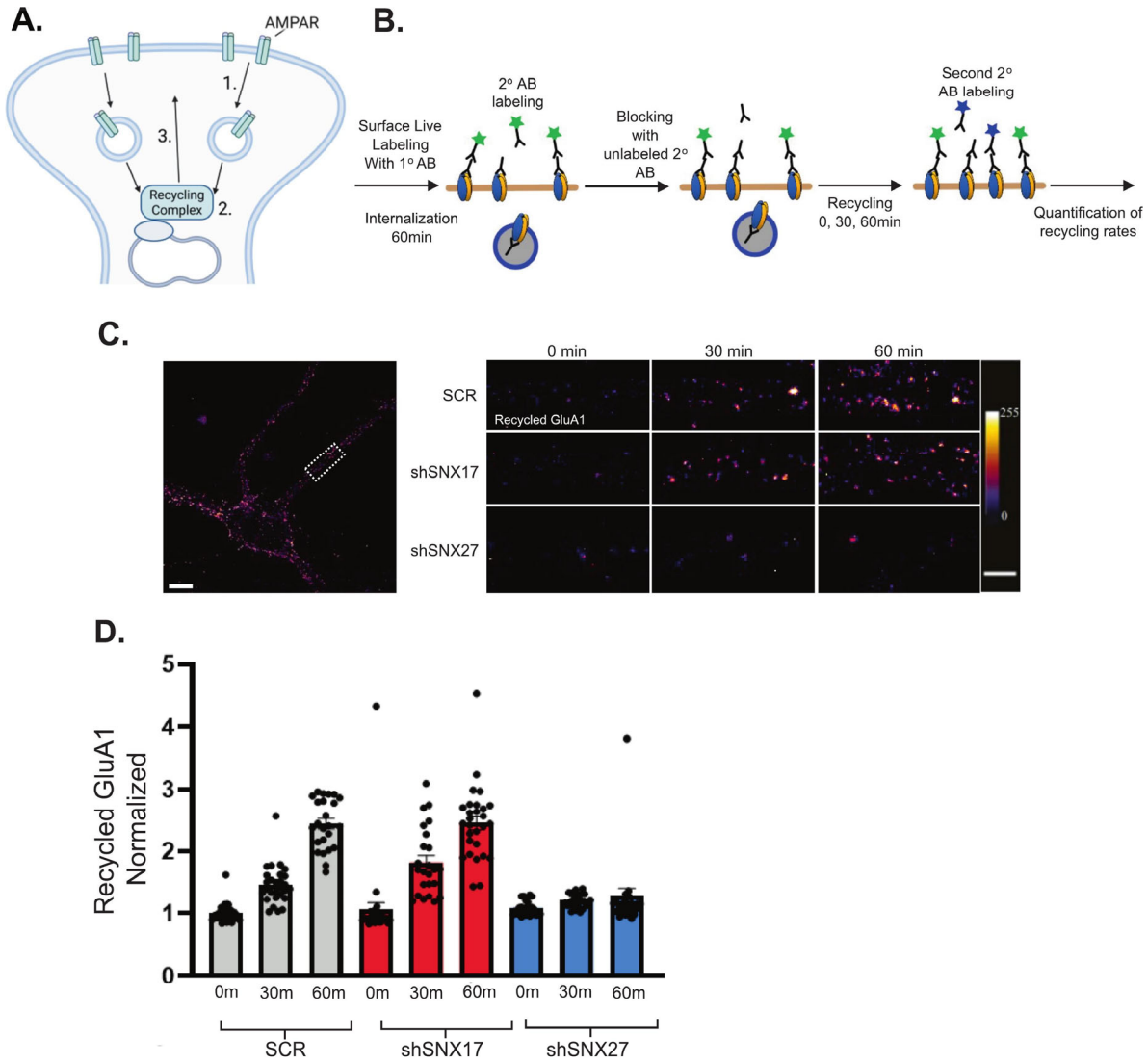


Figure 2.11 AMPARs recycle selectively via the SNX27-Retromer pathway, not the SNX17-Retriever pathway

(A). Simplified cartoon illustrating the internalization and routing of AMPARs to endosomes, followed by AMPAR recycling back to the plasma membrane. **(B).** Experimental schematic of antibody feeding assay for quantifying AMPAR recycling. Neurons are live-labeled with an antibody against a surface epitope of the AMPAR subunit GluA1, allowed to internalize labeled receptors for 60 min, then labeled with an Alexa 555-conjugated secondary antibody to mark AMPARs that remain on the surface. High concentrations of an unlabeled secondary antibody are then applied to saturate this remaining surface AMPAR population. After recycling intervals of 0, 30, or 60 min, internalized receptors that are returned to the surface are labeled with an Alexa488-conjugated secondary antibody (recycled GluA1). **(C).** Left, Representative image of recycled GluA1 in a DIV 14–15 primary hippocampal neuron. Scale bar = 10 µm. Right, Representative images of recycled GluA1 in dendrites of DIV 14–15 hippocampal neurons expressing the indicated shRNAs via lentivirus. Scale bar = 5 µm; intensity (8-bit) denoted by spectrum at right **(D).** Mean ± SEM recycled GluA1 intensity in SCR, shSNX17, and shSNX27 expressing neurons normalized to the 0 min SCR condition. SCR: 0, 30, 60 min, N = 30, 28, and 24 neurons; shSNX17: 0, 30, 60 min, N = 30, 24, and 28 neurons; shSNX27: 0, 30, 60 min, N = 30, 30, and 30 neurons ($F_{8,245} = 44.53$, $p < 0.0001$). Fig. 11A was created in BioRender. Chavis, G. (2025) https://BioRender.com/rcq39ku.

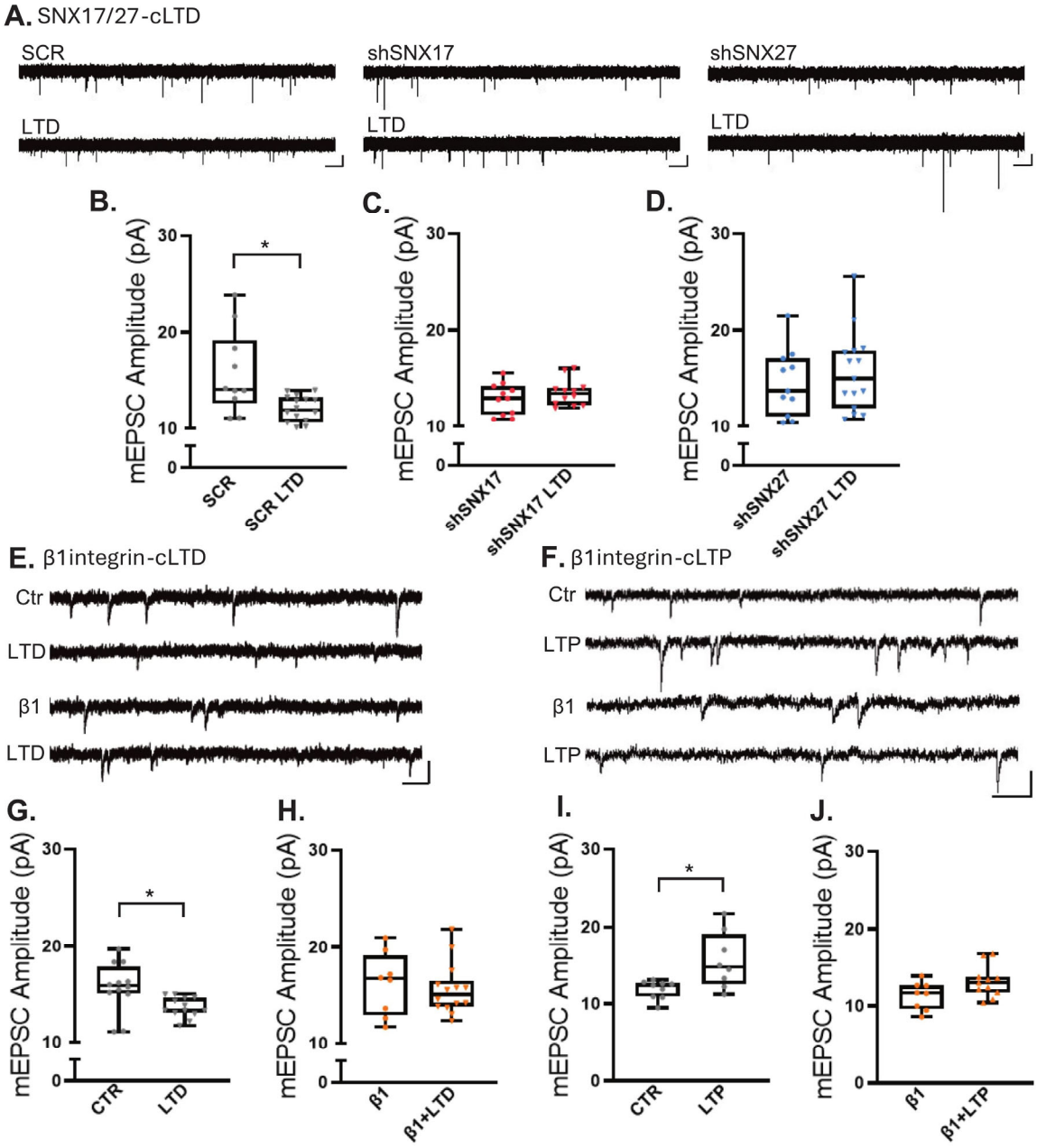


Figure 2.12 SNX17 and SNX27 are both required for long term synaptic depression

(A). Representative mEPSC recordings of DIV 17–20 hippocampal neurons expressing SCR shRNA, or shRNAs against SNX17 or SNX27 with or without chemical LTD induction. Scale bars = 20 pA, 2.5 s. **(B-D).** Box plots of mEPSC amplitude in neurons expressing SCR shRNA **(B)** SNX17 shRNA **(C)**, or SNX27 shRNA **(D)** 20–60 min following cLTD or mock stimulation. SCR, N = 10 neurons; SCR + LTD, N = 16 neurons (t_{24} = 3.27, p = 0.003); shSNX17, N = 11 neurons; shSNX17 + LTD, N = 12 neurons (t_{21} = 1.02, p = 0.32); shSNX27, N = 11 neurons; shSNX27 + LTD, N = 15 neurons (t_{24} = 0.73, p = 0.47). **(E-F).** Representative mEPSC traces in DIV 17–20 hippocampal neurons 20–60 min following cLTD **(E)** or cLTP **(F)** induction in the presence of function blocking β1-integrin or pre-immune (CTR) antibody. Scale bar = 20pA, 50 ms. **(G-H).** Box plots of mEPSC amplitude in neurons treated with pre-immune (CTR, **G**) or function blocking β1-integrin (**H**) antibody prior to and throughout cLTD or mock stimulation. CTR, N = 12 neurons, CTR + LTD, N = 13 neurons (t_{23} = 2.68, p = 0.01); β1 mock, N = 8 neurons, β1 + LTD, N = 14 neurons (t_{20} = 0.42, p = 0.68). **(I-J).** Box plots of mEPSC amplitude in neurons treated with pre-immune (CTR, **I**) or function blocking β1-integrin (**J**) antibody prior to and throughout cLTP or mock

stimulation. CTR, N = 9 neurons, CTR + LTP, N = 8 neurons (t_{15} = 2.99, p = 0.01); β1, N = 8 neurons; β1 + LTP, N = 11 neurons (t_{17} = 2.02, p = 0.07). *P < 0.05

dependent synaptic weakening. To explore this question, neurons were pretreated with a function-blocking β1 integrin antibody (10 μg/mL) for 30 min prior to cLTD induction and this antibody remained in the external solution throughout the experiment. cLTD was induced as above and mEPSCs were recorded 20–60 min post-induction. In vehicle-treated control neurons, cLTD induction resulted in a robust decrease in mEPSC amplitude (Fig. 12F–H), but blocking β1 integrin prevented this synaptic depression (Fig. 12I); the β1 integrin antibody did not alter basal mEPSC amplitude in the absence of cLTD stimulation. Using the same treatment regimen (Fig. 12G–K), we confirmed that blocking β1-integrin similarly disrupts cLTP induction (Rivero Rios et al., 2023). These results reveal an important downstream effector of SNX17-Retriever for LTD and demonstrate that the same cargo, β1 integrin, can play key roles in bidirectional forms of synaptic plasticity.

2.5 Discussion

Our results provide new insights into how the regulation of endomembrane recycling in neurons impacts synapse maintenance and plasticity (summarized in Fig. 13). In recent years, it has become clear that recycling of internalized membrane proteins back to the cell surface is achieved by at least 2 distinct pathways – the SNX27-Retromer and SNX17-Retriever pathways (McNally et al., 2017; Chen et al., 2019; McDonald, 2020). Here, we show that *in vivo* or *in vitro* disruption of either pathway is accompanied by pronounced loss of excitatory synapses and that these pathways function in parallel to maintain synapses (Fig. 13). We also find that both pathways have broad roles in synaptic plasticity as each is required for the induction of cLTP, cLTD, and homeostatic upscaling (Fig. 13). As at least some cargoes are recycled exclusively by a single pathway, our data reveal combinatorial roles of SNX27-Retromer and SNX17-Retriever pathways as a consistent requirement for enduring forms of synaptic plasticity.

2.5.1 An emerging role for SNX17-Retriever in synapse regulation

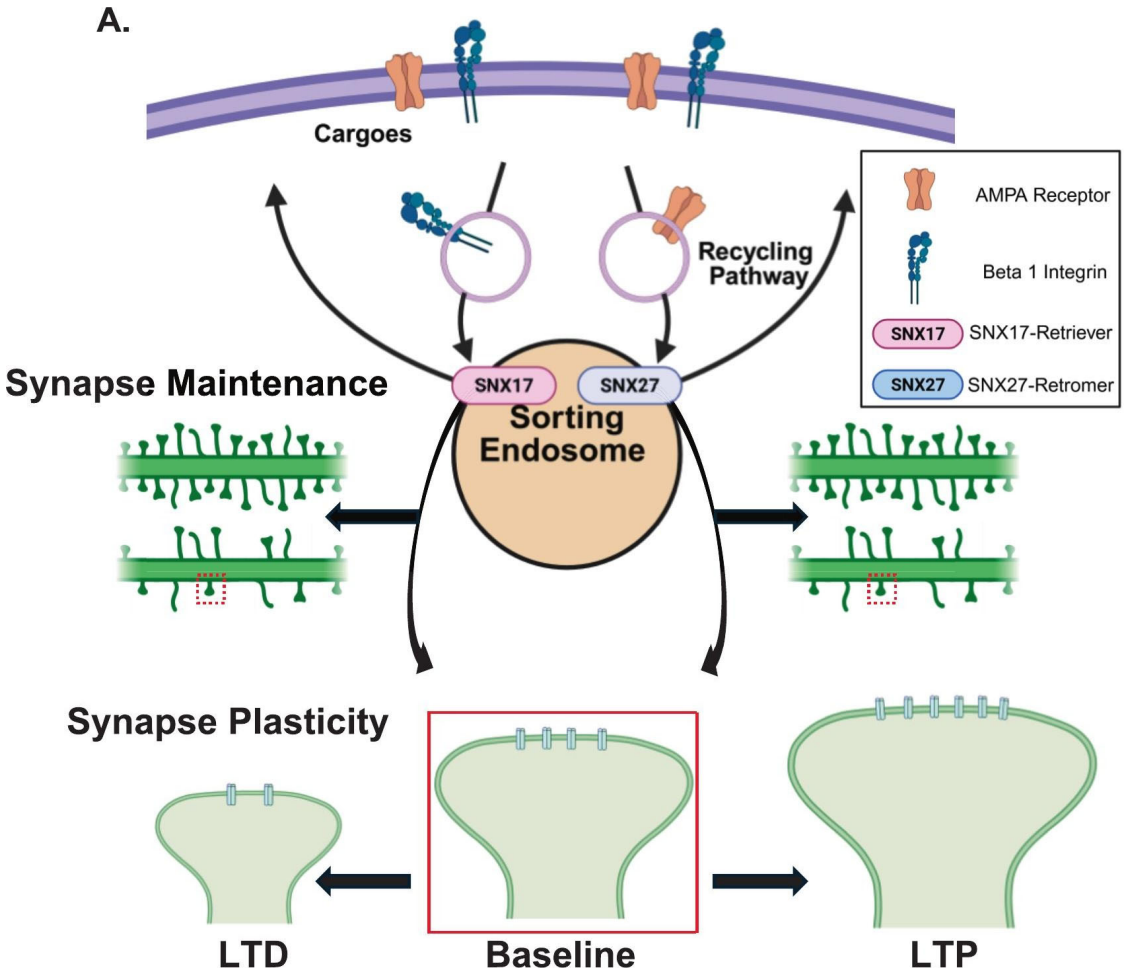


Figure 2.13 Model for functional organization of SNX27-Retromer and SNX17-Retriever pathways at excitatory synapses

SNX17-Retriever and SNX27 Retromer define distinct pathways for recycling internalized protein cargo back to the cell surface. These pathways likely emanate from the same endosome and selectively traffic at least some cargos (e.g., β1-integrin via SNX17-Retriever and AMPARs via SNX27-Retromer). Disrupting SNX17 and SNX27 in isolation or together reveals that they work in parallel to maintain excitatory synapses, and their combinatorial action is required for diverse forms of long-term synaptic plasticity. Fig. 13 was created in BioRender. Chavis, G. (2025) https://BioRender.com/t46imzd; Chavis, G. (2025) https://BioRender.com/gbu5kxu; Chavis, G. (2025) https://BioRender.com/q7qxsc3.

Our results are broadly consistent with previous studies examining the role of SNX17 in excitatory synapse function. Rivero-Rios et al. (2023) reported that acute knockdown of SNX17 (or Retriever subunits) induced a ~40% loss of excitatory synapses in cultured hippocampal neurons and blocked the induction of cLTP. Cui et al. (2024) found that 2–3-month-old SNX17 heterozygous mice exhibit a significant reduction in mature mushroom-shaped spines in CA1 pyramidal neurons, along with significantly reduced amplitude of mEPSCs in that cell

population. Notably, however, they found no significant differences in overall spine density or mEPSC frequency, suggesting that overall synapse density was normal in these mice. Both studies demonstrate a clear role for SNX17 in regulating excitatory synapse function, but reveal different synaptic phenotypes associated with SNX17 deficiency. To partly bridge the approaches used by the two studies, we performed stereotaxic infusion of AAV9 vectors expressing shRNA against SNX17 into hippocampal area CA1 in developing rats (P8-10) and found results that confirmed elements of both studies. Similar to Rivero Rios et al. (2023), we observed a marked reduction in synapse density in CA1 pyramidal neurons 2 weeks post-surgery (P22-24). In addition, similar to Cui et al. (2024), we found a significant decrease in the proportion of mushroom spines relative to less mature spine morphologies, suggesting a similar spine maturation deficit as they reported. Both the overall loss of synapses and specific loss of mushroom spines were recapitulated in cultured hippocampal neurons following SNX17 knockdown, but interestingly, these changes were associated with a decrease in mEPSC frequency (synapse loss), but not mEPSC amplitude.

Two other methodological differences of the Cui et al. (2024) study bear mention: 1) they examined synapses at a slightly older age (2–3 months) than in the other two studies (> 1 month) and 2) they examined synaptic effects of a constitutive (50%) deficiency of SNX17 throughout development, whereas the other studies utilized acute SNX17 knockdown. It is possible that this acute vs. persistent depletion of SNX17 accounts for some of the differences observed (e.g., synapse density).

2.5.2 SNX17-Retriever and SNX27-Retromer operate in the same cellular compartment but regulate synapse maintenance in parallel

Our data show that, in cultured hippocampal neurons, SNX17 and SNX27 exhibit prominent colocalization with each other, as well with Retriever and Retromer, respectively. Moreover, both SNX17 and SNX27 are predominantly localized to endosomes, which is consistent with previous studies examining SNX27 distribution in neurons (Loo et al., 2014; Hussain et al., 2014). Together, this data suggests that both SNX17-Retriever and SNX27-Retromer function in the same cellular compartment and likely reside in the same endosomes, consistent with studies in non-neuronal cells (Chen et al., 2019; McDonald, 2021).

Previous studies have documented loss of excitatory synapses associated with SNX27 or Retromer dysfunction (Asadzadeh et al., 2022; Phadke et al., 2025), consistent with our finding that this pathway is needed to maintain synapses *in vitro* and *in vivo*. We found a similar marked loss of excitatory synapses when we knocked down SNX17 or the core Retriever subunit VPS26C. Despite the fact that SNX17 and SNX27 knockdown each resulted in a prominent loss of synapses on their own, there was an additive effect when both were knocked down together. This result suggests that the two recycling pathways independently contribute to synapse maintenance and thus at least partly function in parallel. One caveat with this interpretation is that the additivity of synapse loss was examined under knockdown, rather than null conditions. However, we also found that coincident knockdown of SNX17 with the Retromer subunit VPS26B, but not the Retriever subunit VPS26C, induced additive spine loss. This latter finding argues against the idea that double knockdown induces more complete disruption of a single pathway and supports the idea that the SNX17-Retriever and SNX27-Retromer pathways control synapse maintenance in parallel.

The parallel control of synapse maintenance by SNX27-Retromer and SNX17-Retriever pathways may have important implications for a number of neurological disorders. Synapse loss is a pathophysiological hallmark of Alzheimer's disease (AD), as well as other debilitating neuropsychiatric disorders such as Schizophrenia. Numerous lines of evidence point to endosomal trafficking dysfunction in both AD patients (Cataldo et al., 2000; Israel et al., 2012) and animal AD models (Small et al., 2005; Muhammad et al., 2008), as well as other neurodegenerative diseases such as Parkinson's disease (Follett et al., 2014; Fan et al., 2025; Young et al., 2023; Collins and Cullen, 2025). Indeed, targeting Retromer and/or SNX27 has been considered as a therapeutic strategy for a variety of neurodegenerative diseases, including AD (Berman et al., 2015; Zhang et al., 2018). The consequences of endomembrane trafficking defects extend to other neurological disorders, as well. For example, SNX27 is downregulated in Down's Syndrome (DS), and restoration of SNX27 levels or stabilization of Retromer can ameliorate cognitive and synaptic defects in the Ts65dn DS mouse model (Wang et al, 2013; Curtis et al., 2023). Finally, recent evidence suggests that the Schizophrenia risk gene C4 induces synapse loss by impairing SNX27- dependent trafficking in neurons (Phadke et al., 2025), suggesting yet another link with neurological disease. Given these associations primarily with

the SNX27-Retromer pathway, a key question that emerges is the extent to which the SNX17-Retriever pathway contributes to the etiology of those disorders and whether it can be targeted for therapeutics.

While our studies focused on the role of endomembrane recycling pathways in regulating excitatory synaptic function, it is of interest to determine whether these principles operate at inhibitory synapses, as well. Of relevance, previous studies have defined an important role for the SNX27-Retromer pathway in controlling inhibitory synapse numbers via regulated recycling of neuroligin-2 (Kang et al., 2014; Halff et al., 2019; Binda et al., 2019). By contrast, the role of the SNX17-Retriever pathway at inhibitory synapses is currently unknown. Understanding how these dual endomembrane recycling pathways work together at inhibitory synapses is an important question for future studies.

2.5.3 Combinatorial roles of SNX17-Retriever and SNX27-Retromer in diverse forms of long-lasting synaptic plasticity

Consistent with several prior studies (Wang et al., 2013; Loo et al., 2014; see also, Temkin et al., 2017), we found that depleting neurons of SNX27 prevented the induction of cLTP. Likewise, we found that knocking down SNX17 or blocking the SNX17-specific cargo β1-integrin prevented the establishment of cLTP, as reported previously (Rivero Rios et al., 2023). Homeostatic synaptic upscaling, induced by chronic network silencing with TTX, is a distinct form of synaptic enhancement where the roles of either recycling pathway were not known. Our results show that depletion of either SNX17 or SNX27 prevents the induction of upscaling, without altering basal synaptic function. These results, for the first time, suggest that recycling of internalized cargo through both the SNX27-Retromer and SNX17-Retriever pathways is required for adaptive synaptic compensation to network silencing. It is now of interest to determine the degree to which the cargoes regulated by these pathways overlap in these Hebbian and non-Hebbian forms of synaptic enhancement.

Although it is presently unclear how many SNX27- or SNX17- dependent cargoes contribute to LTP and upscaling, AMPAR abundance is a critical determinant of synaptic strength. Moreover, recycling of AMPARs via the SNX27-Retromer pathway plays a key role in

LTP (Hussain et al., 2014; Temkin et al., 2017). Given the importance of AMPAR trafficking to synaptic function and plasticity, a major question is whether these receptors are sorted by one or both recycling pathways. We used a dual-labeling approach to specifically monitor the insertion of previously endocytosed AMPARs, and examined AMPAR recycling rates under control conditions, or following SNX27 or SNX17 knockdown. Our results show that AMPAR recycling after SNX17 knockdown is virtually indistinguishable from controls but is almost entirely abolished following SNX27 knockdown. These results demonstrate that AMPARs are recycled exclusively by the SNX27-Retromer pathway, and not the SNX17-Retriever pathway.

In addition to forms of plasticity leading to synaptic enhancement, we examined the roles of both recycling pathways in an enduring form of synaptic weakening – LTD. Again, our results revealed that disrupting either pathway inhibited the induction of cLTD. We also explored the role of a known SNX17 cargo, β1-integrin (Osborne et al., 2015; Rivero-Rios et al., 2023) in cLTD, as recycling of this same cargo has been shown to be necessary for cLTP in hippocampal neurons (Rivero Rios et al., 2023). Using a function-blocking antibody against β1-integrin, we confirmed the role of this cargo in cLTP and demonstrated that it was also necessary for induction of cLTD. These results demonstrate that regulated sorting of the same cargo can have broad roles in distinct forms of plasticity that encompass both strengthening and weakening of synapse function.

Does this broad role for the SNX27-Retromer and SNX17-Retriever pathways in different forms of synaptic plasticity reflect an instructive or permissive role? Our data do not clearly answer this question for homeostatic scaling, but there is strong evidence that each pathway plays an instructive role in LTP. As noted above, SNX27-dependent recycling of AMPARs via Retromer has been shown to add new receptors to synapses during LTP (Wang et al., 2013; Loo et al., 2014; Hussain et al., 2014; Temkin et al., 2017), a clear instructive role. A similar instructive role for SNX17-Retriever can be inferred: LTP stimulation recruits SNX17 to synaptic sites, and SNX17-dependent recycling of β1-integrin via Retriever is necessary for LTP (Rivero-Rios et al., 2023). Similarly, we found that acute blockade of β1-integrin function disrupted cLTD, suggesting an instructive role for this pathway in LTD as well. However, it will

be necessary to more fully characterize the cargoes of these recycling pathways to determine if their active recycling is instructive for LTD and homeostatic scaling.

Our results demonstrate that SNX27-Retromer and SNX17-Retriever function in parallel in maintaining synapses and act combinatorially in several different forms of synaptic plasticity. Together, these findings position SNX17-Retriever and SNX27-Retromer as central components of a dual-pathway trafficking system that ensures both the stability and adaptability of excitatory synapses. Given the extensive association of endosomal trafficking with neurological disorders, elucidating the molecular and cargo-specific mechanisms by which these pathways regulate synaptic composition will be crucial for understanding and potentially targeting synaptic dysfunction in disease.

2.6 References

Asadzadeh, J., Ruchti, E., Jiao, W., Limoni, G., MacLachlan, C., Small, S.A., Knott, G., Santa-Maria, I., McCabe, B.D., (2022). Retromer deficiency in Tauopathy models enhances the truncation and toxicity of Tau. *Nat. Commun*. 13 (1), 5049. https:// doi.org/10.1038/s41467-022-32683-5. PMID: 36030267; PMCID: PMC9420134.

Berman, D.E., Ringe, D., Petsko, G.A., Small, S.A., (2015). The use of pharmacological retromer chaperones in Alzheimer's disease and other endosomal-related disorders. *Neurotherapeutics* 12 (1), 12–18. https://doi.org/10.1007/s13311-014-0321-y. PMID: 25472693; PMCID: PMC4322078.

Binda, C.S., Nakamura, Y., Henley, J.M., Wilkinson, K.A., (2019). Sorting nexin 27 rescues neuroligin 2 from lysosomal degradation to control inhibitory synapse number. *Biochem*. J 476 (2), 293–306. https://doi.org/10.1042/BCJ20180504. PMID: 30602588.

Cataldo, A.M., Peterhoff, C.M., Troncoso, J.C., Gomez-Isla, T., Hyman, B.T., Nixon, R.A., (2000). Endocytic pathway abnormalities precede amyloid beta deposition in sporadic

Alzheimer's disease and down syndrome: differential effects of APOE genotype and presenilin mutations. *Am. J. Pathol*. 157 (1), 277–286. https://doi.org/10.1016/ s0002-9440(10)64538-5. PMID: 10880397; PMCID: PMC1850219.

Chandra, M., Kendall, A.K., Jackson, L.P., (2020). Unveiling the cryo-EM structure of retromer. *Biochem*. Soc. Trans. 48 (5), 2261–2272. https://doi.org/10.1042/ BST20200552.

Chandra, M., Kendall, A.K., Jackson, L.P., (2021). Toward understanding the molecular role of SNX27/retromer in human health and disease. *Front. Cell Dev*. Biol. 9, 642378. https://doi.org/10.3389/fcell.2021.642378.

Chavis GD, Rivero-Ríos P, Uygun T, Tsukahara T, Hayami T, Lee GY, Lee M, Pace C, Czesak FN, Hilde KL, Li F, Iwase S, Murphy GG, Morrow JD, Akil H, Weisman LS, Sutton MA. (2025). Dual endomembrane recycling pathways function in parallel to support synapse maintenance and plasticity. Neuroscience. 15;591:205-221. doi: 10.1016/j.neuroscience.2025.11.009. Epub 2025 Nov 12. PMID: 41238049.

Chen, K.-E., Healy, M.D., Collins, B.M., (2019). Towards a molecular understanding of endosomal trafficking by Retromer and Retriever. *Traffic* 20, 465–478.

Chen, Z., Peppi, M., Kujawa, S.G., Sewell, W.F., (2009). Regulated expression of surface AMPA receptors reduces excitotoxicity in auditory neurons. *J. Neurophysiol*. 102 (2), 1152–1159. https://doi.org/10.1152/jn.00288.2009. Epub 2009 Jun 10. PMID: 19515954; PMCID: PMC2724347.

Choy, R.W., Park, M., Temkin, P., Herring, B.E., Marley, A., Nicoll, R.A., von Zastrow, M., (2014). Retromer mediates a discrete route of local membrane delivery to dendrites. *Neuron* 82 (1), 55–62. https://doi.org/10.1016/j.neuron.2014.02.018. PMID: 24698268; PMCID: PMC4029335.

Collins, B.M., Cullen, P.J., (2025). Separation of powers: a key feature underlying the neuroprotective role of Retromer in age-related neurodegenerative disease? *Curr. Opin. Cell Biol.* 94, 102516. https://doi.org/10.1016/j.ceb.2025.102516. Epub 2025 PMID: 40253888.

Cui, Q., Liang, S., Li, H., Guo, Y., Lv, J., Wang, X., Qin, P., Xu, H., Huang, T.Y., Lu, Y., Tian, Q., Zhang, T., (2024). SNX17 mediates dendritic spine maturation via p140cap. *Mol. Neurobiol*. 61 (3), 1346–1362. https://doi.org/10.1007/s12035-023-03620-4. Epub 2023 Sep 13 PMID: 37704928.

Curtis, M.E., Smith, T., Nenov, M., Blass, B.E., Pratic`o, D., (2023). Retromer stabilization improves cognitive function and synaptic plasticity in a mouse model of down syndrome. J. Alzheimers *Dis.* 94 (2), 513–518. https://doi.org/10.3233/JAD- 230205. PMID: 37334603; PMCID: PMC10357169.

Diering, G.H., Huganir, R.L., (2018). The AMPA receptor code of synaptic plasticity. *Neuron* 100 (2), 314–329. https://doi.org/10.1016/j.neuron.2018.10.018. PMID: 30359599; PMCID: PMC6214363.

Fan, X., Xie, Y., Cao, S., Zhu, L., Wang, X., (2025). VPS35-retromer: multifunctional roles in various biological processes - a focus on neurodegenerative diseases and cancer. *J. Inflamm. Res.* 18, 4665–4680. https://doi.org/10.2147/JIR.S510768. PMID: 40195959; PMCID: PMC11975009.

Fern´andez-Monreal, M., Brown, T.C., Royo, M., Esteban, J.A., (2012). The balance between receptor recycling and trafficking toward lysosomes determines synaptic strength during long-term depression. *J Neurosci*. 32 (38), 13200–13205. https:// doi.org/10.1523/JNEUROSCI.0061-12.2012. PMID: 22993436; PMCID: PMC6621469.

Follett, J., Norwood, S.J., Hamilton, N.A., Mohan, M., Kovtun, O., Tay, S., Zhe, Y., Wood, S.A., Mellick, G.D., Silburn, P.A., Collins, B.M., Bugarcic, A., Teasdale, R.D., (2014). The Vps35

D620N mutation linked to Parkinson's disease disrupts the cargo sorting function of retromer. *Traffic* 15 (2), 230–244. https://doi.org/10.1111/ tra.12136. Epub 2013 Nov 14 PMID: 24152121.

Gallon, M., Cullen, P.J., (2015). Retromer and sorting nexins in endosomal sorting. *Biochem. Soc. Trans.* 43 (1), 33–47. https://doi.org/10.1042/BST20140290.

Halff, E.F., Szulc, B.R., Lesept, F., Kittler, J.T., (2019). SNX27-Mediated recycling of neuroligin-2 regulates inhibitory signaling. *Cell Rep.* 29 (9). https://doi.org/ 10.1016/j.celrep.2019.10.096. PMID: 31775031; PMCID: PMC6899438 2599-2607. e6.

Harbour, M.E., Breusegem, S.Y., Seaman, M.N.J., (2012). Recruitment of the endosomal WASH complex is mediated by the extended 'tail' of Fam21 binding to the retromer protein Vps35. *Biochem. J* 442, 209–220. https://doi.org/10.1042/BJ20111761.

Henry, F.E., Wang, X., Serrano, D., Perez, A.S., Carruthers, C.J.L., Stuenkel, E.L., Sutton, M.A., (2018). A unique homeostatic signaling pathway links synaptic inactivity to postsynaptic mTORC1. *J Neurosci*. 38 (9), 2207–2225. https://doi.org/ 10.1523/JNEUROSCI.1843-17.2017. Epub 2018 Jan 8. PMID: 29311141; PMCID: PMC5830511.

Hussain, N.K., Diering, G.H., Sole, J., Anggono, V., Huganir, R.L., (2014). Sorting Nexin 27 regulates basal and activity-dependent trafficking of AMPARs. *Proc. Natl. Acad. Sci.* USA 111, 11840–11845. https://doi.org/10.1073/pnas.1412415111.

Israel, M.A., Yuan, S.H., Bardy, C., Reyna, S.M., Mu, Y., Herrera, C., Hefferan, M.P., Van Gorp, S., Nazor, K.L., Boscolo, F.S., Carson, C.T., Laurent, L.C., Marsala, M., Gage, F. H., Remes, A.M., Koo, E.H., Goldstein, L.S., (2012). Probing sporadic and familial Alzheimer's disease using induced pluripotent stem cells. *Nature* 482 (7384), 216–220. https://doi.org/10.1038/nature10821. PMID: 22278060; PMCID: PMC3338985.

Kang, Y., Ge, Y., Cassidy, R.M., Lam, V., Luo, L., Moon, K.M., Lewis, R., Molday, R.S., Wong, R.O., Foster, L.J., Craig, A.M., (2014). A combined transgenic proteomic analysis and

regulated trafficking of neuroligin-2. *J. Biol. Chem.* 289 (42), 29350–29364. https://doi.org/10.1074/jbc.M114.549279. Epub 2014 Sep 4. PMID: 25190809; PMCID: PMC4200284.

Kim, M.J., Dunah, A.W., Wang, Y.T., Sheng, M., (2005). Differential roles of NR2A- and NR2B-containing NMDA receptors in Ras-ERK signaling and AMPA receptor trafficking. *Neuron* 46 (5), 745–760. https://doi.org/10.1016/j. neuron.2005.04.031. PMID: 15924861.

Lee, H.K., Kameyama, K., Huganir, R.L., Bear, M.F., (1998). NMDA induces long-term synaptic depression and dephosphorylation of the GluR1 subunit of AMPA receptors in hippocampus. *Neuron* 21 (5), 1151–1162. https://doi.org/10.1016/s0896-6273 (00)80632-7. PMID: 9856470.

Li, C., Shah, S.Z., Zhao, D., Yang, L., (2016). Role of the retromer complex in neurodegenerative diseases. *Front. Aging Neurosci*. 8, 42. https://doi.org/10.3389/ fnagi.2016.00042.

Loo, L.S., Tang, N., Al-Haddawi, M., Stewart Dawe, G., Hong, W., 2014. A role for sorting nexin 27 in AMPA receptor trafficking. Nat. Commun. 5. https://doi.org/10.1038/ ncomms4176.
Lu, W., Man, H., Ju, W., Trimble, W.S., MacDonald, J.F., Wang, Y.T., (2001). Activation of synaptic NMDA receptors induces membrane insertion of new AMPA receptors and LTP in cultured hippocampal neurons. *Neuron* 29 (1), 243–254. https://doi.org/ 10.1016/s0896-6273(01)00194-5. PMID: 11182095.

Mao, L., Liao, C., Qin, J., Gong, Y., Zhou, Y., Li, S., Liu, Z., Deng, H., Deng, W., Sun, Q., Mo, X., Xue, Y., Billadeau, D.D., Dai, L., Li, G., Jia, D., (2021). Phosphorylation of SNX27 by MAPK11/14 links cellular stress-signaling pathways with endocytic recycling. *J. Cell Biol*. 220, e202010048. https://doi.org/10.1083/jcb.202010048.

McCartney, A.J., Zolov, S.N., Kauffman, E.J., Zhang, Y., Strunk, B.S., Weisman, L.S., Sutton, M.A., (2014). Activity-dependent PI(3,5)P2 synthesis controls AMPA receptor trafficking during

synaptic depression. *PNAS* 111 (45). https://doi.org/10.1073/ pnas.1411117111. Epub 2014 Oct 29. PMID: 25355904; PMCID: PMC4234577 E4896-905.

McDonald, F.J., (2020). Explosion in the complexity of membrane protein recycling. *Am. J. Physiol*. Physiol. 320. https://doi.org/10.1152/ajpcell.00171.2020. C483–C494.
McMillan, K.J., Banks, P.J., Hellel, F.L., Carmichael, R.E., Clairfeuille, T., Evans, A.J., Heesom, K.J., Lewis, P., Collins, B.M., Bashir, Z.I., Henley, J.M., Wilkinson, K.A., Cullen, P.J., 2021. Sorting nexin-27 regulates AMPA receptor trafficking through the synaptic adhesion protein LRFN2. *Elife* 10, e59432. https://doi.org/10.7554/ eLife.59432.

McNally, K.E., Faulkner, R., Steinberg, F., Gallon, M., Ghai, R., Pim, D., Langton, P., Pearson, N., Danson, C.M., N¨agele, H., Morris, L.L., Singla, A., Overlee, B.L., Heesom, K.J., Sessions, R., Banks, L., Collins, B.M., Berger, I., Billadeau, D.D., Burstein, E., Cullen, P.J., (2017). Retriever is a multiprotein complex for retromer- independent endosomal cargo recycling. *Nat. Cell Biol.* 19, 1214–1225. https://doi. org/10.1038/ncb3610.

Muhammad, A., Flores, I., Zhang, H., Yu, R., Staniszewski, A., Planel, E., Herman, M., Ho, L., Kreber, R., Honig, L.S., Ganetzky, B., Duff, K., Arancio, O., Small, S.A., (2008). Retromer deficiency observed in Alzheimer's disease causes hippocampal dysfunction, neurodegeneration, and Abeta accumulation. *PNAS* 105 (20), 7327–7332. https://doi.org/10.1073/pnas.0802545105. Epub 2008 May 14. PMID: 18480253; PMCID: PMC2386077.

Osborne, D.G., Piotrowski, J.T., Dick, C.J., Zhang, J.S., Billadeau, D.D., (2015). SNX17 affects T cell activation by regulating TCR and integrin recycling. *J. Immunol*. 194 (9), 4555–4566. https://doi.org/10.4049/jimmunol.1402734. Epub 2015. PMID: 25825439; PMCID: PMC4402276.

Park, M., Penick, E.C., Edwards, J.G., Kauer, J.A., Ehlers, M.D., (2004). Recycling endosomes supply AMPA receptors for LTP. *Science* 305 (5692), 1972–1975. https://doi.org/10.1126/science.1102026. PMID: 15448273.

Phadke, R.A., Brack, A., Fournier, L.A., Kruzich, E., Sha, M., Picard, I., Johnson, C., Stroumbakis, D., Salgado, M., Yeung, C., Escude Velasco, B., Liu, Y.Y., Cruz- Martín, A., (2025). The schizophrenia risk gene C4 induces pathological synaptic loss by impairing AMPAR trafficking. *Mol. Psychiatry* 30 (2), 796–809. https://doi.org/ 10.1038/s41380-024-02701-7. Epub 2024 Sep 3. PMID: 39227431; PMCID: PMC11746135.

Phillips-Krawczak, C.A., Singla, A., Starokadomskyy, P., Deng, Z., Osborne, D.G., Li, H., Dick, C.J., Gomez, T.S., Koenecke, M., Zhang, J.S., Dai, H., Sifuentes-Dominguez, L. F., Geng, L.N., Kaufmann, S.H., Hein, M.Y., Wallis, M., McGaughran, J., Gecz Sluis Bv, J., Billadeau, D.D., Burstein, E., (2015). COMMD1 is linked to the WASH complex and regulates endosomal trafficking of the copper transporter ATP7A. *Mol. Biol. Cell* 26 (1), 91–103. https://doi.org/10.1091/mbc.E14-06-1073.

Rivero-Ríos, P., Tsukahara, T., Uygun, T., Chen, A., Chavis, G.D., Giridharan, S.S.P., Iwase, S., Sutton, M.A., Weisman, L.S., (2023). Recruitment of the SNX17-Retriever recycling pathway regulates synaptic function and plasticity. *J. Cell Biol.* 222, e202207025. https://doi.org/10.1101/2023.02.20.529299.

Saitoh, S., (2022). Endosomal recycling defects and neurodevelopmental disorders. *Cells* 11. https://doi.org/10.3390/cells11010148.

Simonetti, B., Cullen, P.J., (2019). Actin-dependent endosomal receptor recycling. *Curr. Opin. Cell Biol.* 56, 22–33. https://doi.org/10.1016/j.ceb.2018.08.006.

Small, S.A., Kent, K., Pierce, A., Leung, C., Kang, M.S., Okada, H., Honig, L., Vonsattel, J. P., Kim, T.W., (2005). Model-guided microarray implicates the retromer complex in Alzheimer's disease. *Ann. Neurol.* 58 (6), 909–919. https://doi.org/10.1002/ ana.20667. PMID: 16315276.

Steinberg, F., Gallon, M., Winfield, M., Thomas, E.C., Bell, A.J., Heesom, K.J., Tavar´e, J. M., Cullen, P.J., (2013). A global analysis of SNX27-retromer assembly and cargo specificity reveals

a function in glucose and metal ion transport. *Nat. Cell Biol*. 15, 461–471. https://doi.org/10.1038/ncb2721.

Temkin, P., Morishita, W., Goswami, D., Arendt, K., Chen, L., Malenka, R., (2017). The retromer supports AMPA receptor trafficking during LTP. *Neuron* 94 (1). https://doi. org/10.1016/j.neuron.2017.03.020, 74-82.e5.

van Oostrum, M., Campbell, B., Seng, C., Müller, M., Tom Dieck, S., Hammer, J., Pedrioli, P.G.A., F¨oldy, C., Tyagarajan, S.K., Wollscheid, B., (2020). Surfaceome dynamics reveal proteostasis-independent reorganization of neuronal surface proteins during development and synaptic plasticity. *Nat. Commun.* 11 (1), 4990. https://doi.org/10.1038/s41467-020-18494-6.

Wang, X., Zhao, Y., Zhang, X., Badie, H., Zhou, Y., Mu, Y., Loo, L.S., Cai, L., Thompson, R. C., Yang, B., Chen, Y., Johnson, P.F., Wu, C., Bu, G., Mobley, W.C., Zhang, D., Gage, F.H., Ranscht, B., Zhang, Y., Lipton, S.A., Hong, W., Xu, H., (2013). Loss of sorting nexin 27 contributes to excitatory synaptic dysfunction by modulating. *Nature Med*. doi.org/10.1038/nm.3117.

Wen, W., Turrigiano, G.G., (2024). Keeping your brain in balance: homeostatic regulation of network function. Annu. Rev. *Neurosci.* 47 (1), 41–61. https://doi.org/10.1146/ annurev-neuro-092523-110001. Epub 2024 Jul 1 PMID: 38382543.

Willems, J., de Jong, A.P.H., Scheefhals, N., Mertens, E., Catsburg, L.A.E., Poorthuis, R. B., de Winter, F., Verhaagen, J., Meye, F.J., MacGillavry, H.D., (2020). ORANGE: a CRISPR/Cas9-based genome editing toolbox for epitope tagging of endogenous proteins in neurons. *PLoS Biol*. 18 (4), e3000665. https://doi.org/10.1371/journal. pbio.3000665. PMID: 32275651; PMCID: PMC7176289.

Young, J.E., Holstege, H., Andersen, O.M., Petsko, G.A., Small, S.A., (2023). On the causal role of retromer-dependent endosomal recycling in Alzheimer's disease. *Nat. Cell Biol.* 25 (10),

1394–1397. https://doi.org/10.1038/s41556-023-01245-2. PMID: 37803174; PMCID: PMC10788784.

Zhang, H., Huang, T., Hong, Y., Yang, W., Zhang, X., Luo, H., Xu, H., Wang, X., (2018). The retromer complex and sorting nexins in neurodegenerative diseases. *Front. Aging Neurosci*. 10, 79. https://doi.org/10.3389/fnagi.2018.00079. PMID: 29632483; PMCID: PMC5879135.

Chapter 3 Dual Recycling Pathways Function in Presynaptic Terminals

3.1 Abstract

SNX27-Retromer and SNX17-Retriever are endosomal recycling pathways that control the surface expression and trafficking of key synaptic proteins, yet their roles in the presynaptic compartment remain poorly defined. In this presented work I will show how these complexes regulate presynaptic structure and neurotransmission in cultured hippocampal neurons. I first show that SNX17 is expressed in axons and present in presynaptic compartments. Consistent with emerging roles for recycling pathways in synapse stability, shRNA mediated knockdown of either SNX17 or SNX27 reduces the density of presynaptic boutons, demonstrating that both pathways support the maintenance of presynaptic terminals. In contrast, simultaneous depletion of SNX17 and SNX27 does not produce an additive loss of boutons, suggesting that these pathways share presynaptic cargos or sorting hubs. To define functional consequences for neurotransmitter release, I combined optical readouts of spontaneous and evoked synaptic vesicle exocytosis: Spontaneous, action potential independent release is preserved following SNX17 or SNX27 depletion. In contrast, action potential evoked transmission with knockdown of SNX27 or the Retromer subunit VPS26B slows stimulus evoked responses and reduces the density of active boutons, whereas depletion of SNX17 or the Retriever subunit VPS26C leaves the evoked responses largely unchanged. I further show that SNX27 knockdown reduces both the readily releasable and total recycling pools of synaptic vesicles, implicating SNX27 in maintaining the vesicle reservoirs that support sustained neurotransmission. Together, these findings identify presynaptic endosomes as critical sites where sorting nexin dependent recycling pathways stabilize boutons and shape release capacity.

3.2 Introduction

Endosomal recycling pathways are important for regulating the cell-surface expression of many proteins in all eukaryotic cell types, including neurons (Diering and Huganir, 2018; Grant and Donaldson, 2009; Cullen and Steinberg, 2018). Two major endosomal recycling pathways

operate in eukaryotic cells: 1) the SNX27-Retromer pathway, in which the Retromer complex (VPS35, VPS26A/B, and VPS29) works in concert with the cargo adapter sorting nexin 27 (SNX27), and 2) the more recently discovered SNX17-Retriever pathway, in which sorting nexin 17 recognizes endosomal cargos and works with the Retriever complex (VPS35L, VPS26C, and VPS29) to re-insert these at the cell membrane (Steinberg et al., 2013; McNally and Cullen, 2018; Yong et al., 2020). In hippocampal neurons, SNX27 is highly expressed and has been linked to the recycling of glutamate and GABA receptor complexes, which affects synaptic strength and synaptic plasticity (Loo et al., 2014; Hussain et al., 2014; Wang et al., 2013; Chavis et al., 2025). Functional roles for the SNX17-Retriever pathway in neurons are less well understood, as there remain only a handful of studies that have examined this pathway in neurons. Recent studies have suggested that this pathway plays a key role in β1-integrin recycling (and possibly, other adhesion molecules) during activity-dependent plasticity (Rivero-Ríos et al., 2023; Rivero-Rios et al., 2025; Chavis et al., 2025).

Work in cultured hippocampal neurons and *in vivo* models suggests that both SNX27-Retromer and SNX17-Retriever are present at postsynaptic specializations of neuronal synapses and are needed to maintain excitatory synapse number and function (Loo et al., 2014; Wang et al., 2013; McNally and Cullen, 2018; Yong et al., 2020; Chavis et al., 2025). SNX27 binds directly to the Retromer core subunit VPS26 and forms part of a SNX27-Retromer-WASH complex that shapes endosomal tubules and supports recycling of specific synaptic cargos, such as neurotransmitter receptors and adhesion proteins, which in turn influence synaptic strength (Steinberg et al., 2013; Temkin et al., 2011; Seaman, 2012). In parallel, the SNX17-Retriever pathway is recruited to synapses in an activity-dependent manner during chemical LTP (Rivero-Ríos et al., 2023), where it contributes to structural changes of spines and lasting changes in excitatory synaptic transmission, at least in part, by controlling β1-integrin recycling to the cell surface (Böttcher et al., 2012; Bottcher et al., 2017; McNally et al., 2017; Rivero-Ríos et al., 2023; Rivero-Rios et al., 2025; Chavis et al., 2025). Of potential relevance to neuropsychiatric and neurodegenerative disorders, disrupting either recycling pathway postsynaptically leads to a precipitous loss of excitatory synapses (~40 %) both *in vitro* (Wang et al., 2013; McNally and Cullen, 2018; Yong et al., 2020; Rivero-Ríos et al., 2023) and *in vivo* (Chavis et al., 2025). Recent findings indicate that, in the postsynaptic compartment, the SNX27-

Retromer and SNX17-Retriever pathways act largely in parallel for synapse maintenance (Chavis et al., 2025), suggesting that cargoes of both pathways contribute to synapse stability within the same hippocampal circuits, and that both are required to maintain excitatory synapses in CA1 pyramidal neurons and support normal circuit output, suggesting that presynaptic endosomes may be a key site where their functions converge (Rivero-Ríos et al., 2023; Yong et al., 2020; Wang et al., 2020).

While clear roles for the SNX27-Retromer and SNX17-Retriever recycling pathways are emerging at postsynaptic specializations of synapses, the manner by which these pathways regulate the function of the presynaptic terminal is much less understood. Presynaptic terminals contain endosomes that help control synaptic vesicle pools, neurotransmitter transporter trafficking, and the surface levels of proteins that set release probability and short-term plasticity (Brodin and Shupliakov, 2018; Tsuboi and Fukuda, 2006; Uytterhoeven et al., 2011). Retromer components such as VPS35 are found in hippocampal presynaptic boutons, supporting the possibility that SNX27-Retromer dependent trafficking can directly affect transmitter release and presynaptic stability (Sanchez et al., 2018; Inoshita et al., 2017; Temkin et al., 2017). By contrast, we know almost nothing about how the SNX17-Retriever regulates presynaptic function. In particular, we do not know how strongly this pathway acts in presynaptic endosomes, how it shapes presynaptic structure and function, or how it is coordinated with Retromer-associated complexes.

Here, we examine functional roles for the SNX27-Retromer and SNX17-Retriever endosomal recycling pathways in presynaptic terminals of cultured hippocampal neurons. We find that SNX17 is distributed throughout axons and localizes preferentially at presynaptic boutons. Similar to effects observed postsynaptically, we find that presynaptic disruption of each pathway leads to a loss of presynaptic terminals, though the features of this effect presynaptically differ in important ways from that postsynaptically. We also find that basal, action potential-independent, synaptic vesicle release is largely unaffected by disruption of either the SNX27- or SNX17 pathways. By contrast, unique roles for the two pathways were found in evoked synaptic vesicle release – this was largely spared by depleting neurons of SNX17 or the Retriever complex but was strongly disrupted by targeted depletion of SNX27 or Retromer. We further

identified that disruption of the SNX27-Retromer pathway led to the depletion of both the readily releasable and total recycling pool of synaptic vesicles. Together, our results identify novel roles for each pathway in regulating presynaptic stability and neurotransmission.

3.3 Materials and methods

Subjects

Pregnant Female Sprague Dawley rats, purchased from Charles River Laboratories, were housed on a 12hr light-dark cycle and had food and water available *ad libitum*. Neonatal rat pups (P0-1) of either sex were used to generate primary hippocampal neuron cultures. All procedures were in accordance with the Guide for the Care and Use of Laboratory Animals from the National Institutes of Health and were approved by the University Committee on the Use and Care of Animals (PRO00012210; University of Michigan; Ann Arbor, MI).

DNA Constructs

For knockdown experiments, we used the following shRNA lentiviral plasmids: SNX17 (pLKO.1-puro with shRNA target sequence 5'-CCA-GATGACTTGATCGGATAT-3', TRCN0000190340, Millipore Sigma); SNX27 (pLKO.005-puro with shRNA target sequence 5'-AGCTGGA-GAACCAGGTAATAG-3', TRCN0000253473, Millipore Sigma); VPS26C (pGIPZ vector with shRNA target sequence 5'-TAATCTTGATGTCCA-GAGT-3', V3LMM_455807, Horizon Discovery), VPS26B (pLKO.005- puro with shRNA target sequence 5'-TGCAGCCTAGGTAGGGATAAG-3', TRCN0000306336, Millipore Sigma); and scrambled control (MISSION pLKO.1 scrambled non-target shRNA SHC002, Millipore Sigma). The shRNA-resistant variant of SNX17 were previously described (Rivero-Ríos et al., 2023).
To make this construct resistant to SNX27 shRNA, six silent mutations were introduced into the target site (5'- AGCTGGAGAACCAGGTAATAG-3') using two rounds of Q5 Site- Directed Mutagenesis (New England Biolabs). The first round (primers: 5'-CAGGTAATAGCGTTTGAATGGGATGAGATGC-3' and 5'-GTTTTCAAGTTGCCCTTCTTCAGTGCAGG-3') yielded an intermediate sequence (5'-AACTTGAAAACCAGGTAATAG-3'), and the second round (primers: 5'-CAAGTGATAGCGTTTGAATGGGATGAGATGC-3' and 5'-

ATTTTCAAGTTGCCCTTCTTCAGTGCAGG-3') completed the mutation to 5'-AACTTGAAAATCAAGTGATAG-3', resulting in pCDNA4:TO-GFP- SNX27-R.
DNA was prepared from bacterial cultures grown at 37ºC using a Maxiprep kit (Endofree Plasmid Maxiprep System, QIAGEN) according to the manufacturer's instructions. In all cases, the identity of the constructs was verified by sequencing the entire coding region.

Lentiviral Vectors

Lentiviral transduction-ready viral particles were produced for SNX17, SNX27 and scramble shRNAs by the University of Michigan Vector Core with a concentration of 10^7 transduction units per ml. For lentivirus infection, neurons were infected on DIV7 at an MOI of 2, without polybrene. After overnight incubation, the virus-containing medium was replaced with conditioned medium. Experiments were performed 7 days after lentivirus transduction.

Cell Culture and Transfection

Dissociated hippocampal or cortical neuron cultures from P0-2 rat pups of either sex were prepared as previously described (Henry et al., 2018). Hippocampal neurons were plated at a density of 230-460 mm^2 in poly-D-lysine-coated 35-mm glass-bottom Petri dishes (Mattek), while cortical neurons were seeded at 3-4 x10^6 cells/well on 6-well plates (Costar). Neurons were maintained at 37°C and 5% CO^2 in growth medium (Neurobasal A [Invitrogen] containing 2% B27 [Invitrogen] and 1% Glutamax [Invitrogen]) supplemented with 15% glial conditioned media and 10% cortical conditioned media until DIV14; after DIV14, neurons were maintained in growth medium alone until experiments.

For plasmid transfection, neurons were transfected at DIV12-14 using Lipofectamine 2000 (Invitrogen) according to the manufacturer's recommendations and used 4-5 d after shRNA transfection. For lentiviral delivery of shRNAs, neurons were infected on DIV7 and used for experiments on DIV14.

Immunocytochemistry

Neurons were fixed with 4% paraformaldehyde/4% sucrose in phosphate-buffered saline (PBS) with 1 mM $MgCl_2$ and 0.1 mM $CaCl_2$ (PBS-MC) for 15 min, permeabilized with 0.1%

Triton X-100 for 10 min and blocked with 2% BSA for 1 hr. Neurons were then incubated with primary antibody in blocking buffer overnight followed by 3X 5 min washes in PBS-MC and incubation with secondary antibodies for 1 hr. The secondary antibodies used were, Goat Anti-Rabbit Alexa Fluor 555 (#A21429, Invitrogen).

Analysis of presynaptic function used live-labeling with an Oyster 550-conjugated rabbit polyclonal antibody against the luminal domain of synaptotagmin 1 (syt-1; 1:100, Synaptic Systems). Before labeling, neurons were treated with 2 μm TTX for 15 min for isolating spontaneous neurotransmitter release. Neurons were then labeled with anti-syt-1 for 6 min at room temperature in the presence of 1 μm TTX, washed, fixed with 4% PFA/4% sucrose in PBS-MC, permeabilized, and blocked as above, then labeled with a guinea pig polyclonal anti-vglut1 antibody (1: 2500, Millipore Bioscience Research Reagents). The intrinsic fluorescent signal of the anti-syt-1 at synaptic sites was amplified by an Alexa 555-conjugated goat anti-rabbit (1:500) secondary antibody. An Alexa 488-conjugated goat anti-guinea pig (1:1000) secondary antibody (each for 60 min at room temperature) was used to visualize vglut1 staining. Neurons were selected based on vglut1 epifluorescence to ensure blind sampling of syt-1 expression. For analysis, a syt-1 particle was defined as a particle that occupied >10% of the area defined by a vglut1 particle, and the proportion of vglut1 particles containing synaptic syt-1 particles was calculated using custom written analysis routines for ImageJ. Statistical differences were assessed by ANOVA, followed by Fisher's LSD post hoc tests.

Confocal microscopy and analysis

Aside from vGlut-pH imaging, all other images were acquired with an Olympus FV1000 laser-scanning confocal microscope system with a Plan-Apochromat 63 ×/1.4 oil objective. Z-stacks were captured at 0.4 μm intervals with sequential single-wavelength excitation. The same laser settings and acquisition parameters were used for all treatment conditions in individual experiments. Images were analyzed and processed using Image J.

Bouton numbers were quantified manually by an observer blind to the experimental conditions in 30 μm segments of axons. The JACoP FIJI plugin was used to quantify the colocalization between components of SNX17-Retriever and Synaptophysin. Manders' overlap coefficient was obtained after thresholding the images, and the percentage of colocalization was obtained by

multiplying the coefficient by 100. To prepare representative images, the brightness and contrast were adjusted uniformly over all images of the respective assays using Image J.

vglut-pHluorin imaging

Cultured hippocampal neurons in Mattek dishes were transfected at DIV 14–16 with mCherry-vglut-pHluorin for visual identification of boutons in the absence of stimulation (mCherry) and for quantifying synaptic vesicle release (pHluorin). Experiments were conducted 4-5 d post-transfection in HBS containing 10 μM CNQX and 50 μM DL-APV to block synaptic transmission. Action potentials were evoked via a SIU-102 Stimulus Isolation Unit (Warner instrutments) and A310 Accupulser (World Precision Instruments) using a custom fabricated electric field stimulator, which was inserted into each dish just before the start of an experiment. To observe changes in evoked release, we recorded the change in vglut-pHluorin fluorescence intensity elicited by 20 Hz electrical stimulation for 10 s. To measure specific synaptic vesicle pools, we used well-established stimulation protocols (e.g., Fernandez-Alfonso and Ryan, 2008) in the presence of the vesicular ATPase inhibitor bafilomycin (1 μM) to prevent vesicle reacidification. The Readily Releasable Pool was measured with stimulation delivered at 20 Hz for 2 s, the Total Releasable Pool with stimulation at 20 Hz for 45 s, and the Reserve Vesicle Pool measured by remaining changes in fluorescence induced by 50mM ammonium chloride in HBS to neutralize pH differences. Images were taken using a Prime 95B QE Backside illuminated high speed CMOS camera (Photometrics) mounted on an inverted microscope (Olympus IX83) using a 40× 1.3 NA oil-immersion objective (Olympus). pHlourin imaging was acquired with a 472/30 excitation filter, a 495-edge dichroic mirror, and a 520/30 emission filter. Illumination was achieved using a Lumencor SpectraX high intensity LED light engine. All images were captured at 16-bit depth using Olympus cellSens software. Full frame (1200 × 1200) imaging sequences were acquired at a rate of 5 Hz using 50 ms exposure times. Image sequences were analyzed using the "time series" plug-in for ImageJ (http://rsb.info.nih.gov/ij/plugins/time-series.html). Active synapses were identified for each experiment by subtracting the signal before the initiation of the first train from the peak increase in vglut-pHluorin signal elicited by the stimulus. ROIs were placed over each of the resulting puncta in the "difference image." The time-lapse plug-in was then used to measure average fluorescence for each ROI over time, with photobleaching corrections. Fluorescence signals at

each time-point were quantified as the change in fluorescence at time i (F_i) relative to baseline (F_0), divided by basal fluorescence ($\Delta F/ F_0$); F_0 is defined as the average of five sequential images recorded before the onset of stimulation for each ROI.

Statistical Analysis

All experiments were repeated at least three times. Statistical tests and the size of the samples are described in the figure legends. Data distribution was assumed to be normal, but this was not formally tested. Unless stated otherwise, statistical differences between groups were made using unpaired Student's t-test (2 groups) or one-way Analysis of Variance (ANOVA) with Fisher's LSD post hoc tests (>2 groups). All comparisons were 2-tailed. Data was plotted and analyzed using Microsoft Excel and GraphPad Prism 10.

3.4 Results

Previous studies have documented potent roles for the SNX27-Retromer and SNX17-Retriever endosomal recycling pathways in regulating synapse maintenance and plasticity in the postsynaptic compartment (Loo et al., 2014, Hussain et al., 2014; Rivero Rios et al., 2023, 2025; Chavis et al., 2025). By contrast, relatively little is known about how these pathways regulate the function of the presynaptic compartment in neurons. Components of the SNX27-Retromer pathway are known to be present in axons and in presynaptic terminals, but the localization of SNX17 and Retriever subunits in axons is unknown. To determine where SNX17 localizes in neuronal axons, primary hippocampal neurons were co-transfected with GFP-tagged SNX17 and mCherry-synaptophysin to label axons and synaptic terminals (Fig 3.1A). Under these conditions, SNX17 formed discrete puncta in axons that closely paralleled the distribution of synaptophysin-positive boutons (Fig 3.1B-C). High-magnification views of individual processes revealed frequent overlap between SNX17 and synaptophysin signals, visible as yellow puncta in the merged images, demonstrating SNX17 localization at presynaptic sites (Fig 3.1C). Colocalization analysis was performed on confocal image stacks using thresholded images of SNX17 and synaptophysin channels to calculate Mander's colocalization coefficients. A substantial fraction of synaptophysin-positive boutons contained detectable SNX17 signal, and a corresponding proportion of SNX17 puncta overlapped with synaptophysin (~87%), indicating that SNX17 is not uniformly distributed in axons, but is enriched at presynaptic structures (Fig 3.1D).

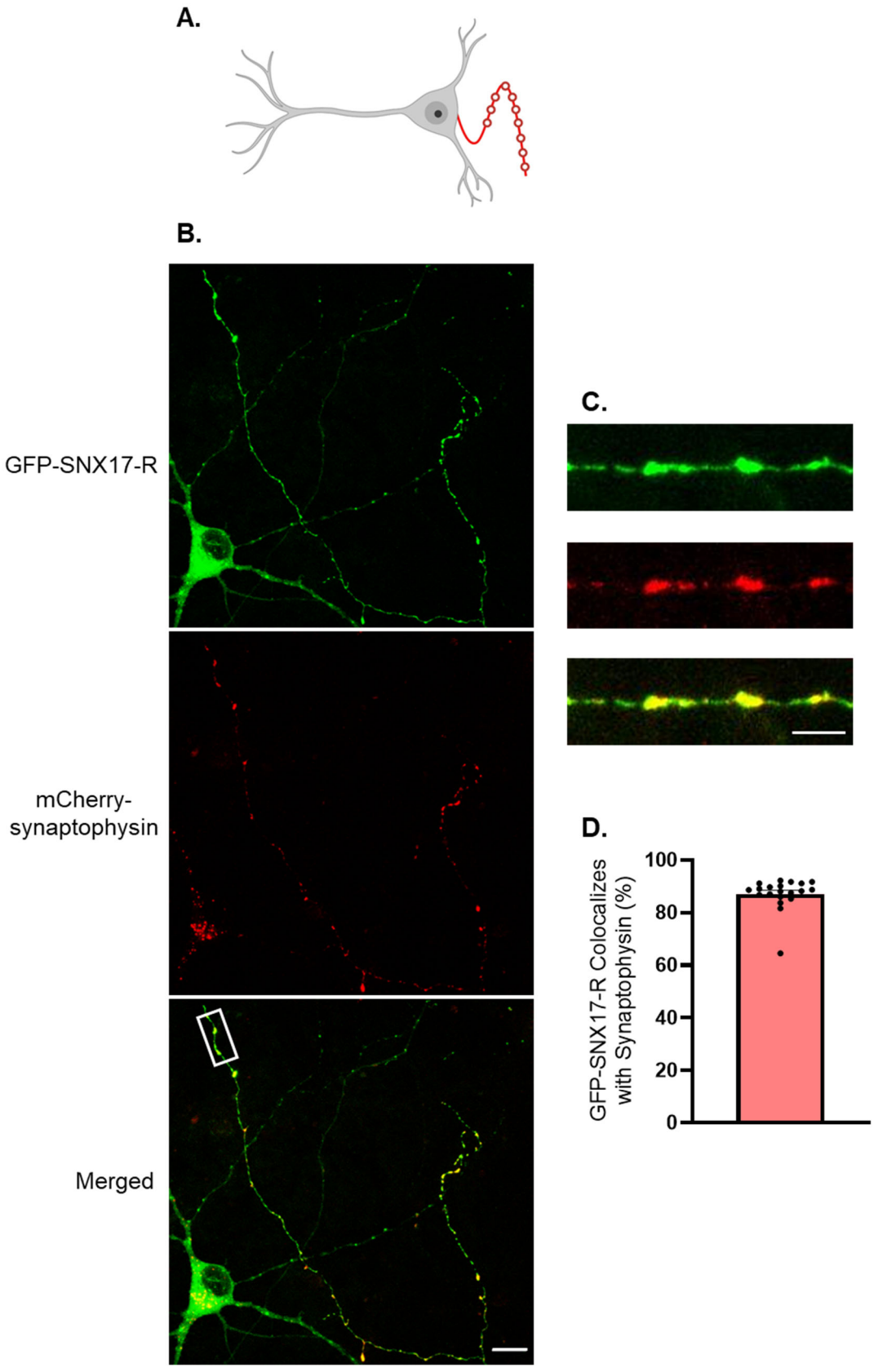

A.
B.
GFP-SNX17-R
mCherry-
synaptophysin
Merged
C.
D.
GFP-SNX17-R Colocalizes
with Synaptophysin (%)
100
80
60
40
20
0

Figure 3.1 SNX17 colocalizes with presynaptic terminals

(A). Cartoon schematic showing "beads on a string" morphology when cells express mCherry-Synaptophysin. **(B-C)**. Representative images of DIV 18-20 primary hippocampal neurons expressing recombinant GFP-SNX17. Scale bars = 20 μm, Scale bars = 5 μm. **(D)**. Mean ± SEM percent of GFP-SNX17 colocalized with mCherry-Synaptophysin (mean = 87.12%, n = 20).

3.4.1 SNX17 and SNX27 are necessary to maintain presynaptic terminals in axons

In the postsynaptic compartment, depletion of SNX17 or SNX27 each lead to pronounced loss of dendritic spines and synapses, and SNX17/27 co-depletion produces additive synapse loss (Chavis et al., 2025). To assess whether SNX17 and SNX27 contribute to synapse maintenance in the presynaptic compartment, DIV 14-16 primary hippocampal neurons were transfected with a plasmid encoding mCherry-Synaptophysin together with shRNAs targeting either SNX17, SNX27, or a non-targeting shRNA control. mCherry-Synaptophysin marks concentrations of synaptic vesicles along axonal processes, thus identifying presynaptic boutons (Fig 3.1A). Presynaptic bouton density was quantified as the number of mCherry-Synaptophysin positive puncta per μm of straightened axonal segment in each condition. Neurons expressing shRNA against SNX17 displayed a significant reduction in bouton density compared with control shRNA expressing neurons (Fig 3.2A-B). Similarly, knockdown of SNX27 resulted in a decrease in bouton density, indicating that both proteins are required to maintain normal numbers of presynaptic boutons (3.2A-B). Together, these results suggest that SNX17- and SNX27-dependent pathways support the maintenance of presynaptic boutons in hippocampal neurons.

To ensure that these effects on presynaptic terminal density are due to specific effects of each shRNA, we examined whether re-introduction of SNX17 or SNX27 would rescue these changes. Neurons were co-transfected with mCherry-Synaptophysin, the corresponding shRNA (targeting SNX17 or SNX27), and an RNAi-resistant SNX17 or SNX27 expression construct (Fig 3.2C-F). Quantification of mCherry-Synaptophysin puncta density in axons showed that RNAi-resistant SNX17 and SNX27 expression significantly rescued the decrease observed with shRNA alone, returning bouton density to control or near control values (Fig 3.2D,F). Recent work shows that depletion of SNX17 and SNX27 in the postsynaptic compartment produces additive loss of excitatory synapses, revealing a parallel organization of the SNX17-

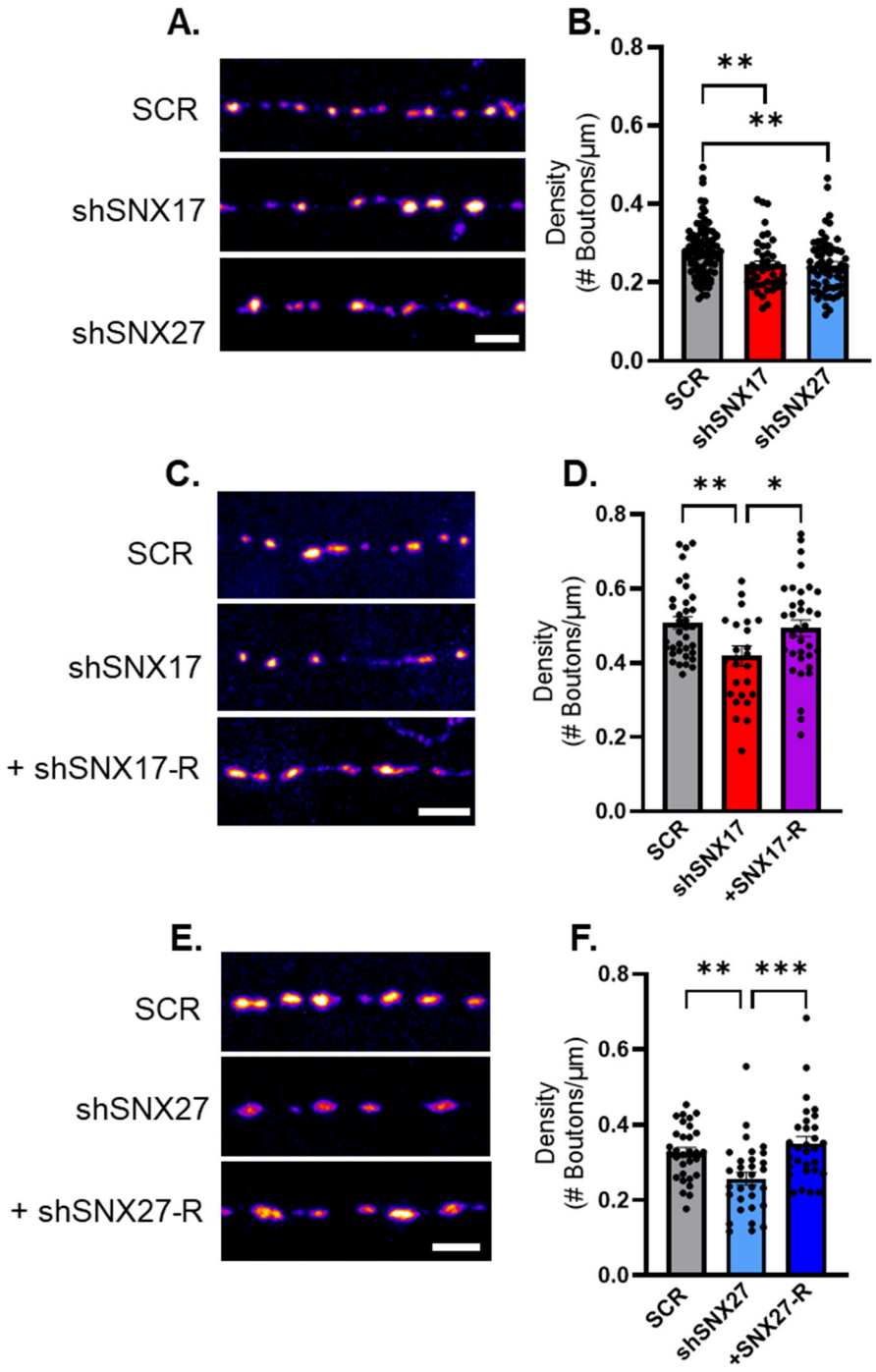


Figure 3.2 SNX17 and SNX27 are necessary to maintain presynaptic terminals in axons

(A). Representative images of straightened axons from DIV 18-20 primary hippocampal neurons (Scale bar = 5 µm) expressing mCherry-Synaptophysin along with shRNA against SNX17 (n = 88 neurons), SNX27 (n = 42 neurons), or a non-targeting shRNA (SCR) as control (n = 63 neurons). **(B).** Quantification of bouton density using mCherry-Synaptophysin as bouton marker and indicated plasmid constructs. Knockdown of SNX17 or SNX27 each induced a significant decrease in bouton density relative to SCR controls ($F_{2,190} = 6.78$, $p = 0.001$; ** $p < 0,01$ by Fisher's LSD). **(C).** Representative straightened axons from DIV 18-20 primary hippocampal neurons co-expressing mCherry-Synaptophysin with shRNA against SNX17 with (n = 34 neurons) or without (n = 26 neurons) expression

of an RNAi-resistant SNX17 or a SCR shRNA control (n = 36 neurons); scale bar = 5 μm. **(D).** Mean ± SEM bouton density in the indicated groups. SNX17 knockdown induced a significant loss of presynaptic terminals, that were rescued by expression of RNAi-resistant SNX17 ($F_{2,93}$ = 4.49, p = 0.01; * p <0.05, ** p < 0.01 vs shSNX17 group by Fisher's LSD). **(E).** Representative images of straightened axons from DIV 18-20 primary hippocampal neurons co-expressing mCherry-Synaptophysin with shRNA against SNX27 with (n = 30 neurons) or without (n = 31 neurons) expression of an RNAi-resistant SNX27 or a SCR shRNA control (n = 31 neurons); scale bar = 5 μm. **(F).** Mean ± SEM bouton density in the indicated groups. SNX27 knockdown induced a significant loss of presynaptic terminals, that was rescued by expression of RNAi-resistant SNX27 ($F_{2,89}$ = 8.92 p = 0.0003; ** p <0.01, *** p < 0.001 vs shSNX27 group by Fisher's LSD).

Retriever and SNX27-Retromer pathways postsynaptically in synapse maintenance (Chavis et al., 2025). To test whether SNX17 and SNX27 act in overlapping or parallel pathways for synapse maintenance in the presynaptic compartment (Fig 3.3A), we next examined whether simultaneous knockdown of both proteins would have additive effects on bouton loss. Primary hippocampal neurons were co-transfected with mCherry-Synaptophysin together with shRNAs targeting SNX17 and SNX27, using the same conditions as in the single knockdown experiments (Fig 3.3B). As before, we found that depletion of SNX17 or SNX27 individually induced a significant reduction in axonal bouton density (Fig 3.3C). Unlike previous findings with postsynaptic SNX17/27 depletion, neurons subjected to double knockdown displayed a reduction in mCherry-Synaptophysin-positive boutons that was comparable to that observed with individual SNX17 or SNX27 knockdown, indicating a lack of an additive effect (Fig 3.3C). These data do not support the idea that SNX17 and SNX27 function in parallel to control bouton maintenance and raise the possibility that perhaps a shared cargo supports presynaptic terminal stability.

3.4.2 SNX17-Retriever and SNX27-Retromer pathways are not required for spontaneous synaptic vesicle release

As a starting point to determine how the SNX17-Retriever and SNX27-Retromer pathways regulate presynaptic function, we disrupted each pathway and monitored spontaneous, action potential (AP)-independent synaptic vesicle release using a previously established optical readout (Jakawich et al., 2010). Here, neurons are live-labeled with an antibody targeting the lumenal domain of synaptotagmin 1 (α-syt1) in the presence of tetrodotoxin (TTX; 2 μM) to block APs, followed by immunocytochemistry against the vesicular glutamate transporter (vGlut1) to mark all excitatory synaptic boutons. Under these conditions, the α-syt1 antibody

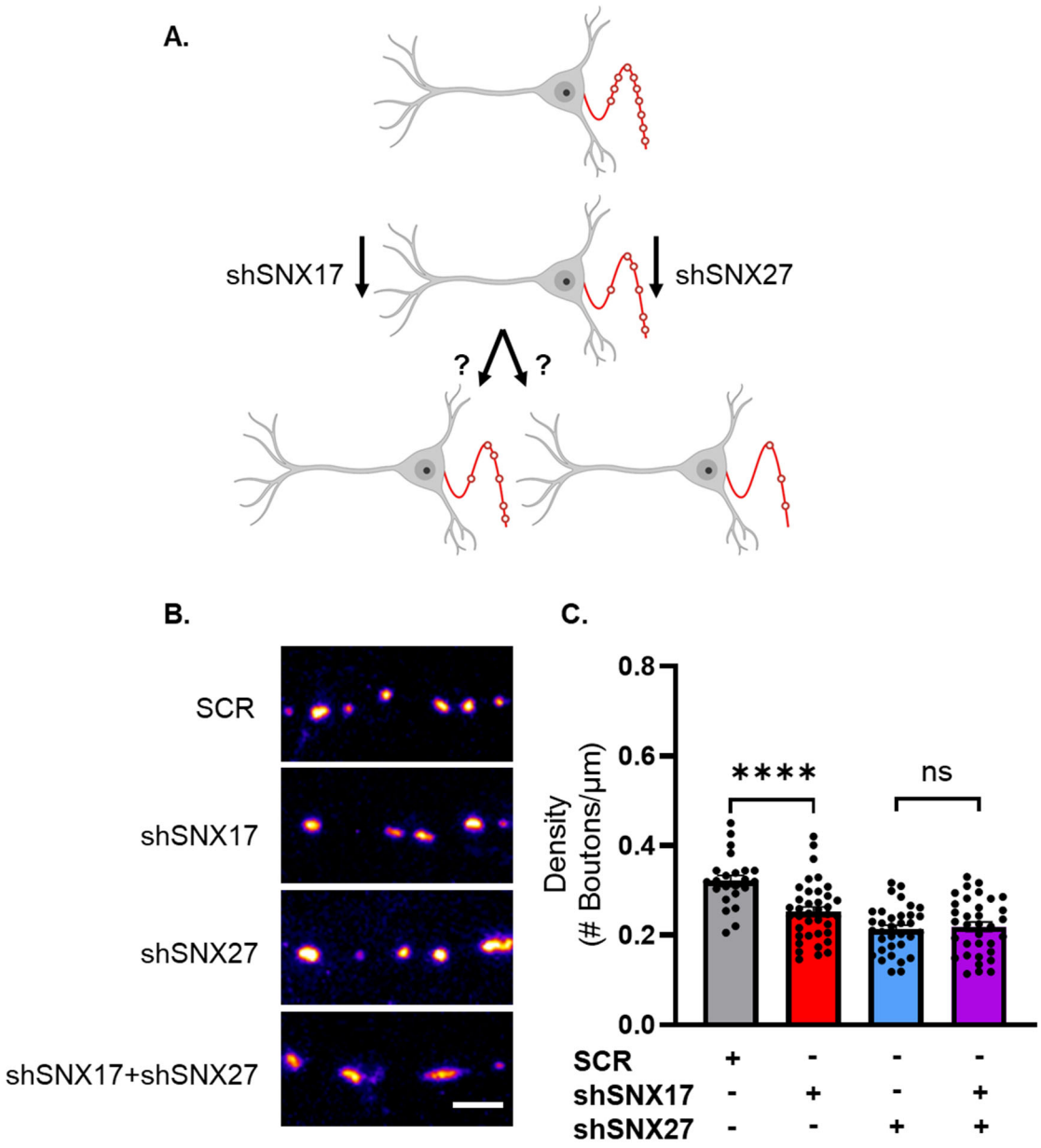


Figure 3.3 Depletion of SNX17 and SNX27 induces non-additive loss of presynaptic boutons

(A). Cartoon schematic showing two potential outcomes arising from coordinate disruption of the SNX17-Retriever and SNX27-Retromer pathways. If these pathways function in parallel for bouton maintenance, we would expect coincident SNX17/27 knockdown to induce additive bouton loss relative to individual SNX17 or SNX27 knockdown (right). If these pathways play overlapping roles in bouton maintenance, synapse loss should be similar to knockdown of SNX17 or SNX27 individually (left). **(B).** Representative mCherry-Synaptophysin images from axons co-expressing SCR shRNA (control; n = 23 neurons) or shRNAs targeting SNX17 (n = 38 neurons), SNX27 (n = 34 neurons), or both SNX17 and SNX27 (n = 34 neurons); scale bar = 5 µm. **(C).** Mean ± SEM bouton density in the indicated groups. SNX17 and SNX27 knockdown induced a significant loss of presynaptic terminals relative to SCR controls ($F_{3,125}$ = 17.92, $p < 0.0001$; *****$p < 0.0001$, by Fisher's LSD); bouton loss following coordinate SNX17/27 knockdown was not significantly different than SNX27 knockdown on its own (ns = $p > 0.05$, by Fisher's LSD).

only has access to its antigen when a synaptic vesicle fuses with the plasma membrane (Fig 3.4A). To validate this assumption, we examined α-syt1 uptake in the presence of TTX under brief labeling conditions (90 s) and used Hi K^+ (60 mM K^+) to directly depolarize presynaptic terminals and drive release. As shown in Fig 3.4B-C, Hi K^+ induced a dramatic increase in α-syt1 uptake specifically at vGlut1-positive synaptic terminals, validating this approach as an optical readout of spontaneous AP-independent synaptic vesicle release.

We next examined how SNX17 or SNX27 depletion affected AP-independent synaptic vesicle release. We exposed DIV7 neurons to lentiviral vectors expressing shRNA against SNX17, SNX27, or a non-targeting scrambled shRNA as a control. 7 days later, DIV14 hippocampal neurons were subjected to live labeling with α-syt1 for 6 min in the presence of 1 μM TTX, then fixed and immunostained for vGlut1 (Fig 3.5A-B). We found that α-syt1 uptake at vGlut1-positive excitatory boutons was comparable among groups and not significantly altered by either SNX17 knockdown or SNX27 knockdown, relative to Scr control neurons (Fig 3.5C). These data suggest that SNX17- and SNX27-dependent pathways influence synapse maintenance without grossly perturbing basal features of presynaptic AP-independent vesicle release.

3.4.3 The SNX27-Retromer pathway, but not SNX17-Retriever, is required for normal evoked synaptic vesicle release

We next examined the role of each endomembrane recycling pathway in supporting normal AP-triggered neurotransmission. To examine this evoked release, we employed vGlut1-pHluorin (vGlut-pH) to visualize synaptic vesicle exocytosis in cultured hippocampal neurons (Balaji and Ryan, 2007; Cazares et al., 2015; Pulido and Ryan, 2021). This approach leverages the fact that fluorescence from the pH-sensitive GFP variant super ecliptic pHluorin is quenched at the pH of the synaptic vesicle lumen (pH ~ 5.5), thus permitting reliable visualization of synaptic vesicle exocytosis at individual boutons via dequenching when the vesicle lumen becomes neutral (Fig 3.6A-B). The vGlut-pH probe was also tagged with mCherry, which

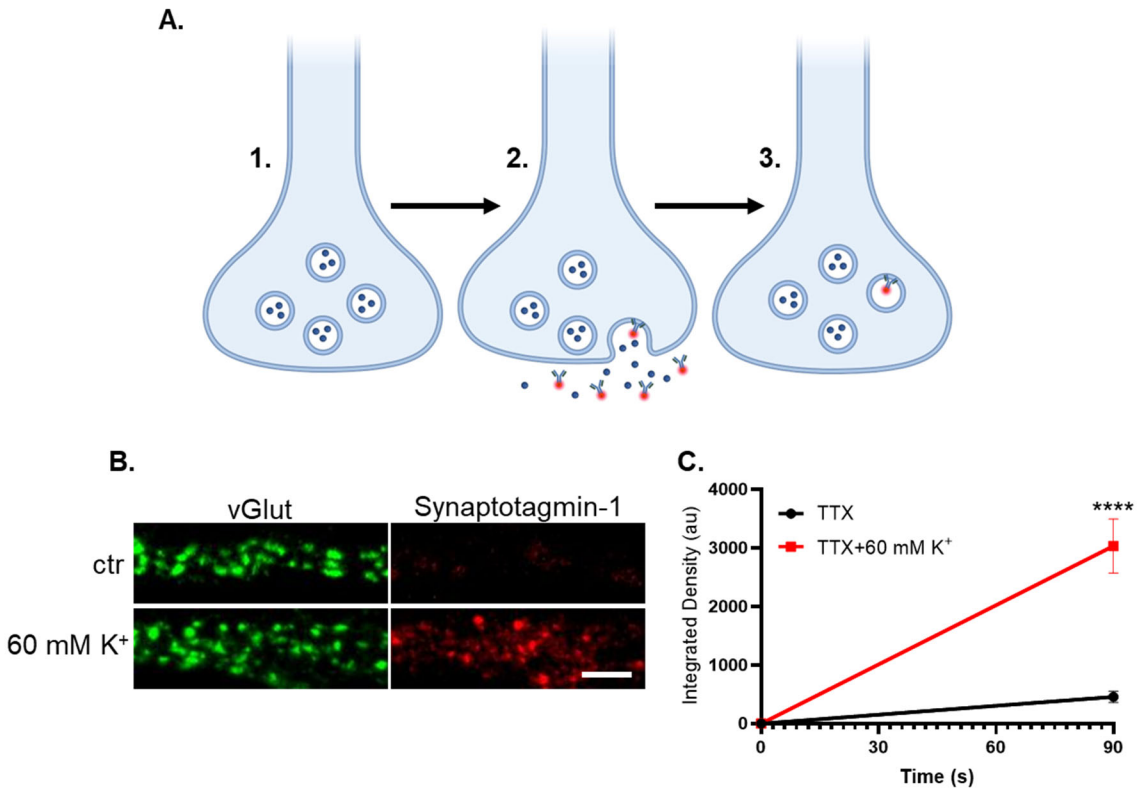


Figure 3.4 Measuring basal AP-independent synaptic vesicle release via live labeling of synaptotagmin 1 in the vesicle lumen

(A). Cartoon schematic denoting the logic of the experimental approach. Neurons are treated with TTX to block APs, then briefly live-labeled with an Oyster 550- conjugated anti-synaptotagmin 1 antibody that targets an epitope confined to the vesicle lumen (α-syt1). Synaptic vesicles within the presynaptic terminal remain unlabeled (panel 1) and only when a vesicle fuses with the plasma membrane does α-syt1 gain access to the epitope (panel 2); vesicles that fused and have been retrieved from the surface remain labeled (panel 3). **(B).** Representative 90s α-syt1 labeling in TTX-treated neurons following direct depolarization of presynaptic terminals with elevated K^+ ($V_m \sim 0$ mV) to drive synaptic vesicle release; following α-syt1 labeling, neurons were fixed, permeabilized, and stained with vGlut1 to mark excitatory boutons; scale = 5 µm **(C).** Mean ± SEM α-syt1 labeling (expressed as Integrated Density) at vGlut1-positive presynaptic terminals. Direct bouton depolarization (n = 9 neurons) induced a significant increase in α-syt1 labeling relative to TTX alone (n = 12 neurons) condition (****$t_{19} = 6.26$, $p < 0.0001$).

allowed us to visualize presynaptic terminals prior to stimulation. A series of baseline images were acquired at a frame rate of 50 ms, then a 20 Hz train (10 s) of APs were elicited via field stimulation between parallel platinum iridium electrodes. Representative vGlut-pH images of neurons are shown in Fig 3.6A-B. Prior to stimulation, mCherry fluorescence is visible as discrete fluorescent puncta along axonal processes, revealing the location of presynaptic boutons (Fig 3.6A). Following electrical field stimulation, we observed robust increases in vGlut-pH fluorescence at individual synaptic terminals followed by exponential decay, reflecting activity-

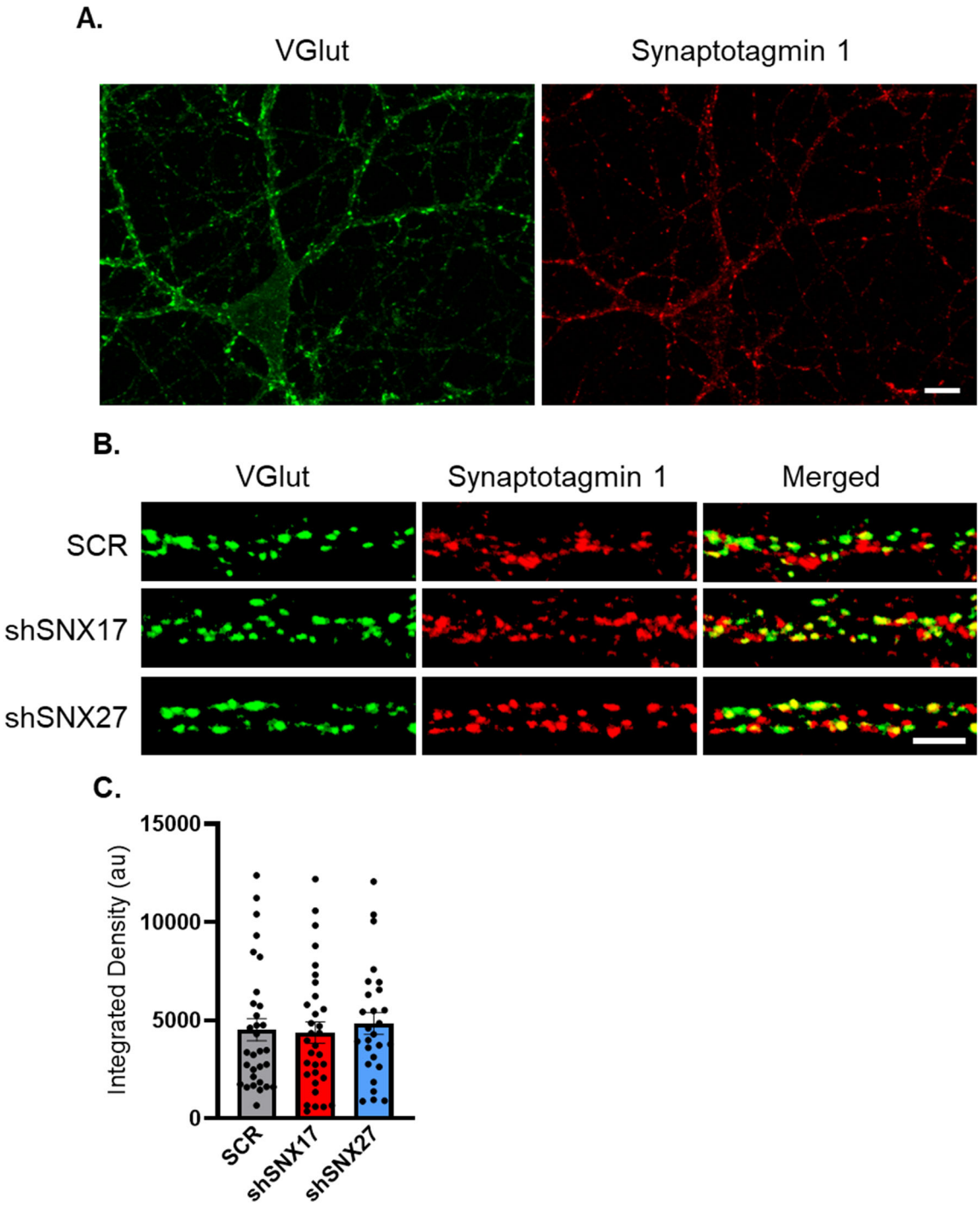


Figure 3.5 SNX17-Retriever and SNX27-Retromer pathways are not required for spontaneous synaptic vesicle release

(A). Representative full-frame images of vGlut1 (Green) and α-syt1 (red) signals from DIV 18-20 primary hippocampal neurons in the presence of TTX; scale bar = 20 µm. **(B).** Representative vGlut1 and α-syt1 images of straightened neurite segments from neurons expressing SCR shRNA (control; n = 31 neurons), SNX17 shRNA (n = 32 neurons), and SNX27 shRNA (n = 27 neurons); scale bar = 5 µm. **(C).** Mean ± SEM α-syt1 labeling (expressed as Integrated Density) at vGlut1-positive presynaptic terminals from the groups described in **(B-C).** Neither SNX17

depletion or SNX27 depletion altered spontaneous AP-independent synaptic vesicle release relative to SCR control neurons ($F_{2,87} = 0.17$, $p > 0.05$).

dependent synaptic vesicle fusion and vesicle reacidification following endocytic retrieval, respectively (Fig 3.6B). These activity-dependent changes in vGlut-pH are consistent with numerous other studies deploying this probe to measure features of AP-triggered synaptic vesicle release (e.g., Balaji and Ryan, 2007; Cazares et al., 2015; Pulido and Ryan, 2021).

To measure the presynaptic impact of SNX17 and SNX27 depletion on AP-triggered release, DIV 14-15 hippocampal neurons were co-transfected with shRNAs targeting SNX17 or SNX27 (or Scr shRNA as a control), along with the mCherry-vGlut-pH probe. Effects of SNX17 or SNX27 knockdown were always assessed with inter-leaved Scr expressing neuron experiments. 4-5 d following transfection, synaptic vesicle exocytosis was elicited as above during image acquisition, then axons were digitally straightened, and vGlut-pH signals were quantified as the change in fluorescence divided by the initial fluorescence ($\Delta F/F_0$). As shown in Fig 3.7A, basal vGlut-pH fluorescence was low prior to stimulation in both Scr- and SNX17 shRNA-expressing neurons, and in both conditions, markedly increased during the stimulus train (Fig 3.7B). We examined the time course of vGlut-pH $\Delta F/F_0$ and found that this was virtually indistinguishable in neurons expressing Scr- or SNX17-targeting shRNA (Fig 3.7B-C). We did find that the axonal density of boutons that exhibited detectable release was significantly reduced by SNX17 depletion (Mean ± SEM, SCR = 0.2337 ± 0.01582, shSNX17 = 0.1682 ± 0.01582; Fig 3.7D), which is consistent with the loss of presynaptic terminals we describe earlier.

While depleting SNX17 expression in neurons had little impact on AP-triggered release, SNX27 knockdown produced a pronounced impairment in evoked release. As before, 20 Hz stimulation drove a robust increase in vGlut-pH signal $\Delta F/F_0$ in Scr-expressing control neurons, but this was markedly reduced in SNX27 shRNA-expressing neurons (Fig 3.7E-H). Time course analysis revealed a slower rate of fluorescence rise compared to control neurons (Fig 3.7F-G) during stimulation. In addition, as with SNX17 knockdown, the density of active boutons was significantly diminished in SNX27 knockdown neurons (Mean ± SEM, SCR = 0.2254 ± 0.01745, shSNX27 = 0.1632 ± 0.01745; Fig 3.7H), again consistent with the effects on terminal

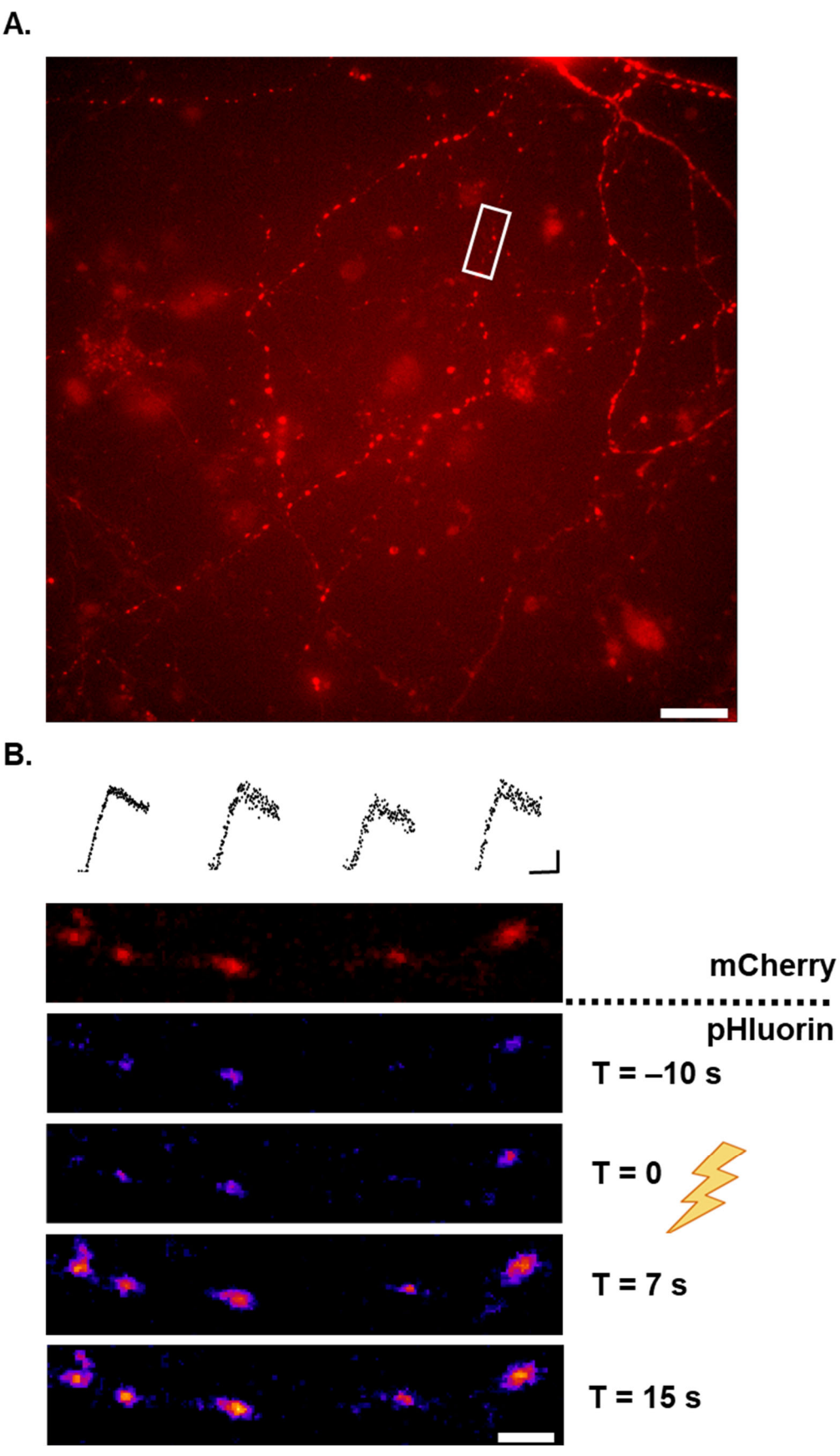

A.
B.
mCherry
pHluorin
T = –10 s
T = 0
T = 7 s
T = 15 s

Figure 3.6 Using mCherry-vGlut1-pHluorin to measure evoked synaptic vesicle release from individual presynaptic boutons

(A). Representative image of mCherry signal (red) from neurons expressing the mCherry-vGlut1-pHluorin construct (scale bar = 20 μm). Bright red puncta mark individual presynaptic terminals **(B).** Higher magnification of boxed region in **(A)** depicting mCherry signal and vglut-pH signal before (T = -10 s, 0), during (T = 7 s), and immediately following a 20 Hz elicited by field stimulation; scale bar = 5 μm. Representative $\Delta F/F_0$ traces are superimposed over 5 individual active boutons; scale bar = 0.25 $\Delta F/F_0$, 10 s.

density we reported earlier. These data demonstrate that SNX27, but not SNX17, is required for efficient evoked synaptic vesicle release during sustained neuronal activity.

To further test whether these effects on evoked release indicate different roles for the SNX17-Retriever and SNX27-Retromer pathways, we also examined effects of depleting the core complex subunits VPS26B (Retromer) and VPS26C (Retriever). Consistent with the SNX27 results, knockdown of VPS26B led to a significant and marked decrease in evoked release relative to Scr controls, whereas VPS26C knockdown produced no detectable effect (Fig 3.8A-C). Again, this impairment was evident as both a slower rise of $\Delta F/F_0$ (Fig 3.8B). and a decrease in the peak $\Delta F/F_0$ intensity (Fig 3.8C) during 20 Hz field stimulation. Together, these results indicate unique roles for the SNX27–Retromer and SNX17-Retriever recycling pathways in supporting AP-triggered neurotransmitter release.

3.4.4 SNX27 regulates multiple vesicle pools that participate in AP-triggered neurotransmission

Synaptic vesicle pools play a key role in determining how presynaptic terminals respond to different patterns of neuronal activity. The readily releasable pool (RRP) supplies vesicles that fuse rapidly in response to brief stimulation, whereas the total recycling pool (TRP) reflects the broader reservoir of vesicles that can be mobilized during sustained firing. Disruptions in these pools can therefore reveal whether a given knockdown primarily affects initial release, ongoing vesicle recycling, or both. To distinguish how SNX27 contributes to these functionally distinct vesicle populations, we applied 20 Hz stimulation for 2 seconds and 45 seconds in the presence of bafilomycin to selectively probe the RRP and TRP, respectively (Fig 3.9A).

Using this paradigm, we found that SNX27 knockdown led to a clear reduction in both the RRP and TRP signals, indicating that loss of SNX27 compromises not only the pool of vesicles immediately available for release, but also the larger recycling reservoir that sustains prolonged activity (Fig 3.9B). These preliminary findings suggest that SNX27 plays a more prominent role

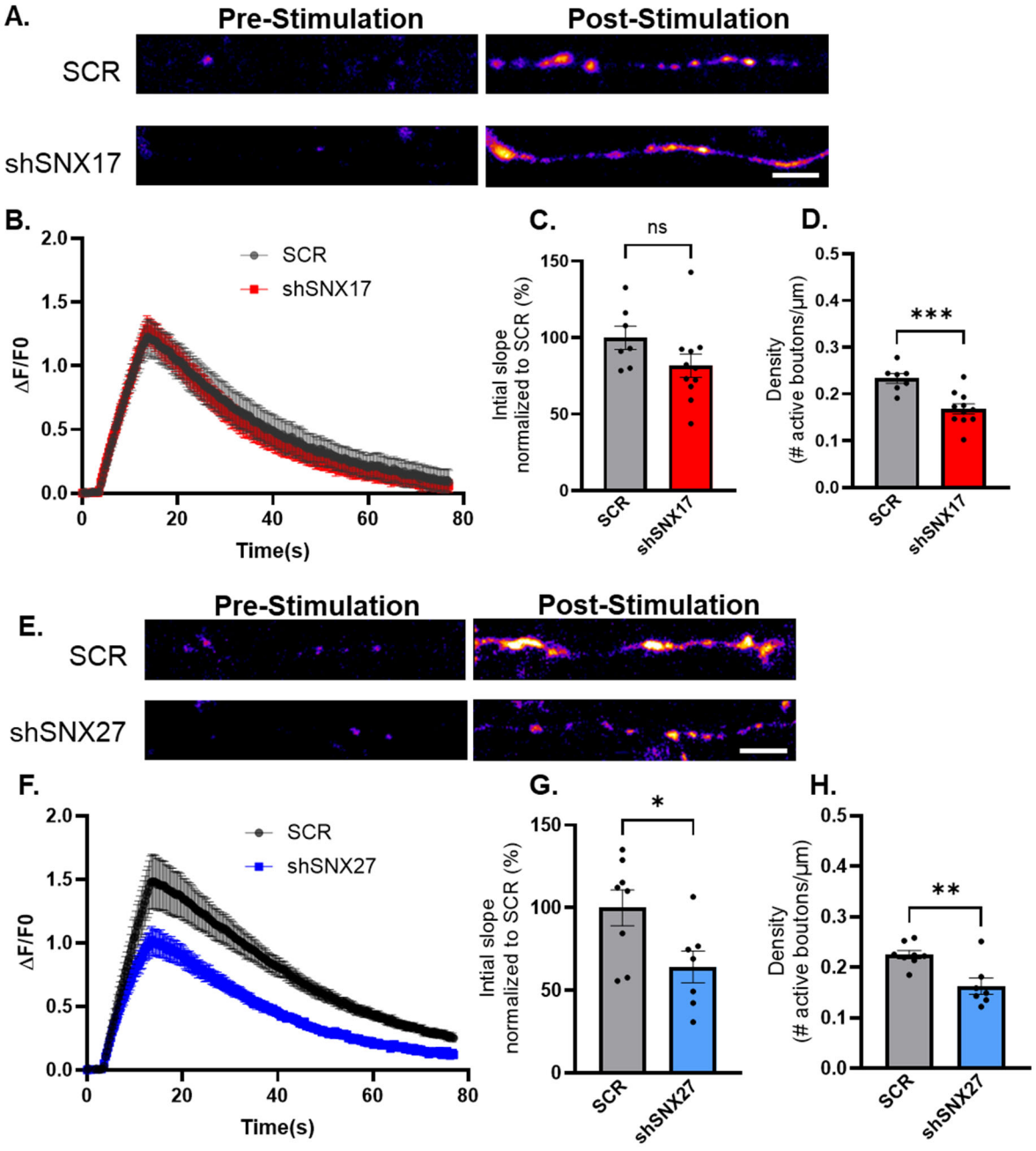


Figure 3.7 The SNX27-Retromer pathway, but not SNX17-Retriever, is required for normal evoked synaptic vesicle release

(A). Representative vGlut-pH images of straightened axonal segments from DIV 18-20 primary hippocampal neurons co-expressing either SCR shRNA (n = 7 neurons) or SNX17 shRNA (n = 11 neurons) before and following

field stimulation; scale bars = 5 μm). **(B-C).** Time course of vglut-pH fluorescence (expressed as $\Delta F/F_0$) in response to a 20 Hz train of APs for 10 s. vglut-pH signals were statistically indistinguishable between SNX17-depleted neurons and SCR controls (Mean ± SEM rising slope (normalized to average SCR), SCR = 100.0 ± 11.30, shSNX17 = 81.81 ± 11.30; $t_{16} = 1.610$, $p > 0.05$). **(D).** Mean ± SEM density of active bouton sites in axons, defined by vGlut-pH signals. SNX17 knockdown neurons exhibited significantly reduced density of active boutons relative to SCR controls ($t_{16} = 4.14$, $p = 0.0008$). **(E).** Representative vGlut-pH images of straightened axonal segments from DIV 18-20 primary hippocampal neurons co-expressing either SCR shRNA (n = 8 neurons) or SNX27 shRNA (n = 7 neurons) before and following field stimulation; scale bars = 5 μm. **(F-G).** Time course of vglut-pH fluorescence (expressed as $\Delta F/F_0$) in response to a 20 Hz train of APs for 10 s. vglut-pH signals revealed significantly diminished evoked release in SNX27-depleted neurons vs SCR controls (Mean ± SEM rising slope (normalized to average SCR), SCR = 100.0 ± 14.67, shSNX27 = 64.33 ± 14.67; $t_{13} = 2.431$, $p < 0.05$). **(H).** Mean ± SEM density of active bouton sites in axons, defined by vGlut-pH signals. SNX27 knockdown neurons exhibited significantly reduced density of active boutons relative to SCR controls ($t_{13} = 3.56$, $p = 0.0035$).

in evoked transmission, at least in part, by regulating multiple functional vesicle pools at presynaptic boutons. However, because these experiments are based on limited replicates, additional recordings will be necessary to rigorously validate the observed differences in vesicle pool size and dynamics.

3.5 Discussion

The SNX17 and SNX27 recycling pathways regulate presynaptic structure and function in distinct ways. This chapter demonstrates that both SNX17-Retriever and SNX27-Retromer complexes localize to and support the maintenance of presynaptic boutons in hippocampal neurons, with SNX27 exerting a more prominent role in synaptic vesicle release and pool maintenance.

While components of the SNX27-Retromer pathway have been previously documented in axons and at presynaptic terminals (Vazquez-Sanchez, S., et al. 2018; Walsh, R. B., et al. 2021; Ye, H., et al. 2020) it was not clear whether the SNX17-Retriever pathway is present in axons. We addressed this issue by expressing recombinant GFP-tagged SNX17 along with mCherry-synaptophysin, which allows the reliable identification of axons and presynaptic terminals based on the unique features of this neuronal process (diameter, length, and "beads-on-a-string" morphology). We find that GFP-SNX17 is prominently expressed in axons, where it extensively co-localizes with synaptophysin-positive axonal boutons, confirming its access to presynaptic endosomal compartments (Fig 3.1). Localization of recycling pathways has been more extensively examined in neuronal dendrites, where SNX17 exhibits tight spatial alignment with

endosomes, the Retriever complex, and SNX27. It is important for future studies to confirm the axonal distribution of endogenous SNX17 and to determine its spatial relationship with endosomes, the Retriever complex, and components of the SNX27-Retromer pathway in axons.

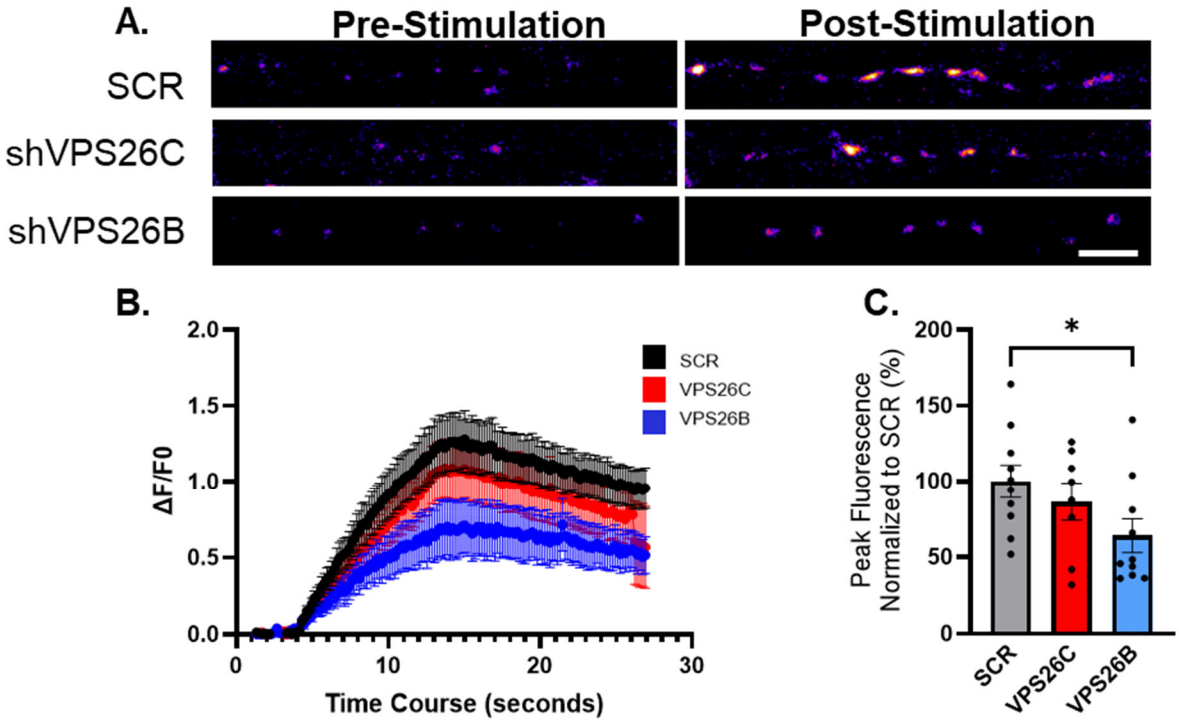


Figure 3.8 Depletion of core Retromer and Retriever subunits reveals unique roles for the SNX27-Retromer and SNX17-Retriever pathways in regulating evoked vesicle release

(A). Representative vGlut-pH images of straightened axonal segments from DIV 18-20 primary hippocampal neurons co-expressing either SCR shRNA (n = 10 neurons), shRNA targeting the Retromer subunit VPS26B (n = 8 neurons), or shRNA targeting the Retriever subunit VPS26C (n = 10 neurons) before and following field stimulation; scale bar = 5 µm). **(B).** Time course of vglut-pH fluorescence (expressed as $\Delta F/F_0$) in response to a 20 Hz train of APs for 10 s. vglut-pH signals were similar VPS26C-depleted neurons and SCR controls, but significantly diminished in VPS26B-depleted neurons (Mean ± SEM rising slope (normalized to average SCR), SCR = 100.0 ± 34.20, shVPS26C = 95.24 ± 34.20, $t_{11} = 0.1392$, $p = 0.4459$; shVPS26B = 71.59 ± 25.49, $t_{14} = 1.115$, $p = 0.1419$. **(C).** Mean ± SEM peak vGlut-pH response, normalized to average in SCR controls. Peak vGlut-pH responses were significantly reduced in VPS26B-depleted neurons, relative to SCR controls and VPS26C-depleted neurons ($t_{18} = 2.33$, $p = 0.032$)

3.5.1 The SNX27-Retromer and SNX17-Retriever pathways contribute to the maintenance of axonal boutons.

Previous work has demonstrated that a precipitous loss of dendritic spines and excitatory synapses accompanies depletion of either SNX17, SNX27, or core subunits of the Retriever and

Retromer complexes (Rivero-Rios et al., 2023; Chavis et al., 2025). We found that knockdown of either SNX17 or SNX27 reduced presynaptic bouton density along axons without altering overall neuronal morphology, axon length, or individual bouton size (Fig 3.2). These structural deficits were fully rescued by shRNA-resistant constructs, establishing specificity and indicating that both recycling adaptors are required for bouton maintenance, as they are for dendritic spines in the postsynaptic compartment (Chavis et al., 2025). The lack of gross morphological changes

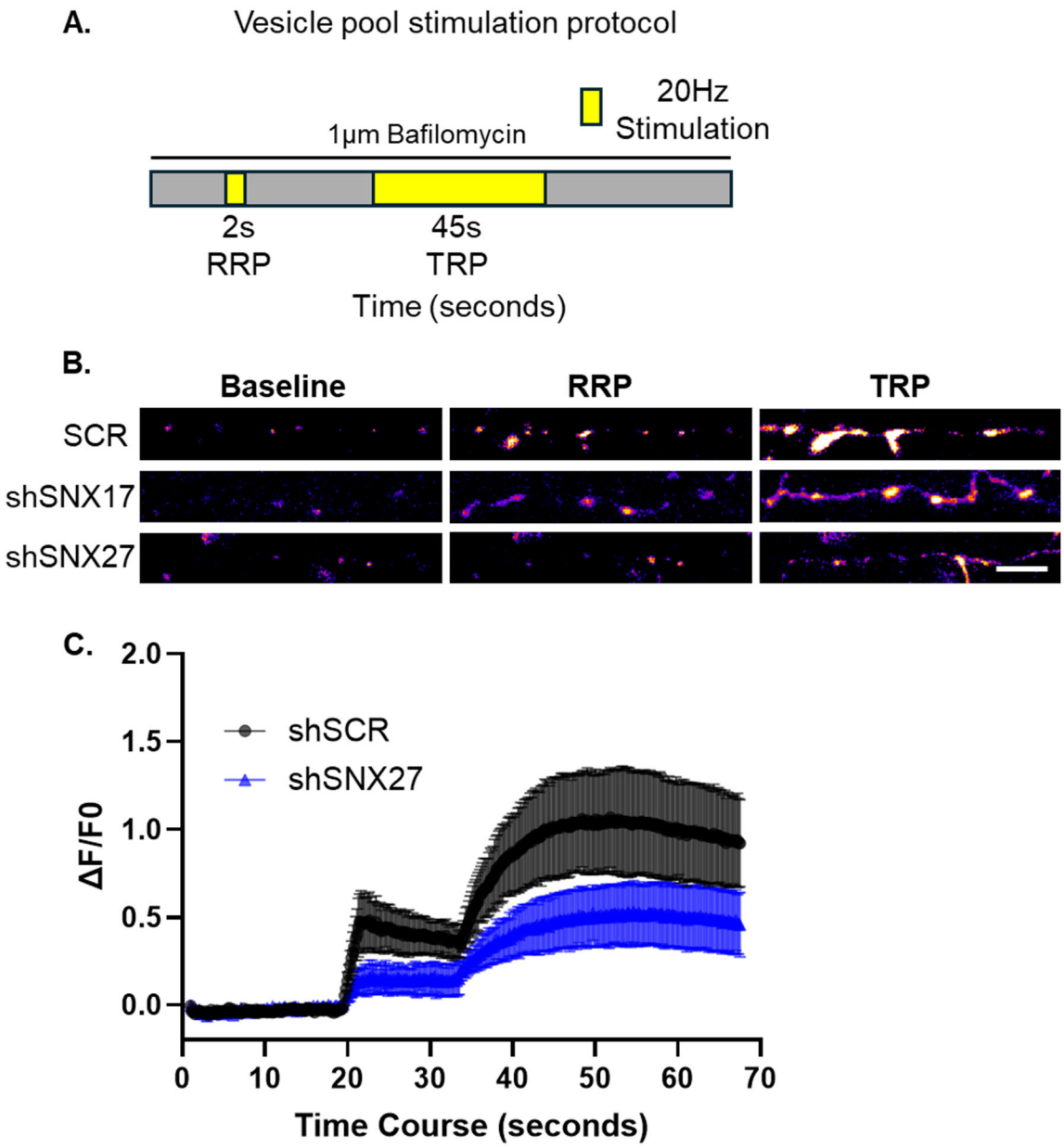


Figure 3.9

Figure 3.9 The SNX27-Retromer pathway regulates multiple synaptic vesicle pools that participate in evoked neurotransmission

(A). Experimental paradigm with stimulation protocols for measuring the Readily Releasable Pool (RRP) and the Total Recycling Pool (TRP) of synaptic vesicles. RRP and TRP are measured in succession in the presence of 1 μM Bafilomycin to prevent vesicle reacidification. **(B).** Representative vGlut-pH images of straightened axonal segments from DIV 18-20 primary hippocampal neurons co-expressing SCR shRNA (n = 3) or SNX27 shRNA (n = 3); scale bar = 5 μm. **(C).** Time course of vGlut-pH fluorescence ($\Delta F/F_0$) over the course of the experiment – the early rise represents the RRP, while the later rise represents the TRP. Relative to SCR controls, SNX27 depletion significantly reduced the size of both the RRP (Group x time 2 factor ANOVA, Main effect of group, $F_{1,1604} = 4896$, $p < 0.0001$, mean of SCR = 0.1234, shSNX27 = -0.0099) and the TRP (Main effect of group, $F_{1,1600} = 2562$, $p < 0.0001$, mean of SCR = 0.4633, shSNX27 = 0.1363).

suggests these pathways specifically stabilize presynaptic sites rather than broadly disrupt axonal development. This aligns with established roles of endosomal recycling in regulating adhesion molecules and scaffolding proteins that anchor synaptic contacts (Böttcher et al., 2012; Loo et al., 2014). Notably, SNX17's presynaptic enrichment extends its previously documented postsynaptic functions in β1-integrin trafficking during activity-dependent plasticity (McNally et al., 2017; Rivero-Ríos et al., 2023).

Despite this overall similarity between pre- and post-synaptic roles of SNX17/27 in synapse stability, we note two important differences in effects driven by knockdown in the pre- vs post-synaptic compartment. First, the magnitude of synapse loss was noticeably more modest when depleting either SNX17 or SNX27 presynaptically, as compared to postsynaptic knockdown. The loss of boutons in axons is ~ 15-20% in each case, while postsynaptic depletion produces a more robust ~ 40% loss of dendritic spines and functional synapses (Chavis et al., 2025). The reasons for this difference are not obvious but could reflect a stronger maintenance role for ongoing protein recycling in the postsynaptic, relative to the presynaptic compartment. A second major difference between pre- and postsynaptic effects of SNX17/27 depletion is that combined presynaptic SNX17/SNX27 knockdown failed to produce additive reductions in bouton density (Fig 3.3). Coincident SNX17/27 knockdown postsynaptically induces additive loss of dendritic spines and excitatory synapses (Chavis et al., 2025), indicating that each pathway regulates synapse maintenance in parallel. The non-additive effects seen presynaptically suggests the two complexes either cooperate at common endosomal sorting hubs or recycle partially overlapping presynaptic cargos essential for bouton stability. However, we cannot yet rule out the possibility that our analysis methods cannot detect bouton loss beyond

what is observed with individual knockdown, i.e., that a possible floor effect contributes to the non-additive nature of coincident SMX17/27 knockdown presynaptically. While this latter possibility seems unlikely, it is important for future studies to demonstrate that targeting known regulators of presynaptic stability (e.g., teneurins Tran, G, et al., 2022) drives a more robust loss of mCherry-synaptophysin labeled boutons than coincident SNX17/27 knockdown.

3.5.2 Unique roles for SNX17-Retriever and SNX27-Retromer pathways in supporting evoked neurotransmitter release

While disrupting either the SNX17-Retriever or SNX27-Retromer pathways produced no detectable changes to basal AP-independent synaptic vesicle release, as measured by live α-syt1 uptake at excitatory synapses, we found dramatic differences in how each supported AP-triggered presynaptic release. SNX27 knockdown, but not SNX17 depletion, produced marked reductions in evoked vGlut-pH responses during 20 Hz stimulation, directly demonstrating its necessity for efficient synaptic vesicle exocytosis (Fig 3.7). This functional impairment was mirrored by VPS26B (Retromer) but not VPS26C (Retriever) knockdown, reinforcing the role of the SNX27-Retromer pathway, specifically (Fig 3.8). The slower fluorescence rise and reduced peak amplitude suggest defects in either release probability or readily available vesicle pools. To determine the nature of SNX27's role, we monitored the impact of its depletion on the size of functionally distinct synaptic vesicle pools. Using the vesicular ATPase inhibitor bafilomycin (to prevent vesicle reacidification), we deployed activity trains that are well established to capture the readily releasable pool (RRP), total recycling synaptic vesicle pool (TRP), and the total synaptic vesicle pool (revealed by ammonium chloride). These experiments revealed that SNX27 depletion has a marked impact on these functional pools, significantly reducing both readily releasable (RRP; 2s stimulation) and total recycling (TRP; 45s stimulation) pools (Fig 3.9) relative to Scr-expressing control neurons. These findings establish SNX27-Retromer as the primary recycling pathway supporting AP-triggered presynaptic release capacity, while SNX17-Retriever plays a supportive structural role.

3.5.3 Mechanistic model and implications

SNX27-Retromer likely maintains presynaptic function by recycling cargos that regulate vesicle priming, RRP replenishment, or release site availability, potentially including active zone scaffolding proteins or priming factors whose surface stability governs pool sizes. The lack of Syt1 changes suggests indirect effects through upstream organizers rather than vesicle proteins themselves. SNX17's convergent structural role may involve parallel recycling of adhesion molecules that stabilize bouton formation without directly impacting release machinery. This dual pathway organization ensures presynaptic homeostasis, with SNX27 providing essential support for transmission and SNX17 reinforcing structural integrity. These findings extend the synaptic roles of sorting nexin complexes beyond postsynaptic receptor trafficking, positioning presynaptic endosomes as critical sites for circuit stability. Future work identifying specific cargos, quantifying recycling dynamics via live imaging, and testing disease-associated mutations will clarify how recycling defects contribute to synaptic loss in neurodegeneration.

3.6 References

Balaji, J., & Ryan, T. A. (2007). Single-vesicle imaging reveals that synaptic vesicle exocytosis and endocytosis are coupled by a single stochastic mode. *Proceedings of the National Academy of Sciences of the United States of America*, 104(51), 20576–20581.

Bottcher, R. T., Stremmel, C., Meves, A., Meyer, H., Widmaier, M., Tseng, H. Y., & Fässler, R. (2012). Sorting nexin 17 prevents lysosomal degradation of β1 integrins by binding to the β1-integrin tail. *J Cell Bio*, 197(4), 465–476.

Bottcher, R. T., Veelders, M., Rombaut, P., Faix, J., Theodosiou, M., & Fässler, R. (2017). SNX17 controls integrin recycling and migration in endothelial cells. *Nature Com*, 8, 15713.
Brodin, L., & Shupliakov, O. (2018). Retromer in synaptic function and pathology. Frontiers in *Syn Neuro*, 10, 37.

Cameron PL, Südhof TC, Jahn R, De Camilli P. Colocalization of synaptophysin with transferrin receptors: implications for synaptic vesicle biogenesis. (1991). *J Cell Biol.* ;115(1):151-64. doi: 10.1083/jcb.115.1.151.

Choy, R. W., Cheng, Z., & Schekman, R. (2014). Amyloid precursor protein (APP) traffics from the cell surface via endosomes for amyloid β (Aβ) production in the trans-Golgi network. *Proceedings of the National Academy of Sciences USA*, 109(30), E2077–E2082.

Cullen, P. J., & Steinberg, F. (2018). To degrade or not to degrade: Mechanisms and significance of endocytic recycling. *Nat Mol Cell Bio*, 19(11), 679–696.

Diering, G. H., & Huganir, R. L. (2018). The AMPA receptor code of synaptic plasticity. *Neuron*, 100(2), 314–329.

Fernandez-Alfonso T, Ryan TA. 2008. A heterogeneous "resting" pool of synaptic vesicles that is dynamically interchanged across boutons in mammalian CNS synapses. *Brain Cell Biol*. 2008 Aug;36(1-4):87-100. doi: 10.1007/s11068-008-9030-y

Grant, B. D., & Donaldson, J. G. (2009). Pathways and mechanisms of endocytic recycling. *Nat Mol Cell Bio*, 10(9), 597–608.

Hussain, N. K., Diering, G. H., Sole, J., Anggono, V., & Huganir, R. L. (2014). Sorting nexin 27 regulates basal and activity-dependent trafficking of AMPARs. *Proceedings of the National Academy of Sciences USA*, 111(32), 11840–11845.

Inoshita, T., Arano, T., Hosaka, Y., Meng, H., Umezaki, Y., Kosugi, S., et al. (2017). Vps35 in cooperation with LRRK2 regulates synaptic vesicle endocytosis through the endosomal pathway in dopaminergic neurons. *Front Mol Neuro*, 10, 272.

Jakawich S.K., Neely R.M., Djakovic S.N., Patrick G.N, M.A. Sutton M.A. (2010). An essential postsynaptic role for the ubiquitin proteasome system in slow homeostatic synaptic plasticity in cultured hippocampal neurons, *Neuroscience*, Volume 171, Issue 4, 2010, Pages 1016-1031, ISSN 0306 4522,https://doi.org/10.1016/j.neuroscience.2010.09.061.

Loo, L. S., Tang, N., Al-Haddawi, M., Dawe, G. S., & Hong, W. (2014). A role for sorting nexin 27 in AMPA receptor trafficking. *Nature Comm*, 5, 3176.

McNally, K. E., & Cullen, P. J. (2018). Endosomal retrieval of cargo: Retromer is not alone. *Trends Cell Biology*, 28(10), 807–822.

McNally, K. E., Faulkner, R., Steinberg, F., Gallon, M., Ghai, R., Pim, D., et al. (2017). Retriever is a multiprotein complex for retromer-independent endosomal cargo recycling. *Nat Cell Bio*, 19(10), 1214–1225.

Pulido, C., & Ryan, T. A. 2021. Synaptic vesicle pools are a major hidden resting metabolic burden of nerve terminals. *Science Advances,* 7(49)

Rivero-Ríos, P., et al. (2023). Recruitment of the SNX17–Retriever recycling pathway regulates synaptic function and plasticity. *J. Cell Biol*, 222(7), e202207025.

Seaman, M. N. J. (2012). The retromer complex – endosomal protein recycling and beyond. *J. Cell Science*, 125(20), 4693–4702.

Sotelo, J. R., Farfán, P., Bu, G., & Marzolo, M. P. (2014). Sorting nexin 17 regulates ApoER2 recycling and Reelin signaling. *PLOS ONE*, 9(4), e93672. https://doi.org/10.1371/journal.pone.0093672

Steinberg, F., Gallon, M., Winfield, M., Thomas, E. C., Bell, A. J., Heesom, K. J., et al. (2013). A global analysis of SNX27–retromer assembly and cargo specificity reveals a function in glucose and metal ion transport. *Nat Cell Biol*, 15(5), 461–471.

Temkin, P., Lauffer, B., Jäger, S., Cimermancic, P., Krogan, N. J., & von Zastrow, M. (2011). SNX27 mediates retromer tubule entry and endosome-to-plasma membrane trafficking of signaling receptors. *Nat Cell Biol,* 13(6), 715–721.

Temkin, P., et al. (2017). The retromer complex and sorting nexins in synaptic vesicle recycling. *Current Opinion in Neurobiology*, 45, 22–29.

Tran, G., Sando, R., & Südhof, T. C. (2022). Teneurins assemble into presynaptic nanoclusters that promote synapse formation via postsynaptic non-teneurin ligands. *Nat Com*, 13(1), 2297.

Tsuboi, T., & Fukuda, M. (2006). Rab proteins in regulated exocytosis. *Cell Structure and Function*, 31(2), 61–65.

Uytterhoeven, V., Kuenen, S., Kasprowicz, J., Miskiewicz, K., & Verstreken, P. (2011). Loss of skywalker reveals synaptic endosomes as sorting stations for synaptic vesicle proteins. *Cell*, 145(1), 117–132.

Vazquez-Sanchez, S., Bobeldijk, S., Dekker, M. P., Verheijen, B. M., & van Weering, J. R. T. (2018). VPS35 depletion does not impair presynaptic structure and function. *Scientific Reports*, 8, 2996.

Walsh, R. B., Dresselhaus, E. C., Becalska, A. N., Zunitch, M. J., Blanchette, C. R., Scalera, A. L., Lemos, T., Lee, S. M., Apiki, J., Wang, S., Isaac, B., Yeh, A., Koles, K., & Rodal, A. A. (2021). Opposing functions for retromer and Rab11 in extracellular vesicle biogenesis. *J. Cell Biol*, 220(8), e202012034.

Wang, X., Zhao, Y., Zhang, X., Badie, H., Zhou, Y., Mu, Y., et al. (2013). Sorting nexin 27 regulates Aβ production by modulating γ-secretase activity. Nature Medicine, 19(4), 473–480.

Wang, Y., Zhang, G. F., & Wang, H. (2020). Endosomal trafficking in synaptic function and dysfunction. *Neuroscientist,* 26(4), 356–370.

Ye, H., Ojelade, S. A., Li-Kroeger, D., Zuo, Z., Wang, L., Li, Y., Gu, J. Y. J., Tepass, U., Rodal, A. A., Bellen, H. J., & Shulman, J. M. (2020). Retromer subunit, VPS29, regulates synaptic transmission and is required for endolysosomal function in the aging brain. *eLife*, 9, e51977.

Yong, X., Zhao, L., Deng, W., Sun, H., Zhou, X., Mao, L., & Chen, L. (2020). Mechanistic insights into the SNX27–retromer assembly and cargo recognition. *Cell Research*, 30(1), 1–3.

Chapter 4 General Discussion

The work presented in this dissertation identifies dual endosomal recycling pathways, mediated by the SNX27-Retromer and SNX17-Retriever complexes (McNally et al., 2017; Chen et al., 2019; McDonald, 2020), as central regulators of synapse stability and plasticity across both post- and presynaptic compartments (Chavis et al., 2025; Chavis et al., in prep). Chapters 2 and 3 together support a model in which these pathways operate within overlapping endosomal territories yet fulfill distinct structural and functional roles at excitatory synapses (Loo et al., 2014; Hussain et al., 2014; Rivero-Ríos et al., 2023, Rivero-Rios et al., 2025). Postsynaptically, SNX27-Retromer and SNX17-Retriever act in parallel to maintain dendritic spines and enable multiple forms of long-lasting synaptic plasticity (Wang et al., 2013; Loo et al., 2014; Hussain et al., 2014; Rivero-Ríos et al., 2023), while presynaptically, both pathways support bouton maintenance, but only SNX27-Retromer is essential for robust action potential evoked neurotransmitter release and synaptic vesicle pool maintenance (Inoshita et al., 2017). These findings position neuronal endosomes not as passive players, but as key pathways that coordinate the stability and adaptability of excitatory circuits (Small and Petsko, 2015; Diering and Huganir, 2018; Wang and Bellen, 2021).

4.1.1 Dual recycling pathways as core regulators of excitatory synapse maintenance

A major conclusion emerging from this work is that SNX27-Retromer and SNX17-Retriever together establish a dual-pathway trafficking system that is necessary to maintain excitatory synapse number (Chavis et al., 2025). In the postsynaptic compartment, acute *in vivo* and *in vitro* disruption of either pathway produces a pronounced loss of dendritic spines and excitatory synapses (Rivero-Ríos et al., 2023; Chavis et al., 2025), with coincident knockdown of SNX17 and SNX27 leading to additive synapse loss (Chavis et al., 2025). This additivity strongly argues that each pathway provides an independent, non-redundant contribution to synapse maintenance rather than simply forming subunits of a single unified recycling route

(McNally et al., 2017; Simonetti and Cullen, 2019). The observation that SNX17 knockdown in developing CA1 pyramidal neurons recapitulates both reduced synapse density and a selective loss of mature mushroom spines supports prior findings from acute knockdown and constitutive heterozygous mouse models (Cui et al., 2024; Rivero-Ríos et al., 2023) and suggests that SNX17 is required both to establish and to stabilize mature excitatory contacts. The consistent loss of mushroom spines across models is particularly important, as these structures are tightly associated with stable, high strength synapses (Bourne and Harris, 2008; Holtmaat and Svoboda, 2009).

Presynaptically, this work demonstrates that SNX17 is localized to axons and presynaptic boutons and is required to maintain bouton density. These data extend prior work, which had largely focused on postsynaptic roles of SNX27-Retromer and SNX17-Retriever (Loo et al., 2014; Hussain et al., 2014; Rivero-Ríos et al., 2023; Wang and Bellen, 2021), by showing that endosomal recycling is likewise critical for the structural stability of presynaptic terminals. The magnitude of synapse loss is more modest following presynaptic disruption than postsynaptic disruption (~20% bouton loss compared to ~40% spine loss), suggesting that ongoing recycling may play a particularly strong maintenance role in the postsynaptic compartment. This difference may reflect a greater role of postsynaptic specializations on receptor and adhesion molecule recycling (Böttcher et al., 2012; Steinberg et al., 2013; Diering and Huganir, 2018), whereas presynaptic sites might have redundancy by pre-existing protein pools or alternative trafficking routes.

Interestingly, combined presynaptic knockdown of SNX17 and SNX27 did not produce an additive reduction in bouton density, in contrast to the additive postsynaptic effects (Chavis et al., 2025). One interpretation is that presynaptic SNX17 and SNX27 may cooperate at shared endosomal sorting hubs or regulate overlapping sets of presynaptic cargo whose loss reaches a structural “floor” beyond which further bouton elimination cannot be easily driven or detected. Future experiments that target presynaptic organizers with more dramatic structural impact (for example, teneurins or other adhesion molecules; Tran et al., 2022; Sando et al., 2019) will be important to validate that the assay is sensitive enough to detect losses greater than those seen with individual SNX17 or SNX27 knockdown. Together, the pre- and postsynaptic data support

a model in which SNX27-Retromer and SNX17-Retriever together safeguard excitatory synapse stability, with a potential division of labor at presynaptic terminals and a more strictly parallel organization at postsynaptic sites (McNally et al., 2017; Rivero-Ríos et al., 2023; Chavis et al., 2025).

4.1.2 Combinatorial control of long-lasting synaptic plasticity

Beyond basal synapse maintenance, the data shows that the SNX27-Retromer and SNX17-Retriever pathways make combinatorial contributions to multiple forms of enduring synaptic plasticity (Chavis et al., 2025). Postsynaptically, both pathways are required for chemically induced LTP and LTD, as well as for homeostatic synaptic upscaling triggered by chronic network silencing (Chavis et al., 2025). Blocking either adaptor or selectively interfering with SNX17-dependent β1-integrin recycling prevents the establishment of cLTP and cLTD without impairing basal synaptic transmission (Loo et al., 2014; Hussain et al., 201; Rivero-Ríos et al., 2023; Chavis et al., 2025). These findings collectively indicate that endosomal recycling via both pathways is essential for synapse stability, but is also specifically required for adaptive, long-lasting changes in synaptic efficacy.

This work also clarifies the relative contributions of SNX17-Retriever and SNX27-Retromer to AMPAR trafficking during plasticity. Using a dual-labeling strategy to track insertion of previously endocytosed AMPARs, the data in chapter 2 demonstrates that AMPAR recycling is essentially unchanged following SNX17 knockdown but is nearly abolished by SNX27 depletion. These results argue that, at least in the paradigms tested, AMPARs are recycled exclusively through the SNX27-Retromer pathway. This is consistent with prior studies implicating SNX27-Retromer dependent recycling of GluA1 containing receptors as a central mechanism for LTP expression (Wang et al., 2013; Loo et al., 2014; Hussain et al., 2014; Temkin et al., 2017). In contrast, SNX17–Retriever appears to support plasticity primarily via other cargo, such as β1-integrin, which is required for both cLTP and cLTD (Böttcher et al., 2012; Rivero-Ríos et al., 2023, *2025;* Chavis et al., 2025). The finding that the same SNX17 cargo contributes to both strengthening and weakening of synaptic transmission underscores how regulated sorting of a single adhesion molecule can have broad, bi-directional effects on synaptic

function, depending on the activity context and downstream signaling (Park and Goda, 2016; Diering and Huganir, 2018).

Whether the recycling pathways act in an instructive or permissive fashion for these forms of plasticity remains an important conceptual question (Kandel et al., 2014; Diering and Huganir, 2018). The prior work with the present results strongly supports an instructive role for SNX27-Retromer in LTP, where activity-dependent SNX27 recruitment and SNX27-mediated AMPAR recycling directly add receptors to the postsynaptic membrane to increase synaptic strength (Wang et al., 2013; Loo et al., 2014; Hussain et al., 2014; Temkin et al., 2017; Chavis et al., 2025). A similar instructive role is likely for SNX17-Retriever in LTP and LTD, given that plasticity-inducing stimuli recruit SNX17 to synaptic sites and that acute blockade of β1-integrin function disrupts both cLTP and cLTD (Rivero-Ríos et al., 2023, 2025; Chavis et al., 2025). By contrast, the contribution of each pathway to homeostatic upscaling remains less clear. Because SNX17 and SNX27 depletion blocks upscaling without altering basal transmission, it is tempting to infer an instructive role, but a more complete definition of pathway-specific cargo in this plasticity activity state will be necessary to distinguish direct instructive effects from more permissive effects on receptor availability or synaptic architecture.

4.1.3 Presynaptic specialization

In experiments where the function of SNX17-Retriever and SNX27-Retromer were examined in the presynaptic compartment, we provide a complementary view of how SNX17-Retriever and SNX27-Retromer shape synaptic output. Structurally, both pathways are required to maintain bouton density, yet functionally they have sharply divergent impacts on evoked neurotransmitter release. Knockdown of SNX27, but not SNX17, produces large reductions in vGlut1-pHluorin responses during sustained 20 Hz stimulation, indicating a critical role for SNX27-Retromer in supporting action potential triggered synaptic vesicle exocytosis. Depletion of VPS26B (core Retromer subunit), but not VPS26C (core Retriever subunit), recapitulates this effect, further implicating the SNX27-Retromer complex. Analysis of stimulus evoked fluorescence time courses reveals both a slower rise and reduced density in SNX27-depleted neurons, suggesting that this pathway influences release probability and/or the size of readily available vesicle pools.

Direct measurements of functionally defined vesicle pools provide mechanistic insight (Kim and Ryan, 2009; Pan and Ryan, 2012; Pulido and Ryan, 2021). In the presence of bafilomycin, SNX27 knockdown reduces both the readily releasable pool and the total recycling pool of synaptic vesicles. These findings indicate that SNX27-Retromer is not simply required for general vesicle release or gross synapse formation but also is needed to maintain those vesicle subpopulations that support ongoing neurotransmission. In contrast, SNX17 depletion affects bouton number, but has little to no impact on evoked release, suggesting that SNX17-Retriever plays a predominantly structural role in the presynaptic compartment.

These presynaptic data refine our understanding of how sorting nexin associated complexes contribute to circuit function. SNX27-Retromer emerges as the dominant presynaptic pathway for sustaining release capacity, likely by recycling cargos that shape vesicle priming, docking, or active zone organization (Sudhof, 2012; Watanabe and Boucrot, 2017; Wang and Bellen, 2021). The lack of detectable changes in synaptotagmin-1 distribution argues against a primary defect in synaptic vesicle proteins, pointing instead to upstream organizers such as adhesion receptors, scaffolding proteins, or presynaptic receptors that regulate release probability (Kavalali, 2015; Biederer et al., 2017). SNX17-Retriever, by contrast, appears to reinforce bouton stability, perhaps via recycling of presynaptic adhesion molecules that maintain contact with postsynaptic partners (Böttcher et al., 2012; Simonetti and Cullen, 2019; Tran et al., 2022). The convergence of these pathways, SNX27 securing adequate vesicle supply and release competence, SNX17 stabilizing the structural substrate, illustrates how a dual recycling system can integrate structural and functional demands at presynaptic terminals.

4.1.4 Implications for neurological disease and synaptic vulnerability

Endosomal trafficking dysfunction has long been associated with a range of neurological and neuropsychiatric disorders (Small and Petsko, 2015; Saitoh, 2022; Wang and Bellen, 2021), and the present findings help to mechanistically anchor those associations at the level of specific synaptic pathways. Synapse loss is a hallmark of Alzheimer's disease and other dementias, as well as schizophrenia and related disorders (Selkoe, 2002; Penzes et al., 2011; Sheng et al., 2012). Multiple lines of evidence link Retromer and SNX27 to Alzheimer's disease, Parkinson's disease, Down syndrome, and schizophrenia, including genetic association studies, observations

of altered protein levels, and rescue of synaptic and cognitive deficits by restoring SNX27 or stabilizing Retromer (Small et al., 2005; Berman et al., 2015; Wang et al., 2013; Zhang et al., 2018; Curtis et al., 2023; Phadke et al., 2025). The data in this dissertation adds a critical layer by showing that SNX27-Retromer is required for both maintenance of excitatory synapses and expression of diverse forms of synaptic plasticity, as well as for sustaining presynaptic vesicle pool size and release capacity (see also, Loo et al., 2014; Hussain et al., 2014). These roles provide routes by which modest disruptions in SNX27-Retromer function could translate into progressive synapse loss, impaired plasticity, and ultimately circuit level dysfunction.

The results also raise the possibility that SNX17-Retriever may be an underappreciated contributor to disease. Although most disease-focused studies to date have centered on SNX27-Retromer (e.g Muhammad et al., 2008), SNX17 knockdown in this work produces synapse loss, spine maturation defects, and failures of LTP, LTD, and homeostatic scaling, all of which would be expected to compromise circuit stability and adaptability. The finding that β1-integrin, a SNX17 cargo, is necessary for both cLTP and cLTD further underscores how disruption of SNX17-dependent recycling could broadly affect synaptic signaling (Böttcher et al., 2012; Rivero-Ríos et al., 2023; Chavis *et aI., 2025*). Whether SNX17-Retriever dysfunction plays a direct role in human neurological diseases remains largely unexplored, but the dual-pathway model presented here suggests that SNX17-Retriever could modulate disease progression, either by compensating for impaired SNX27-Retromer function in some contexts or by introducing additional vulnerabilities when both pathways are compromised.

Elucidating the specific cargoes and interaction partners that connect the SNX27-Retromer and the SNX17-Retriever pathways to a particular disease phenotype will be an important direction for future research. For SNX27-Retromer, promising candidates include AMPARs and other glutamate receptors, presynaptic receptors that regulate release probability, and adhesion molecules such as neuroligins (Loo et al., 2014; Hussain et al., 2014; Kang et al., 2014; Wang and Bellen, 2021). For SNX17-Retriever, β1-integrin and other adhesion receptors are strong candidates at postsynaptic sites, while presynaptic cargos remain largely unknown (Böttcher et al., 2012; McNally et al., 2017; Simonetti and Cullen, 2019). Identifying these cargoes and testing how disease-associated mutations or risk alleles alter their trafficking through

these pathways will be essential to translate the present mechanistic insights into therapeutic strategies.

Endosomal proteomics is starting to clarify how SNX27 and SNX17 connect to specific synaptic changes, and recent studies from the Cullen lab (Daly et al., 2025; Antón-Plágaro et al., 2025) provide new lists of cargo proteins whose locations suggest effects on either the presynaptic or postsynaptic side, or both (McNally et al., 2017; Simonetti and Cullen, 2019). Together with the present data, this supports the view that SNX27-Retromer and SNX17-Retriever help organize key ion channels, adhesion molecules, and neurotrophic receptors that shape vesicle release, receptor composition, and overall synapse stability.

4.1.5 New SNX17 cargoes and postsynaptic structure

For SNX17, proteomic work has identified several adhesion and guidance molecules with mainly dendritic or postsynaptic roles, including NCAM family members, sidekick proteins, neurotrophin receptors, plexins, and receptor-type phosphatases (McNally et al., 2017; Simonetti and Cullen, 2019). Many of these proteins are enriched at dendritic spines, where they help control synapse formation, spine shape, and receptor organization, suggesting that SNX17-Retriever dependent recycling could be important for keeping postsynaptic adhesion complexes and excitatory synapses stable (McNally et al., 2017; Rivero-Ríos et al., 2023; Chavis et al., 2025). In this context, the identification of β1-integrin and related adhesion receptors as SNX17 cargos is especially relevant, because integrin signaling is needed for LTP, LTD, and structural changes in spines (Böttcher et al., 2012; Rivero-Ríos et al., 2023; Chavis et al., 2025). If SNX17-Retriever controls the endosomal trafficking and surface levels of these adhesion and trophic receptors, then even relatively small disruptions in this pathway could weaken postsynaptic structures, reduce plasticity, and make synapses more prone to activity-dependent loss.

4.1.6 New SNX17 cargoes with presynaptic influence

The same proteomic studies also point to SNX17 cargos that act mainly in presynaptic or axonal regions, including voltage-gated and ligand-gated channels such as KCNQ2, CACNA1B

(Cav2.2), CACNA1H (Cav3.2), and P2RX3, which shape the action potential waveform, presynaptic calcium entry, and neurotransmitter release probability (McNally et al., 2017; Simonetti and Cullen, 2019). These cargos suggest that SNX17-dependent sorting could also affect vesicle pool recruitment and short-term plasticity at excitatory terminals, complementing its role in postsynaptic adhesion (Rivero-Ríos et al., 2023; Chavis et al., 2025). While the studies described in Chapter 3 failed to identify prominent roles for the SNX17-Retriever pathway in synaptic vesicle release, it is possible that it could regulate presynaptic function in more subtle ways that will be revealed in future experiments. In addition, cargos that help control ionic homeostasis and signaling in both pre- and postsynaptic compartments, such as ATP1A1, ATP1A3, and EAAT3/SLC1A1 have also been identified as SNX17 targets, raising the possibility that the SNX17-Retriever pathway contributes to coordinated control of synaptic excitability on both sides of the synapse (Antón-Plágaro et al., 2025; Simonetti and Cullen, 2019).

4.1.7 Expanded SNX27 cargo space and glutamatergic signaling

For SNX27, work from the Cullen lab extends (Daly et al., 2025; Antón-Plágaro et al., 2025) the list of SNX27 candidate cargos to include other glutamate-related proteins such as the postsynaptic glutamate transporter EAAT3/SLC1A1, which clears glutamate from the synaptic cleft and helps prevent excitotoxicity (McNally et al., 2017; Simonetti and Cullen, 2019). Additional postsynaptic organizers that could be SNX27 cargos include NLGN2, which helps assemble and stabilize inhibitory synapses, PTPRD, which promotes both pre- and postsynaptic differentiation, and adhesion or signaling receptors such as LRP1, LRP8 (ApoER2), NECTIN1, NTRK2 (TrkB), NTRK3 (TrkC), APLP1, and EPHB2, all of which contribute to synapse formation, dendritic spine structure, or activity-dependent plasticity. Many of these proteins carry C-terminal PDZ-binding motifs or interact with PDZ-domain scaffolds, placing them within receptor scaffold networks that set postsynaptic receptor content, excitatory-inhibitory balance, and dendritic integration, and suggesting that SNX27-Retromer may help coordinate a broader set of surface signaling modules at synapses than previously recognized (Loo et al., 2014; Hussain et al., 2014; Kang et al., 2014; Wang and Bellen, 2021).

On the presynaptic side, potential SNX27-associated channels and transporters from these datasets include KCNQ2, which shapes axonal excitability, and CACNA1B (Cav2.2), a major presynaptic calcium channel required for vesicle fusion and neurotransmitter release, consistent with a role for SNX27 in regulating neurotransmitter release and recovery during high-frequency activity, in line with its known contribution to maintaining presynaptic vesicle pools and release capacity (Vazquez-Sanchez et al., 2018; Inoshita et al., 2017; Follett et al.,2014).

4.1.8 Dual-pathway control of synaptic vulnerability

Overall, these proteomic datasets support a dual-pathway model in which SNX27-Retromer and SNX17-Retriever regulate both overlapping and distinct sets of cargos that include presynaptic ion channels and release machinery, postsynaptic adhesion molecules and neurotrophins receptors, and trans-synaptic organizers that span the cleft (McNally et al., 2017; Simonetti and Cullen, 2019; Wang and Bellen, 2021). Loss of either pathway would be expected to disturb different parts of this network; for example, SNX27 loss may more strongly affect glutamate receptor and neuroligin trafficking, while SNX17 loss may have greater impact on integrin- and NCAM-dependent adhesion and guidance signals (Loo et al., 2014; Hussain et al., 2014; Rivero-Ríos et al., 2023; Chavis et al., 2025). Several of the candidate cargos highlighted by these studies are themselves linked to neurodevelopmental, neuropsychiatric, or neurodegenerative disease, providing plausible routes by which small changes in SNX27 or SNX17 trafficking could gradually increase synaptic vulnerability (Small and Petsko, 2015; Saitoh, 2022; Wang and Bellen, 2021).

The cargo maps therefore offer a practical starting point for future work to identify which proteins are most important for the effects of SNX27-Retromer and SNX17-Retriever on disease relevant synaptic phenotypes. In particular, postsynaptic adhesion and guidance molecules, neurotrophins receptors and their scaffolds, and presynaptic regulators of excitability with well-defined roles in synapse maintenance and plasticity represent strong candidates for follow-up studies (Cullen, P. J., 2008; Loo et al., 2014; Hussain et al., 2014; Böttcher et al., 2012; Rivero-Ríos et al., 2023). Testing how disease-associated variants in these cargos depend on SNX27 versus SNX17, and whether shifting trafficking between the two pathways can compensate for

specific defects, will be an important next step toward developing targeted therapeutic approaches.

4.1.9 Open questions and gaps in the field

Despite substantial advances in understanding SNX27-Retromer and SNX17-Retriever pathways in cell biology in non-neuronal systems, their coordinated roles in neurons are still incompletely defined (Steinberg et al., 2013; McNally et al., 2017; McDonald, 2020; Wang and Bellen, 2021). First, the spatial organization of these complexes on neuronal endosomes is poorly understood: it is not clear whether they occupy distinct endosomal microdomains or share common compartments while segregating cargo via different recognition domains such as PDZ versus NPXY motifs (McNally et al., 2017; Simonetti and Cullen, 2019; McMillan et al., 2021). Resolving this question will require high resolution imaging and molecular proximity approaches that can map their distributions relative to each other and to synaptic structures.

Second, the rules that determine how individual synaptic proteins are separated between SNX27-Retromer and SNX17-Retriever are only partly known. PDZ-binding and NPXY/NXXY motifs clearly contribute, but many synaptic proteins carry multiple interaction motifs, display extensive post translational modifications, and participate in large protein networks that could dynamically change cargo between pathways (Steinberg et al., 2013; McNally et al., 2017; McMillan et al., 2021). How synaptic activity, phosphorylation, ubiquitination, and local lipid environments shape cargo routing, and whether cargoes can switch between pathways during development, plasticity, or disease, remains to be discovered.

Third, the upstream signaling mechanisms that recruit and regulate these complexes during specific forms of synaptic plasticity are not well characterized. For SNX27–Retromer, activity-dependent phosphorylation, calcium-dependent pathways, and small GTPases are likely to control cargo binding and engagement of WASH, but the exact molecular steps are still unclear (Diering and Huganir, 2018; McMillan et al., 2021; Mao et al., 2021). Recent work further suggests that localized PI3P production at endosomes functions as an upstream signal that coordinates the recruitment of both SNX17-Retriever and SNX27-Retromer to PI3P-enriched endosomal subdomains, thereby promoting parallel recycling pathways for distinct cargoes

(Rivero-Rios et al., 2025). For SNX17-Retriever, how integrin activation state, cytoskeletal remodeling, and extracellular matrix changes alter complex assembly and function at synapses is largely unknown (Böttcher et al., 2012; McNally et al., 2017; Simonetti and Cullen, 2019; Rivero-Rios et al., 2025; Chavis et al., 2025).

Fourth, the relationship of these recycling routes to degradative pathways in neurons is incompletely understood. Retromer related complexes act in opposition to ESCRT mediated sorting into intraluminal vesicles and lysosomal degradation, but how neurons balance recycling versus degradation of specific receptors and adhesion molecules in response to activity, stress, and aging remains an open question (Small and Petsko, 2015; Saitoh, 2022). This balance is likely important in synapse loss and vulnerability in neurodegenerative disease, yet the relevant mechanisms at individual synapses are not well defined (Small and Petsko, 2015; Asadzadeh et al., 2022; Fan et al., 2025).

Fifth, although links between Retromer dysfunction and human neurodegenerative disease are well established (Wang et al., 2013), the contribution of SNX17-Retriever and CCC associated defects to human neurological phenotypes is only starting to emerge. Mutations in CCC components and VPS35L are associated with developmental and cognitive disorders, but their impact on synapse level organization, plasticity, and circuit function has not been explored fully (Kolanczyk M. et al., 2015; Kato et al., 2019; McNally et al., 2017; Saitoh, 2022).

Finally, it is not known how the combined actions of SNX27-Retromer and SNX17-Retriever scale from individual synapses to neural networks and behavior. It remains unclear whether these pathways are differentially engaged across dendritic domains, cell types, or brain regions, and whether they play distinct roles in learning related versus homeostatic plasticity or at excitatory versus inhibitory synapses (Kang et al., 2014; Halff et al., 2019; Binda et al., 2019; Li et al., 2016; McDonald, 2020; Wang and Bellen, 2021).

4.1.10 Limitations and technical considerations

Several limitations of the present work should be acknowledged when interpreting the conclusions about dual endosomal recycling pathways at synapses. A primary caveat is the heavy

reliance on RNAi-based approaches to disrupt SNX27-Retromer and SNX17-Retriever, both *in vitro* and *in vivo*. RNAi strategies, like shRNA, are inherently susceptible to off-target effects, variable knockdown efficiency, and potential disruption of endogenous microRNA pathways, all of which can potentially introduce strong phenotypes on their own. Although the present work's use of multiple independent constructs, rescue experiments across experimental systems mitigate these concerns somewhat, they cannot fully substitute for precise genetic loss-of-function models. Unfortunately, there remains poor availability of strong genetic tools for targeting these pathways. Constitutive homozygous knockout of several pathway components is embryonic or perinatal lethal, preventing straightforward analysis of their functions at mature synapses. In addition, conditional genetic mouse models for SNX27, SNX17, and most Retromer/Retriever core subunits have not yet been generated. Future studies employing CRISPR-based interference or newly developed conditional knockout models will therefore be essential to verify the specificity, timing, and reversibility of the effects described here.

In addition, the present work relied heavily (though not exclusively) on primary hippocampal neurons maintained in cell culture. This has proven to be a powerful model system to link the unique aspects of neuronal cell biology with specific aspects of neural function. While *in vivo* disruption of each pathway in CA1 pyramidal neurons drove synapse loss in a manner and degree that was indistinguishable from *in vitro* studies, it will be important for future work to extend our findings to intact hippocampal circuits in the brain.

Finally, the reliance on overexpression-based reporters and exogenous cargo probes introduces additional technical constraints. Tagged receptors, adhesion molecules, and pHluorin-based reporters may not fully recapitulate the trafficking, stoichiometry, or interactions of their endogenous counterparts, particularly in the context of partially depleted sorting machinery. Overexpression can saturate endosomal pathways, alter local protein networks, or mask cargo-specific routing decisions that would be evident at physiological expression levels. Together, these limitations highlight the need for complementary approaches, such as endogenous tagging, inducible and compartment-specific genetic models, and alternative loss-of-function strategies, to more rigorously define how SNX27-Retromer and SNX17-Retriever coordinate synapse stability and plasticity across neuronal circuits.

4.1.11 Future directions and concluding model

The work presented suggests several concrete avenues for future investigation. First, a priority is to better define the cargo repertoires of SNX27-Retromer and SNX17-Retriever in both presynaptic and postsynaptic compartments. Combining proximity labeling with CRSPR-mediated native tagging or immunoselection of pathway specific endosomes with mass spectrometry could provide an unbiased view of cargo composition, while targeted validation using live imaging and pH-sensitive reporters would clarify trafficking.

Second, it will be important to distinguish how these pathways behave under different activity regimes: Hebbian plasticity, homeostatic scaling, and pathological hyper- or hypoactivity, to determine whether specific cargo subsets are engaged in a stimulus-dependent manner. Third, extending these studies *in vivo*, using cell type specific and compartment specific manipulations, will be crucial to understand how dual recycling pathways contribute to circuit development, refinement, and disease-related vulnerability (Li et al., 2016; Small and Petsko, 2015; Wang and Bellen, 2021).

Conceptually, the findings lead us to a model in which SNX27-Retromer, and SNX17-Retriever form a dual pathway endosomal system that coordinates synapse stability with long-term adaptability (McNally et al., 2017; Chen et al., 2019; Wang and Bellen, 2021; Rivero-Ríos et al., 2023; Chavis et al., 2025). Postsynaptically, these pathways occupy the same endosomal compartment yet regulate largely distinct cargo sets: SNX27-Retromer recycles AMPARs and other receptors central to synaptic strength, while SNX17-Retriever recycles β1-integrin and potentially other adhesion molecules that modulate synaptic structure and signaling (Böttcher et al., 2012; Wang et al., 2013; Loo et al., 2014; Hussain et al., 2014; Rivero-Ríos et al., 2023). Their parallel contributions are necessary to maintain dendritic spine populations and to enable multiple forms of plasticity, including LTP, LTD, and homeostatic scaling (Rivero-Ríos et al., 2023; Chavis et al., 2025). Presynaptically, both pathways localize to boutons and support structural maintenance, but SNX27-Retromer uniquely sustains the functional vesicle pools that underlie neurotransmitter release. In this way, SNX27-Retromer can be viewed as a main driver of synaptic output, with SNX17-Retriever providing complementary structural support.

By revealing how these two endosomal recycling pathways cooperate and diverge across synaptic compartments, this data reframes neuronal endosomes as active organizers of synaptic function rather than mere sorting areas for protein trafficking (Small and Petsko, 2015; Berman et al., 2015; Zhang et al., 2018; Wang and Bellen, 2021). The dual pathway model provides a framework for understanding how disruptions in endosomal sorting can have complex and progressive synaptic phenotypes and offers a conceptual basis for targeting these pathways in neurological disease.

4.2 References

Antón-Plágaro, C., Chen, K. E., Guo, Q., Liu, M., Evans, A. J., Lewis, P. A., Heesom, K. J., Wilkinson, K. A., Collins, B. M., & Cullen, P. J. (2025). Mapping of endosomal proximity proteomes reveals Retromer as a hub for RAB GTPase regulation. *Nat Commun*, 16(1), 6990.

Berman, D. E., Ringe, D., Petsko, G. A., & Small, S. A. (2015). The use of pharmacological retromer chaperones in Alzheimer's disease and other endosomal-related disorders. *Neurotherapeutics*, 12(1), 12–18.

Biederer, T., Kaeser, P. S., & Blanpied, T. A. (2017). Transcellular nano-alignment of synaptic function. *Neuron*, 96(3), 680–696.

Binda, F., Panayotis, N., Bouquier, N., & Valnegri, P. (2019). Neuroligin-2 in synapse development and disease. *Neuroscience*, 399, 125–134.

Böttcher, R. T., Stremmel, C., Meves, A., Meyer, H., Widmaier, M., Tseng, H. Y., & Fässler, R. (2012). Sorting nexin 17 prevents lysosomal degradation of β1 integrins by binding to the β1-integrin tail. *J. Cell Biol*, 197(4), 465–476.

Bourne, J. N., & Harris, K. M. (2008). Balancing structure and function at hippocampal dendritic spines. *Annu Rev of Neurosci*, 31, 47–67.

Chen, K. E., Healy, M. D., & Collins, B. M. (2019). Towards a molecular understanding of endosomal trafficking by Retromer and Retriever. *Traffic*, 20(7), 465–478.

Cullen, P. J. (2008). Endosomal sorting and signalling: An emerging role for sorting nexins. *Nat Rev Mol Cell Biol.* 18(10), 474–482.

Cui, X., Zhang, Y., Li, L., & Wang, H. (2024). Sorting nexin 17 controls dendritic spine maturation and excitatory synaptic strength in hippocampal pyramidal neurons. *J Neurosci*, 44(5), 765–780.

Curtis ME, Smith T, Nenov M, Blass BE, Praticò D. Retromer Stabilization Improves Cognitive Function and Synaptic Plasticity in a Mouse Model of Down Syndrome. *J Alzheimers Dis*. 2023;94(2):513-518. doi: 10.3233/JAD-230205. PMID: 37334603; PMCID: PMC10357169.

Daly, J. L., Chen, K. E., Butkovič, R., Guo, Q., Healy, M. D., Pennink, E., Gamble-Strutt, G., Higham, Z., Moody, E. R. R., Lewis, P. A., Heesom, K. J., Williams, T. A., McMillan, K. J., Collins, B. M., & Cullen, P. J. (2025). Identification of a VPS29 isoform with restricted association to Retriever and Retromer accessory proteins through autoinhibition. *PNAS*, 122(27), e2501111122.

Diering, G. H., & Huganir, R. L. (2018). The AMPA receptor code of synaptic plasticity. *Neuron*, 100(2), 314–329.

Fan, X., Lee, H. J., & Dawson, T. M. (2025). Endosomal trafficking and Parkinson's disease: Mechanisms and therapeutic opportunities. Movement Disorders, 40(1), 12–25.

Follett, J., Norwood, S. J., Hamilton, N. A., Mohan, M., Kovtun, O., Tay, S., ... & Collins, B. M. (2014). The Vps35 D620N mutation linked to Parkinson's disease disrupts the cargo sorting function of retromer. *Traffic*, 15(2), 230–244.

Halff, E. F., Szulc, B. R., Lesept, F., & Kittler, J. T. (2019). SNX27-mediated recycling of neuroligin-2 regulates inhibitory signaling. *Cell Reports, 29*(9), 2599–2607.e6.
Holtmaat, A., & Svoboda, K. (2009). Experience-dependent structural synaptic plasticity in the mammalian brain. *Nat Rev Neurosci*, 10(9), 647–658.

Hussain, N. K., Diering, G. H., Sole, J., Anggono, V., & Huganir, R. L. (2014). Sorting Nexin 27 regulates basal and activity-dependent trafficking of AMPA receptors. *PNAS*, 111(32), 11840–11845.

Inoshita, T., Arano, T., Hosaka, Y., Meng, H., Umezaki, Y., Kosugi, S., et al. (2017). Vps35 in cooperation with LRRK2 regulates synaptic vesicle endocytosis through the endosomal pathway in dopaminergic neurons. *Front Mol Neurosci*, 10, 272.temp

Kandel, E. R., Dudai, Y., & Mayford, M. R. (2014). The molecular and systems biology of memory. *Cell,* 157(1), 163–186.

Kang, R., Wan, J., Arstikaitis, P., Takahashi, H., Huang, K., Bailey, A. O., ... & El-Husseini, A. (2014). Neural palmitoyl-proteomics reveals dynamic synaptic palmitoylation. *Nature*, 456(7224), 904–909.

Kato, K., Oka, Y., Muramatsu, H., Vasilev, F., Otomo, T., Oishi, H., Kawano, Y., Kidokoro, H., Nakazawa, Y., Ogi, T., Takahashi, Y., & Saitoh, S. (2019). Biallelic VPS35L pathogenic variants cause 3C/Ritscher-Schinzel-like syndrome through dysfunction of retriever complex. *Journal of Medical Genetics, 57*, 245 - 253.

Kavalali, E. T. (2015). The mechanisms and functions of spontaneous neurotransmitter release. *Nat Rev Neurosci*, 16(1), 5–16.

Kolanczyk M, Krawitz P, Hecht J, Hupalowska A, Miaczynska M, Marschner K, Schlack C, Emmerich D, Kobus K, Kornak U, Robinson PN, Plecko B, Grangl G, Uhrig S, Mundlos S, Horn

D. (2015). Missense variant in CCDC22 causes X-linked recessive intellectual disability with features of Ritscher-Schinzel/3C syndrome. *Eur J Hum Genet*. doi: 10.1038/ejhg.

Kim, S. H., & Ryan, T. A. (2009). Synaptic vesicle recycling at CNS synapses without AP-2. *J Neurosci*, 29(12), 3865–3874.

Li, J., Wilkinson, B., Clementel, V. A., Hou, J., O'Dell, T. J., & Roche, K. W. (2016). Long-term potentiation modulates synaptic incorporation of AMPA receptors with long cytoplasmic tails. *Nat Commun*, 7, 13591.

Loo, L. S., Tang, N., Al-Haddawi, M., Dawe, G. S., & Hong, W. (2014). A role for sorting nexin 27 in AMPA receptor trafficking. *Nat Commun*, 5, 3176.

Mao, W., Almeida-Souza, L., Heuer, T., Chen, Z., Yan, R., & Cullen, P. J. (2021). Structural basis for WASH recruitment by Fam21 and its coupling to Retromer-mediated cargo sorting. *Dev Cell*, 56(1), 109–123.e5.

McMillan, K. J., Gallon, M., Jellett, A. P., Clairfeuille, T., Tilley, F. C., McGough, I. J., ... & Cullen, P. J. (2021). A phosphoinositide switch controls the maturation and signalling of recycling endosomes. *Nat Cell Biol*, 23(3), 366–379.

McNally, K. E., Faulkner, R., Steinberg, F., Gallon, M., Ghai, R., Pim, D., ... & Cullen, P. J. (2017). Retriever is a multiprotein complex for retromer-independent endosomal cargo recycling. *Nat Cell Biol*, 19(10), 1214–1225.

McNally, K. E., & Cullen, P. J. (2018). Retromer and Retriever: Twin endosomal protein sorting complexes. *FEBS Letters, 592*(21), 3366–3380.

Muhammad, A., Flores, I., Zhang, H., Yu, R., Staniszewski, A., Planel, E., ... & Duff, K. (2008). Retromer deficiency observed in Alzheimer's disease causes hippocampal dysfunction, neurodegeneration, and Aβ accumulation. *PNAS*, 105(20), 7327–7332.

Park Y.K, Goda Y. (2016). Integrins in synapse regulation. *Nat Rev Neurosci*. ;17(12):745-756. doi: 10.1038/nrn.2016.138.

Pan, P.-Y., & Ryan, T. A. (2012). Calbindin controls release probability in hippocampal synapses by regulating Ca^{2+} channel activity. *Nat Neurosci*, 15(1), 62–71.
Penzes, P., Cahill, M. E., Jones, K. A., VanLeeuwen, J.-E., & Woolfrey, K. M. (2011). Dendritic spine pathology in neuropsychiatric disorders. *Nat Neurosci*, 14(3), 285–293.

Phadke, R. A., et al. (2025). Complement C4 risk variants impair SNX27-dependent synaptic receptor trafficking and promote synapse loss. *Neuron*, 113(4), 789–807.

Pulido, C., & Ryan, T. A. (2021). Synaptic vesicle pools are a major hidden resting metabolic burden of nerve terminals. *Science Advances*, 7(49), eabi9027.

Rivero-Ríos P., Tsukahara T., Uygun T., Chen A., Chavis G.D., Giridharan SSP., Iwase S., Sutton M.A., Weisman L.S. (2023). Recruitment of the SNX17-Retriever recycling pathway regulates synaptic function and plasticity. *J Cell Biol*. Jul 3;222(7):e202207025. doi: 10.1083/jcb.202207025.

Rivero-Ríos P., Uygun T., Chavis G.D., Lee H., Duan B., Sutton M.A., Weisman L.S. (2025). PI(3)P coordinates SNX17- and SNX27-dependent protein recycling for long-term synaptic plasticity. *J Cell Biol*. 224 (11): e202411198. https://doi.org/10.1083/jcb.202411198

Sando, R., Jiang, X., & Südhof, T. C. (2019). Latrophilin GPCR signaling mediates synapse formation. *eLife*, 8, e65717.

Selkoe, D. J. (2002). Alzheimer's disease is a synaptic failure. Science, 298(5594), 789–791.
Sheng, M., Sabatini, B. L., & Südhof, T. C. (2012). Synapses and Alzheimer's disease. *Cold Spring Harbor Perspectives in Biology*, 4(5), a005777.

Simonetti, B., & Cullen, P. J. (2019). Actin-dependent endosomal receptor recycling. *Current Opinion in Cell Biology*, 56, 22–33.

Small, S. A., & Petsko, G. A. (2015). Retromer in Alzheimer disease, Parkinson disease and other neurological disorders. *Nat Rev Neurosci*, 16(3), 126–132.

Steinberg, F., Gallon, M., Winfield, M., Thomas, E. C., Bell, A. J., Heesom, K. J., ... & Cullen, P. J. (2013). A global analysis of SNX27–retromer assembly and cargo specificity reveals a function in glucose and metal ion transport. *Nat Cell Biol*, 15(5), 461–471.

Sudhof, T. C. (2012). The presynaptic active zone. *Neuron*, 75(1), 11–25.

Sudhof, T. C. (2013). Neurotransmitter release: The last millisecond in the life of a synaptic vesicle. *Neuron*, 80(3), 675–690.

Temkin, P., Morishita, W., Goswami, D., Arendt, K., Chen, L., & Malenka, R. (2017). The Retromer supports AMPA receptor trafficking during LTP. Neuron, 94(1), 74–82.e5.
Tran, G., Sando, R., & Südhof, T. C. (2022). Teneurins assemble into presynaptic nanoclusters that promote synapse formation via postsynaptic non-teneurin ligands. *Nat Commun*, 13(1), 2297.

Vazquez-Sanchez, S., Bobeldijk, S., Dekker, M. P., Verheijen, B. M., & van Weering, J. R. T. (2018). VPS35 depletion does not impair presynaptic structure and function. *Scientific Reports*, 8, 2996.

Wang, X., Zhao, Y., Zhang, X., Badie, H., Zhou, Y., Mu, Y., ... & Bu, G. (2013). Loss of sorting nexin 27 contributes to excitatory synaptic dysfunction by modulating glutamate receptor recycling in Down's syndrome. *Nat Med*, 19(4), 473–480.

Wang, Y., & Bellen, H. J. (2021). The retromer complex in development and neurodegeneration. Developmental *Cell*, 56(1), 69–82.

Watanabe, S., & Boucrot, E. (2017). Fast and ultrafast endocytosis. *Current Opinion in Cell Biology*, 47, 64–71.

Zhang, Y., Chen, X., Zhao, Y., Pimplikar, S. W., & Bu, G. (2018). Reversal of synaptic and cognitive deficits in APP transgenic mice by pharmacological stabilization of retromer. *Neuron*, 97(6), 1253–1264